Title

A study on circadian regulation of the cardiovascular system: dysfunction in the BACHD Huntington's Disease model and Vasoactive Intestinal Peptide-deficient mice and the use of scheduled exercise to rescue circadian deficits.

Author

Schroeder, Analyne

Publication Date

2012

Peer reviewed|Thesis/dissertation

UNIVERSITY OF CALIFORNIA

Los Angeles

A study on circadian regulation of the cardiovascular system: dysfunction in the BACHD Huntington's Disease model and Vasoactive Intestinal Peptide-deficient mice and the use of scheduled exercise to rescue circadian deficits.

A dissertation submitted in partial satisfaction of
the requirements for the degree Doctor of Philosophy in
Molecular, Cellular and Integrative Physiology

by

Analyne Manzano Schroeder

2012

ABSTRACT OF THE DISSERTATION

A study on circadian regulation of the cardiovascular system:
dysfunction in the BACHD Huntington's Disease model and
Vasoactive Intestinal Peptide-deficient mice and
the use of scheduled exercise to rescue circadian deficits.

by

Analyne Manzano Schroeder
Doctor of Philosophy in Molecular, Cellular and Integrative Physiology
University of California, Los Angeles, 2012
Professor Christopher S. Colwell, Chair

The circadian system coordinates rhythms of behavior, physiology and gene expression with the external cues of light and dark, and the dysfunction of this system leads to the development of disease. Huntington's disease patients experience circadian symptoms and are at an increased risk for serious cardiovascular events that often lead to death. We, therefore, explored circadian and cardiovascular dysfunction in the BACHD model of Huntington's disease (HD). Diurnal and circadian rhythms of heart rate (HR), heart rate variability (HRV) and body temperature were significantly blunted along with dysfunction of the autonomic nervous system as measured by baroreceptor reflex. Circadian disruption could be attributed to reduced Vasoactive Intestinal Peptide (VIP) signaling in HD, therefore, we examined whether cardiovascular rhythms were

disrupted in the VIP-deficient mouse. We detected deficits in the diurnal and circadian rhythms of HR, HRV, body temperature and cage activity in VIP-deficient mice, suggesting that VIP is crucial for the circadian regulation of physiological outputs, including the cardiovascular system. Stabilization and realignment of the circadian system with the light/dark cycle may help decrease the risk of cardiovascular disease. Therefore, we explored the ability of scheduled exercise to drive and reorganize rhythms in behavior, physiology and gene expression in WT and VIP-deficient mice. Many of the deficits in diurnal rhythms displayed by VIP-deficient mice were rescued by exercise during the late night. In summary, these studies examined mechanisms by which the circadian system regulates the cardiovascular system using BACHD and VIP-deficient mice. We also introduced a new tool to help temporally restructure behavior, which improved various parameters of the circadian system in a circadian compromised mouse model. This tool could potentially be applied to humans with circadian symptoms, to help deter the development of cardiovascular disease associated with circadian disruption.

The dissertation of Analyne Manzano Schroeder is approved.

Gene D. Block

Kenneth D. Philipson

Kenneth P. Roos

James A. Waschek

Christopher S. Colwell, Committee Chair

University of California, Los Angeles

2012

Dedicated to my family,

I wish we could hang out more often!

TABLE OF CONTENTS **Page**

ACKNOWLEDGEMENTS

I would like to thank my parents for raising, loving and educating me. I know I wasn't always a good student, but you never gave up on me... look! Who would have ever thought I would be putting a dissertation together and completing a Ph.D. degree. Not me! And I never could have accomplished this without the both of you! Thank you for always encouraging me, asking me about my experiments, and helping me to become better.

Thank you to my younger brothers who are always there for me no matter what, and who keep me grounded, but keep me on my toes.

I would like to thank Dr. Chris Colwell, who has very patiently guided me through graduate school and helped me produce a body of work that I am proud to have accomplished. Thank you to my committee members, Drs. Gene Block, Kenneth Philipson, Kenneth Roos and James Waschek for their support and intellectual guidance through the years!

I'd like to thank everyone in the Colwell Lab and Waschek Lab for being part of this journey. No matter when in the path I met you, you are part of my life and you have filled my world with joy and meaningful substance.

To everyone who has touched my life in these past few years, Thank You! I wouldn't be where I am at this moment and I wouldn't be who I am without all of you. Thank you for your guidance, smiles, jokes, stories, encouragement and company! I only hope that I add to your lives as well.

My little heart is overflowing with love and gratitude for you all. And I can not say thank you enough!

Analyne Manzano Schroeder

Education

Ph.D. Doctoral Candidate, Molecular, Cellular and Integrative Physiology
University of California – Los Angeles
Los Angeles, California
2005-current
Master of Science, Molecular and Cellular Biology
Brandeis University
Waltham, Massachusetts
Received May 2005
Bachelor of Science, Major: Medical and Integrative Biology; Minor: Management
Beloit College
Beloit, Wisconsin
Received May 2002

Employment

Employment
Research Technologist-- Ravi Allada: PI, Northwestern University (06/04-08/05)
Supervising Researcher—Ravi Allada: Owner, Nunetix Inc. (02/05-08/05)

Selected Grants, Honors and Awards

GRADUATE
Brandeis University Master's Scholarship 2003
NIH Training Grant 2005-2006
UCLA Neural Microcircuits Training Grant 2008
Society for Research on Biological Rhythms Travel Award 2008
Best Poster Presentation Award MCIP Retreat 2008
UCLA Laboratory of Neuroendocrinology Training Grant 2009, 2010
Symposium on VIP, PACAP and Related Peptides Travel Grant 2009
UCLA Graduate Fellowship 2009
Ruth L. Kirschstein National Research Service Award (NRSA) Fellowship 2010-2011
UCSD Center for Chronobiology Symposium Best Poster Award 2010
Circadian Clocks and Metabolic Disease Travel Grant 2012
Society for Research on Biological Rhythms Merit Award 2012

UNDERGRADUATE
Departmental Honors in Biology
Dean's Honor List 2000-2002
Research Experience for Undergraduates (REU) research grant – summer 2001

Publications

Schroeder AM, Loh DH, Jordan MC, Roos KP, Colwell CS. Scheduled exercise alters diurnal rhythms of behaviour, physiology and gene expression in WT and Vasoactive Intestinal Peptide-deficient mice. *Submitted manuscript.*

Schroeder AM, Loh DH, Jordan MC, Roos KP, Colwell CS. (2011) Baroreceptor reflex dysfunction in the BACHD mouse model of Huntington's disease. *PLoS Curr.* 3:RRN1266.

Loh DH, Dragich JM, Kudo T, **Schroeder AM**, Nakamura TJ, Waschek JA, Block GD, Colwell CS. (2011) Effects of vasoactive intestinal Peptide genotype on circadian gene expression in the suprachiasmatic nucleus and peripheral organs. *J Biol Rhythms*. 26:200-9.

Kudo T, **Schroeder A**, Loh DH, Kuljis D, Jordan MC, Roos KP, Colwell CS. (2011) Dysfunctions in circadian behavior and physiology in mouse models of Huntington's disease. *Exp. Neurol*. 228: 80-90.

Schroeder A, Loh D, Jordan MC, Roos KP, Colwell CS. (2011) Circadian regulation of Cardiovascular Function: a role for VIP. *Am J Physiol Heart Circ Physiol*. 300:H241-50.

Itri JN, Vosko AM, **Schroeder A**, Dragich JM, Michel S, Colwell CS. (2010) Circadian regulation of a-type potassium currents in the suprachiasmatic nucleus. *J. Neurophysiol.* **103:** 632-40.

Hee Joo Choi, C. Justin Lee, **Analyne Schroeder**, Yoon Sik Kim, Seung Hoon Jung, Jeong Sook Kim, Do Young Kim, Eun Ju Son, Hee Chul Han, Sung Kil Hong, Christopher S. Colwell, and Yang In Kim. (2008) Excitatory Actions of GABA in the Suprachiasmatic Nucleus. *J. Neurosci.* **28:** 5450-9.

L.M. Wang, **A. Schroeder**, D. Loh, D. Smith, K. Lin, J.H. Han, S. Michel, D. L. Hummer, J.C. Ehlen, H.E. Albers, and C.S. Colwell. (2008) Role for the NR2B subunit of the N-methyl-d-aspartate receptor in mediating light input to the circadian system. *Eur. J. Neurosci.* **27:**1771-9.

Andrew M. Vosko, **Analyne Schroeder**, Dawn H. Loh, and Christopher S. Colwell. (2007) Vasoactive Intestinal Peptide and the Mammalian Circadian System. *Gen. Comp. Endocrinol.* **152:** 165-75.

Jui-Ming Lin, **Analyne Schroeder**, Ravi Allada**.** (2005) In Vivo Circadian Function of Casein Kinase 2 Phosphorylation Sites in Drosophila PERIOD. *J. Neurosci*. **25**: 11175-11183.

Bridget C. Lear, C. Elaine Merrill, Jui-Ming Lin, **Analyne Schroeder**, Luoying Zhang, and Ravi Allada. (2005) A G Protein-Coupled Receptor, *groom-of-PDF*, Is Required for PDF Neuron Action in Circadian Behavior. *Neuron.* **48**: 221-227.

Selected Conferences and Presentations

SRBR (Society for Research on Biological Rhythms) 13th Biennial Meeting 2012: Poster
Experimental Biology 2012: Poster
Circadian Clocks and Metabolic Disease 2012: Talk
23nd Annual UCLA BRI Poster Session 2011: Poster
Molecular, Cellular and Integrative Physiology Annual Retreat 2011: Poster
SRBR (Society for Research on Biological Rhythms) 12th Biennial Meeting 2010: Poster
UCSD Center for Chronobiology Symposium 2010: Best Poster Award
Molecular, Cellular and Integrative Physiology Annual Retreat 2010: Talk
Laboratory of Neuroendocrinology Seminar 2010: Talk
21st Annual UCLA BRI Poster Session 2009: Poster
4th Annual Neural Microcircuits Training Program Symposium 2009: Talk
UCLA Mental Retardation Research Center Annual Retreat 2008: Poster
SRBR (Society for Research on Biological Rhythms) 11th Biennial Meeting 2008: Poster
Molecular, Cellular and Integrative Physiology Annual Retreat 2008: Best Poster Presentation
3rd Annual Neural Microcircuits Training Program Symposium 2008: Poster
Student Seminars: Molecular, Cellular and Integrative Physiology 2008: Talk
2nd Annual Neural Microcircuits Training Program Symposium 2007: Poster
NCUR (National Conference for Undergraduate Research) 2002: Poster
Beloit College Annual Student Symposium 2002 : Talk

CHAPTER 1

i. Introduction

Overview

Life has evolved under the influence of daily light/dark cycles, which is evident in most biological processes that display circa (about) dian (day) oscillations including behavior, physiology, and gene expression. The ability of life forms, ranging from unicellular microorganisms to complex, multi-system, social animals such as humans, to adapt and anticipate the daily onset of light and dark, provides advantages in survival either by avoiding the DNA damaging effects of the sun, anticipating food availability, or preventing disease. In context of current human challenges, it is becoming evident that disruptions of the daily cycle correlate with increased incidence of disease that include heart failure, diabetes and cancer to name a few. This emphasizes the need to examine how circadian inputs regulate biological processes in order to study the mechanisms involved in the development of disease as a result of circadian disruption. Lastly, by understanding what goes wrong, methods to prevent or minimize negative effects can be conceived.

The suprachiasmatic nucleus as the master pacemaker

Circadian rhythms are an endogenous timing mechanism that enables the coordinated timing of behavioral, physiological, and biochemical processes with the 24-hour cycles of light and dark (Takahashi *et al.*, 2008). Through lesion and rescue experiments, a paired nuclei located in the hypothalamus called the suprachiasmatic nucleus (SCN) was determined necessary for the generation of normal circadian rhythms (Stephan & Zucker, 1972; Moore & Eichler, 1972; Lehman *et al.*, 1987). These SCN neurons have the intrinsic ability to generate circadian rhythms

in electrical activity, secretion, and metabolism driven by a cell-autonomous molecular feedback loop made up of key clock genes such as *period (Per1, Per2), crypto chrome (Cry1, Cry2), clock (Clk)* and *Bmal1* that are themselves rhythmically transcribed and translated (Hastings *et al.*, 2003). These molecular and cellular processes within the SCN are reset by light at certain phases of the endogenous cycle (Kuhlman & McMahon, 2006). Light is the major entrainor of the circadian system, which is detected by melanopsin receptors in the retina and transmitted to the SCN via the retinohypothalamic tract using glutamatergic signals (Gooley *et al.*, 2001; Güler *et al.*, 2007). The SCN also receives input signals from other regions of the brain such as the limbic system, Intergeniculate Leaflet (IGL), paraventricular nucleus (PVN) and raphe nucleus (Moga & Moore, 1997). These inputs utilize various neurotransmitters and neuropeptides that provide feedback information from the body to modulate the SCN. Changes in SCN function subsequently alter rhythms of behavior and other biological processes.

Recently, it has become clear that most cells outside of the SCN also display oscillations in clock gene expression; however, unlike the SCN, the generation and synchronization of these rhythms are dependent upon periodic signals from the SCN (Ko & Takahashi, 2006). SCN lesions result in the disruption of robust rhythms in clock gene expression in many tissues, but a recent study suggests that low amplitude rhythms continue (Tahara *et al.* 2012). Also, studies utilizing transgenic rodent models in which the *Per1* gene promoter or *Per2* gene are linked to a luciferase reporter (Yamazaki *et al.*, 2000; Abe *et al.*, 2002; Yoo *et al.*, 2004) demonstrate that cultured extra-SCN and peripheral tissues display oscillations in *Per1* or PER2 driven bioluminescence, but these oscillations quickly dampen as synchrony among cells is lost. Rhythms can be restored by external cues such as media changes or treatment with the cAMP agonist forskolin. The SCN on the other hand, when placed in culture sustain molecular

oscillations indefinitely without requiring any external cues, mediated by the circuitry among neurons as well as through the release of the neuropeptide Vasoactive Intestinal Peptide (VIP; (Vosko *et al.*, 2007). The ability for sustained oscillations of isolated SCN cultures suggests a hierarchal order in the control of rhythms with the SCN being the master pacemaker.

In addition to molecular and cellular oscillations, rhythms in behavior and physiology are also driven by the SCN. Behaviors such as activity and feeding, and physiological processes such HR and body temperature, all display day/night differences that are lost when the SCN is lesioned (Abe *et al.*, 1979; Warren *et al.*, 1994). Disruption of the molecular clock in mice also leads to the loss of circadian rhythms of behavior and physiology (Bae *et al.*, 2001). The role of the circadian system is to temporally compartmentalize biological processes in the body and drive rhythms in behavior, physiology and cellular processes with appropriate phase relationships with each other (Dibner *et al.*, 2010). Furthermore, daily organization allows for anticipation of incoming stimuli. The organization and anticipation allows for optimization of biochemical reactions in the body and prevent or minimize radical production and cell damage. Therefore, one can easily imagine that the lack of temporal regulation could cause cellular dysfunction that could lead to disease and death (Takahashi *et al.*, 2008; Colwell, 2011).

Circadian regulation of cardiovascular function

Mammals exhibit robust circadian rhythms in cardiovascular function that enables the daily anticipation of physical activity and physiological demands of the organism. Cardiovascular parameters such as heart rate (HR), heart rate variability (HRV), ejection fraction and blood pressure (BP) are elevated during periods of wake and depressed during sleep (Hu *et al.*, 2004). These cardiovascular rhythms are dependent upon an intact SCN, whereby SCN lesioned

animals fail to display rhythms in HR (Warren *et al.*, 1994; Sano *et al.*, 1995; Scheer *et al.*, 2001).

At a molecular and cellular level, studies using various methods have shown that cardiac cells, tissue and explants exhibit rhythmic expression of clock genes (Oishi *et al.*, 1998; Sakamoto & Ishida, 2000; Guo *et al.*, 2005; Davidson *et al.*, 2005; Durgan *et al.*, 2005) consistent with the idea that cardiovascular tissue contains circadian oscillators that are independent from the SCN. These oscillations in clock genes are thought to integrate SCN and metabolic input to drive heart specific rhythmic outputs (Bray & Young, 2008; Wu *et al.*, 2011). Micro-array studies have found that hundreds of genes (~10-15% of total genome) oscillate in the heart ((Storch *et al.*, 2002; Martino *et al.*, 2004; Rudic *et al.*, 2005). These rhythmic genes code for proteins such as ion channels, neurotransmitter receptors, and proteins involved in calcium flux, which are likely to have substantial effects on cardiac function. For example, the potassium channels Kv1.5 and 4.2 exhibit oscillations in expression as well as in current that could influence the flow of ions regulating heart rate and function (Yamashita *et al.*, 2003; Jeyaraj *et al.*, 2012). The rhythmic gene expression in the heart may well explain why the response to a variety of environmental stimuli varies depending on the time of day (Young, 2006). Disruptions of the molecular feedback loop lead to altered protein expression, blood pressure as well as an increased risk of cardiac hypertrophy (Ikeda *et al.*, 2007; Sei *et al.*, 2008; Vukolic *et al.*, 2010; Wang *et al.*, 2010).

Recent studies suggest that the regulation of cardiac rhythms is dependent on both the intrinsic molecular clock in the heart as well as by exogenous factors. E*x vivo* heart preparations that examine contractile function of the heart without influence from the autonomic nervous system or circulating factors, suggest that the function of some cardiac parameters, such as

cardiac power, and cardiac efficiency, oscillate dependent on the time of day, while other parameters do not show rhythms (Bray *et al.*, 2008). The disruption of the molecular clock in the cardiomyocytes eliminates these oscillations in function. Studies using mice with cardiomyocyte specific clock mutation (CCM), which disrupts the molecular feedback loop only in the heart, further identifies the role of the molecular clock in heart (Bray *et al.*, 2008). In CCM mice, blood pressure, cage activity levels and cage activity rhythms are not different compared to WT controls. While day/night differences in HR persist, the amplitude of the rhythm is significantly dampened, and 24hr average HR is significantly reduced suggesting that the clock may be involved in the regulation of HR. Furthermore, CCM mice displayed a reduced capacity for exercise (Ko *et al.*, 2011). When presented with a running wheel, CCM mice ran less, had a similar number of bouts but with shortened bout length. Measurement of cell signaling molecules in the heart of WT mice provided wheel access showed daily fluctuations in phosphorylation states (ERK, AKT, GSK, p38, Voltage gated Calcium channels), while CCM mice displayed rhythms only in p38 phosphorylation. These studies demonstrate that the molecular clock regulates heart function including HR, and is required to accommodate increased cardiovascular demand during exercise. Furthermore, subsets of molecules are under direct control of the molecular clock within cardiomyocytes, while other signaling molecules respond to the rhythmic exogenous cues that remain intact in CCM animals. (Wu and Bray durgan fatty acid). Overall, both intrinsic and exogenous factors are required for daily fluctuations, baseline and adaptive cardiovascular function.

The pathways by which the SCN is coupled to these physiological and molecular oscillations in the heart are not yet known. Humoral mechanisms such as glucocorticoid signaling are implicated in resetting phase of clock genes in peripheral tissues, including the heart (Balsalobre

et al., 2000). However, transplantation of SCN tissue into an SCN-lesioned hamster rescued rhythms in wheel running activity without rescuing rhythms in HR or gene expression (Guo *et al.*, 2006)). Similarly, a parabiosis set up that allows blood exchange between a control and SCN-lesioned animal, resulted in the rescue of gene expression in a number of peripheral tissues such as the liver and kidney, but failed to rescue rhythms in the heart (Guo *et al.*, 2005). These results suggest that the interaction between the SCN and heart is primarily through a neuronal mechanism rather than paracrine/humoral regulation. This idea was further supported by retrograde pseudorabies virus tracing, where injections of the virus into the right atrium labeled a multi-synaptic pathway to the SCN via the spinal cord and paraventricular nucleus (PVN) of the hypothalamus (Scheer *et al.*, 2001). This same neural pathway is broadly implicated in the circadian regulation of the autonomic nervous system (ANS; Teclemariam-Mesbah *et al.*, 1999; Larsen, 1999; Buijs *et al.*, 2003).

The ANS regulates cardiac function through the balance of the sympathetic pathway releasing norepinephrine/epinephrine (NE/E) and the parasympathetic release of acetylcholine (ACh). There is evidence implicating the ANS in the rhythmic regulation of HR but whether clock gene expression is also altered has yet to be determined. For example, the pharmacological blockade of peripheral NE in rats resulted in the dampening of circadian rhythms in HR (Warren *et al.*, 1994). However, a recent study found that oscillations of clock genes were preserved in the hearts of dopamine beta-hydroxylase knockout mice that cannot synthesize either NE or E (Reilly *et al.*, 2008). In culture, isoproterenol application boosts rhythms in Per2:LUC driven bioluminescence rhythms, but whether there is an effect on phase is unknown (Durgan *et al.*, 2005). The role of ACh and the parasympathetic branch in regulation of rhythms in heart rate or gene expression in the heart has not been studied in rodents. In

humans, there is indirect evidence that a daily rhythm in vagal cardiac tone is responsible for the rhythm in HR (Scheer *et al.*, 2004). The ANS also secretes neuropeptides, such as VIP and PACAP, onto the heart but the role of these peptides in the regulation of HR and gene expression are still unclear, but could potentially be factors relaying information from the SCN (Beaulieu & Lambert, 1998). It appears that a number of mechanisms are in place that regulates rhythms in peripheral tissues including the heart.

Vasoactive Intestinal Peptide critical for SCN function and potential mediator of circadian information to the periphery

VIP is expressed in a subset of SCN neurons called the ventro-lateral neurons. These neurons receive photic input and relay information to other parts of the SCN effectively synchronizing the rhythms among individual SCN neurons (Vosko *et al.*, 2007). The loss of VIP leads to reduced amplitude of population rhythms in clock gene expression (Loh *et al.*, 2011) as well as firing rate rhythms (Brown *et al.*, 2007) in the SCN. CCD camera imaging of *VIP*-/-; *Per2:luc* mice or MUA recording of VIP-/- mice identified that the reduced rhythms were due in part by reduced number of oscillating neurons but mostly there was a loss of population coherence and synchrony; thereby implicating VIP as a coupling agent (Aton *et al.*, 2005). Behaviorally, the loss of VIP results in the disruption of circadian rhythms in wheel running activity (Colwell *et al.*, 2003), as well as abnormal entrainment of metabolic rhythms (Bechtold *et al.*, 2008). These findings demonstrate the importance of VIP in the regulation of rhythms.

VIP is also expressed in SCN efferents projecting onto pre-autonomic neurons of the PVN (Teclemariam-Mesbah *et al.*, 1997) and is likely involved in the circadian regulation of autonomic processes such as HR (Kalsbeek *et al.*, 2006). VIP is also expressed in the

parasympathetic postganglion neurons that innervate the heart (Halimi *et al.*, 1997), suggesting that VIP may play a role in coupling the circadian system to the cardiovascular system, by regulating rhythms of autonomic function (as suggested by Kalsbeek *et al.*, 2006) or direct actions on the heart that couple independent cellular circadian oscillators (similar to its function in the SCN). Thus, VIP is a likely candidate to be involved in the circadian regulation of cardiovascular function.

Circadian Disruption and cardiovascular disease

According to the American Heart Association, cardiovascular disease (CVD) is the leading cause of death in the United States, surpassing other illnesses such as cancer, diabetes and respiratory diseases (AHA Statistical Fact Sheet 2007). The onset of cardiovascular events such as myocardial ischemia, infarctions, and arrhythmias cluster around the morning period suggesting influence by the circadian system (Muller *et al.*, 1985, 1989). Furthermore, the time of day at which cardiac injury occurs determines the extent of damage as well as patient prognosis. Disruptions of the circadian system such as shiftwork, is associated with increased incidence of cardiovascular disease and mortality (Knutsson *et al.*, 1986; Tüchsen, 1993). Patients with neurodegenerative diseases including Parkinson's disease and Huntington's disease exhibit abnormal cardiac function including the loss in the daily rhythm in cardiac output (e.g. Andrich *et al.*, 2002; Kobal *et al.*, 2004; Hawkes *et al.*, 2007; Bär *et al.*, 2008). This loss of rhythmicity is speculated to contribute to increased incidence of cardiovascular disease in these patient populations.

Work using animal models supports the view that circadian rhythmicity may be a critical aspect of cardiovascular health. Circadian perturbations have been shown to exacerbate heart

disease and decrease survival in cardiomyopathic hamsters (Penev *et al.*, 1998). Mice placed in normal 12:12 LD conditions that have undergone aortic banding, a model inducing cardiac hypertrophy and increased peripheral pressure, undergo normal remodeling of the heart (Martino *et al.*, 2007). In contrast, mice placed in 10:10LD conditions do not show signs of a remodeled heart and therefore the hearts are unable to compensate for the increased peripheral pressure, which decreases cardiac output. This cardiac remodeling is rescued when mice are returned to the normal 12:12LD condition. Another study, reported that heterozygous *tau* mutant hamsters (*tau*/+), that have a circadian period of approximately 22 hours, kept in a 14:10 LD cycle showed extensive cardiac pathology including hypertrophy and fibrosis (Martino *et al.*, 2008). When *tau*/+ mice were housed in a 12:10 LD cycle, a period consistent with their endogenous clock, assessment of cardiac tissue showed no cardiac pathology. These studies suggest that the interactions between circadian rhythms and cardiovascular function can impact cardiovascular disease progression and raise the possibility that disrupted circadian rhythms can cause cardiac dysfunction. Indeed, in many models of cardiovascular disease, alterations in circadian clocks have been demonstrated (Durgan & Young, 2010).

Dysynchrony appears to be the mechanism by which circadian dysfunction leads to cardiovascular disease. In healthy individuals, shear stress, or the force placed upon the lining of the blood vessels, brought on by activity and exercise during the active phase leads to physiological hypertrophy of the heart, which is a beneficial adaptive response of the cardiovascular system (Iemitsu *et al.*, 2001). However, shear stress at inappropriate times in the sleep phase, as is the case in individuals with non-dipping hypertension or shift work, tends to lead to pathological hypertrophy, which is a compensatory adaptation of the cardiovascular system to increased work load that often leads to heart failure (Iemitsu *et al.*, 2001; Durgan &

Young, 2010). It is hypothesized that the circadian system prepares the cardiovascular system to anticipate increased shear stress during the active phase. During the rest phase, the cardiovascular system may fail to provide the necessary components to appropriately respond to increased demand, which leads to pathological progression. In this example, dysfunction is caused by mismatches between the demand on the system and the ability of the system to respond. This appears to be the case during reentrainment to a new light/dark cycle, such as long distance travel, whereby the molecular clock within the heart and blood vessels take many more days to shift to a new LD cycle compared to blood pressure rhythms that take 1-2 days to adjust (Davidson *et al.*, 2008; Scheer *et al.*, 2009; Castillo *et al.*, 2011). The differences in the rate of reentrainment in the cells of the heart, endothelial cells and the rest of the cardiovascular system implies a mismatch or dysynchrony and could explain the increased incidence of cardiovascular disease observed in individuals that experience frequent jetlag or shiftwork. Another level of dysynchrony may be a result of mismatches in metabolism. Cardiovascular function is closely tied to metabolic processes in order to meet energy demands (Goodwin *et al.*, 1998; Neubauer, 2007). Imbalances in energy metabolism have negative consequences on cardiac function that could lead to disease (Neubauer, 2007). Recent research is demonstrating interactions of circadian and metabolic pathways (Young, 2006). For example, cardiac metabolic gene transcription, nonoxidative fatty acid and glucose metabolism display rhythms that are intrinsic in nature and driven by the molecular clock (Young *et al.*, 2001; Bray & Young, 2008). There are also feedback loops between circadian and metabolic genes indicating that they may regulate each other. CLOCK acetylates BMAL1 protein, which then induces SIRT1 deacetylase activity (Grimaldi *et al.*, 2009). SIRT1 has multiple targets and is involved in the regulation of oxidative metabolism, oxidative stress response as well as insulin signaling. SIRT1 also feeds back to the

molecular clock by deacetylating and altering BMAL1 function. This loop demonstrates the temporal regulation of SIRT1 activity that modulate rhythms in metabolic processes. Therefore, disruptions of the circadian system could tilt the supply and demand balance of metabolic reactions causing impaired cardiovascular function and lead to cardiovascular disease.

Circadian disruption and cardiovascular dysfunction in Huntington's Disease

Huntington's Disease is a progressive neurodegenerative disease characterized by movement abnormalities, emotional disturbances and cognitive impairment(Margolis & Ross, 2003). The disease is a result of an expansion of the CAG repeat in the huntingtin gene that when translated produces an elongated polyQ tract that promotes the aggregation of huntingtin protein and accumulation of nuclear inclusions that cause cellular dysfunction and cell death. While neuronal loss appears to be concentrated in the striatum, the huntingtin protein and aggregates are also expressed in most cells of the body.

In addition to the movement disorder associated with Huntington's Disease, patients also suffer from sleep disturbances that impair their quality of life (Chokroverty, 1996; Morton *et al.*, 2005; Hurelbrink *et al.*, 2005; Wulff *et al.*, 2010). HD patients experience sleep disturbances at night as well as an elongated sleep latency. This sleep behavior correlates with the delayed onset of diurnal melatonin observed in HD patients (Aziz *et al.*, 2009). These set of symptoms suggest possible circadian dysfunction, but it is unknown whether the disruption is within the SCN or due to the disruption of signals to peripheral outputs. In addition to the movement and sleep disorders, most HD patients develop cardiovascular disease that often leads to death; in fact cardiovascular disease is the second leading cause of death in this patient group(Chiu & Alexander, 1982; Lanska *et al.*, 1988). Possible mechanisms causing cardiovascular disease may

be through the dysregulation of the autonomic nervous system and possible local metabolic dysfunction in cardiomyocytes (Sharma *et al.*, 1999; Andrich *et al.*, 2002; Kobal *et al.*, 2004, 2010; Bär *et al.*, 2008; Aziz *et al.*, 2010*b*). While cellular dysfunction as a result of huntingtin protein may be the main culprit in disease progression, it is plausible that the concurrent disruption of the circadian system may be contributing to the development of symptoms and disease associated with HD including cardiovascular dysfunction.

In order to further study the mechanism of the dysfunction, mouse models of Huntington's Disease have been created. The R6/2 line is a well-studied model that recapitulates many of the human symptoms, including the disruptions in rest/activity cycles (Morton *et al.*, 2005). In support of circadian dysfunction as part of the disease etiology of HD, rhythms of clock genes within the SCN were disrupted. Furthermore, VIP and VIP receptor (VIPR2) expression in the biological clock of R6/2 mice are decreased (Fahrenkrug *et al.*, 2007) suggesting a mechanism for circadian disruption and dysregulation in rhythms of peripheral outputs including cardiovascular function. The R6/2 mice develop cardiac failure by 12 weeks of age and display mitochondrial alteration in cardiomyocytes indicating metabolic stress (Mihm *et al.*, 2007). The lifespan of these mice are approximately 3-4 months long, which is particularly aggressive when compared to the human disease progression. The fragile state of these mice makes long-term circadian investigations more difficult to pursue.

The BACHD mouse is another HD model of interest: a transgenic that expresses the expanded form of the human huntingtin gene (Gray *et al.*, 2008). Initial studies of the mouse model suggest parallels with the human disease such as huntingtin protein accumulations in the brain and classical progressive motor deficits. The longer life spans of these mice enables long-term studies of cardiovascular function to explore the extent of the circadian phenotype as well

as determine whether BACHD mice phenocopy the autonomic dysfunction and cardiovascular disease described in humans.

Entrainment of the Circadian System: Exercise as a Zeitgeber

Uncovering the mechanisms by which disruption of the circadian system contributes to disease progression is an important direction of study, just as it is important to develop methods to help improve or prevent disease progression. As mentioned above, disruptions of the circadian system and mismatches of the endogenous cycle with environmental cues of light and dark have been linked to increased incidence of disease. While disrupted rhythms may make cardiovascular disease worse, there are some indications that stabilizing rhythms may decrease risk for cardiovascular disease and improve recovery from injury. For example, patients in strong temporally structured environments have better prognosis for recovery from cardiovascular events (Guo & Stein, 2003).

Although light is the primary driver of the circadian system, under certain conditions such as aging and disease, light may not be sufficient to drive normal diurnal behaviors thereby affecting the quality of life in these individuals. There are other environmental cues in addition to light that have been shown to modulate the circadian system. Changes in metabolism appear to be a potent entrainer of rhythms. Scheduled feeding for example can drive feeding and activity behavior as well as alter molecular rhythms in several peripheral tissues (Hara *et al.*, 2001; Sheward *et al.*, 2007). This manipulation does not seem to shift rhythms in the SCN, except under conditions in which the SCN is in an already dysfunctional state, such as constant light (Nováková *et al.*, n.d.). Alternatively, on the demand side of metabolic processes, increased activity or exercise when timed at appropriate times of day may provide metabolic

cues to peripheral tissues and SCN, which could potentially drive rhythms of the circadian system. Timing of these metabolic events can be utilized to help realign and strengthen the relationship and interactions between the endogenous clock and the external environment, which could potentially deter or slow down disease progression attributed to circadian dysfunction.

There is evidence that stimulated activity and exercise in rodents and humans, respectively, alter the circadian system. In humans, exercise can shift the phase of the circadian clock depending on the time of exercise (Buxton *et al.*, 2003; Baehr *et al.*, 2003; Yamanaka *et al.*, 2006; Atkinson *et al.*, 2007). Although single bouts of exercise result in small shifts, multiple daily bouts may have additive effects (Barger *et al.*, 2004). In mice, stimulated activity or arousal cause greater shifts in the phase of the circadian system where some shifts are as large as those induced by light, suggesting that exercise maybe a powerful tool to alter rhythms(Reebs & Mrosovsky, 1989; Mrosovsky, 1996). The presence of the wheel can also alter the rate of reentrainment to an inversed LD cycle (Mrosovsky & Salmon, 1987; Dallmann & Mrosovsky, 2006; Castillo *et al.*, 2011). Wheel access provided in phase to the new LD cycle speeds up reentrainment while wheel access provided out of phase to the new LD cycle delays reentrainment. Lastly, stimulated activity has been shown to alter the SCN. Arousal at certain times of the day phase advances the molecular clock and firing rate of SCN neurons (Maywood *et al.*, 1999; Yannielli *et al.*, 2002). Measurements of both *in vivo* SCN firing rate and activity in the same animal suggest a direct relationship between the two factors, whereby activity leads to immediate decreases in firing rate activity in the SCN(Schaap & Meijer, 2001; Houben *et al.*, 2009). The ability of stimulated activity to influence the circadian clock makes it a potential tool to structure environmental input to the circadian system and stabilize rhythms.

Summary

In my studies, I examined various aspects of the circadian control of activity, cardiovascular and gene expression rhythms. In the BACHD disease model of HD that displays disruptions in their activity rhythms, we found that diurnal and circadian rhythms of physiological outputs such as body temperature and HR were also altered. Furthermore, Heart Rate Variability and baroreceptor function measurements indicated that the activity and rhythms of the ANS are disrupted, which could be a possible mechanism that alters HR as well as lead to the development of cardiovascular disease in the patient group. Because VIP is critical for normal circadian rhythms in activity and the R6/2 HD model display decreased expression of VIP and VIPR2 in the SCN (Fahrenkrug *et al.*, 2007), I also explored the circadian phenotype of the cardiovascular system in VIP-deficient mice. VIP-deficient mice display significant disruptions in HR and body temperature rhythms under both LD and DD conditions, indicating the importance of this neuropeptide in the regulation of physiological rhythms that include HR. Lastly, using scheduled exercise, I was able to alter and reorganize rhythms of behavior, physiology and gene expression in WT mice. When applied to VIP-deficient mice, the temporal structuring of exercise rescued several circadian parameters, suggesting that exercise may be used as a tool to improve and maybe even rescue a disrupted circadian system.

ii. Bibliography

Abe K, Kroning J, Greer MA & Critchlow V (1979). Effects of Destruction of the Suprachiasmatic Nuclei on the Circadian Rhythms in Plasma Corticosterone, Body Temperature, Feeding and Plasma Thyrotropin. *Neuroendocrinology* **29,** 119–131.

Abe M, Herzog ED, Yamazaki S, Straume M, Tei H, Sakaki Y, Menaker M & Block GD (2002). Circadian rhythms in isolated brain regions. *J Neurosci* **22,** 350–356.

Andrich J, Schmitz T, Saft C, Postert T, Kraus P, Epplen JT, Przuntek H & Agelink MW (2002). Autonomic nervous system function in Huntington's disease. *J Neurol Neurosurg Psychiatr* **72,** 726–731.

Atkinson G, Edwards B, Reilly T & Waterhouse J (2007). Exercise as a synchroniser of human circadian rhythms: an update and discussion of the methodological problems. *Eur J Appl Physiol* **99,** 331–341.

Aton SJ, Colwell CS, Harmar AJ, Waschek J & Herzog ED (2005). Vasoactive intestinal polypeptide mediates circadian rhythmicity and synchrony in mammalian clock neurons. *Nat Neurosci* **8,** 476–483.

Aziz NA, Anguelova GV, Marinus J, Lammers GJ & Roos RAC (2010). Sleep and circadian rhythm alterations correlate with depression and cognitive impairment in Huntington's disease. *Parkinsonism & Related Disorders* **16,** 345–350.

Aziz NA, Pijl H, Frölich M, Schröder-van der Elst JP, van der Bent C, Roelfsema F & Roos RAC (2009). Delayed onset of the diurnal melatonin rise in patients with Huntington's disease. *J Neurol* **256,** 1961–1965.

Bae K, Jin X, Maywood ES, Hastings MH, Reppert SM & Weaver DR (2001). Differential functions of mPer1, mPer2, and mPer3 in the SCN circadian clock. *Neuron* **30,** 525–536.

Baehr EK, Eastman CI, Revelle W, Olson SHL, Wolfe LF & Zee PC (2003). Circadian phase-shifting effects of nocturnal exercise in older compared with young adults. *Am J Physiol Regul Integr Comp Physiol* **284,** R1542–1550.

Balsalobre A, Brown SA, Marcacci L, Tronche F, Kellendonk C, Reichardt HM, Schütz G & Schibler U (2000). Resetting of circadian time in peripheral tissues by glucocorticoid signaling. *Science* **289,** 2344–2347.

Bär KJ, Boettger MK, Andrich J, Epplen JT, Fischer F, Cordes J, Koschke M & Agelink MW (2008). Cardiovagal modulation upon postural change is altered in Huntington's disease. *Eur J Neurol* **15,** 869–871.

Barger LK, Wright KP, Hughes RJ & Czeisler CA (2004). Daily exercise facilitates phase delays of circadian melatonin rhythm in very dim light. *American Journal of Physiology - Regulatory, Integrative and Comparative Physiology* **286,** R1077 –R1084.

Beaulieu P & Lambert C (1998). Peptidic regulation of heart rate and interactions with the autonomic nervous system. *Cardiovasc Res* **37,** 578–585.

Bechtold DA, Brown TM, Luckman SM & Piggins HD (2008). Metabolic rhythm abnormalities in mice lacking VIP-VPAC2 signaling. *Am J Physiol Regul Integr Comp Physiol* **294,** R344–351.

Bray MS, Shaw CA, Moore MWS, Garcia RAP, Zanquetta MM, Durgan DJ, Jeong WJ, Tsai J-Y, Bugger H, Zhang D, Rohrwasser A, Rennison JH, Dyck JRB, Litwin SE, Hardin PE, Chow C-W, Chandler MP, Abel ED & Young ME (2008). Disruption of the circadian clock within the cardiomyocyte influences myocardial contractile function, metabolism, and gene expression. *Am J Physiol Heart Circ Physiol* **294,** H1036–1047.

Bray MS & Young ME (2008). Diurnal variations in myocardial metabolism. *Cardiovasc Res* **79,** 228–237.

Brown TM, Colwell CS, Waschek JA & Piggins HD (2007). Disrupted neuronal activity rhythms in the suprachiasmatic nuclei of vasoactive intestinal polypeptide-deficient mice. *J Neurophysiol* **97,** 2553–2558.

Buijs RM, la Fleur SE, Wortel J, Van Heyningen C, Zuiddam L, Mettenleiter TC, Kalsbeek A, Nagai K & Niijima A (2003). The suprachiasmatic nucleus balances sympathetic and parasympathetic output to peripheral organs through separate preautonomic neurons. *J Comp Neurol* **464,** 36–48.

Buxton OM, Lee CW, L'Hermite-Baleriaux M, Turek FW & Van Cauter E (2003). Exercise elicits phase shifts and acute alterations of melatonin that vary with circadian phase. *Am J Physiol Regul Integr Comp Physiol* **284,** R714–724.

Castillo C, Molyneux P, Carlson R & Harrington ME (2011). Restricted wheel access following a light cycle inversion slows re-entrainment without internal desynchrony as measured in Per2Luc mice. *Neuroscience* **182,** 169–176.

Chiu E & Alexander L (1982). Causes of death in Huntington's disease. *Med J Aust* **1,** 153.

Chokroverty S (1996). Sleep and degenerative neurologic disorders. *Neurol Clin* **14,** 807–826.

Colwell CS (2011). Linking neural activity and molecular oscillations in the SCN. *Nature Reviews Neuroscience* **12,** 553–569.

Colwell CS, Michel S, Itri J, Rodriguez W, Tam J, Lelievre V, Hu Z, Liu X & Waschek JA (2003). Disrupted circadian rhythms in VIP- and PHI-deficient mice. *Am J Physiol Regul Integr Comp Physiol* **285,** R939–949.

Dallmann R & Mrosovsky N (2006). Scheduled wheel access during daytime: A method for studying conflicting zeitgebers. *Physiol Behav* **88,** 459–465.

Davidson AJ, London B, Block GD & Menaker M (2005). Cardiovascular tissues contain independent circadian clocks. *Clin Exp Hypertens* **27,** 307–311.

Davidson AJ, Yamazaki S, Arble DM, Menaker M & Block GD (2008). Resetting of central and peripheral circadian oscillators in aged rats. *Neurobiology of Aging* **29,** 471–477.

Dibner C, Schibler U & Albrecht U (2010). The mammalian circadian timing system: organization and coordination of central and peripheral clocks. *Annu Rev Physiol* **72,** 517–549.

Durgan DJ, Hotze MA, Tomlin TM, Egbejimi O, Graveleau C, Abel ED, Shaw CA, Bray MS, Hardin PE & Young ME (2005). The intrinsic circadian clock within the cardiomyocyte. *Am J Physiol Heart Circ Physiol* **289,** H1530–1541.

Durgan DJ & Young ME (2010). The cardiomyocyte circadian clock: emerging roles in health and disease. *Circ Res* **106,** 647–658.

Fahrenkrug J, Popovic N, Georg B, Brundin P & Hannibal J (2007). Decreased VIP and VPAC2 receptor expression in the biological clock of the R6/2 Huntington's disease mouse. *J Mol Neurosci* **31,** 139–148.

Goodwin GW, Taylor CS & Taegtmeyer H (1998). Regulation of energy metabolism of the heart during acute increase in heart work. *J Biol Chem* **273,** 29530–29539.

Gooley JJ, Lu J, Chou TC, Scammell TE & Saper CB (2001). Melanopsin in cells of origin of the retinohypothalamic tract. *Nat Neurosci* **4,** 1165.

Gray M, Shirasaki DI, Cepeda C, André VM, Wilburn B, Lu X-H, Tao J, Yamazaki I, Li S-H, Sun YE, Li X-J, Levine MS & Yang XW (2008). Full-length human mutant huntingtin with a stable polyglutamine repeat can elicit progressive and selective neuropathogenesis in BACHD mice. *J Neurosci* **28,** 6182–6195.

Grimaldi B, Nakahata Y, Kaluzova M, Masubuchi S & Sassone-Corsi P (2009). Chromatin remodeling, metabolism and circadian clocks: the interplay of CLOCK and SIRT1. *Int J Biochem Cell Biol* **41,** 81–86.

Güler AD, Altimus CM, Ecker JL & Hattar S (2007). Multiple photoreceptors contribute to nonimage-forming visual functions predominantly through melanopsin-containing retinal ganglion cells. *Cold Spring Harb Symp Quant Biol* **72,** 509–515.

Guo H, Brewer JM, Champhekar A, Harris RBS & Bittman EL (2005). Differential control of peripheral circadian rhythms by suprachiasmatic-dependent neural signals. *Proc Natl Acad Sci USA* **102,** 3111–3116.

Guo H, Guo H, Brewer JM, Lehman MN & Bittman EL (2006). Suprachiasmatic regulation of circadian rhythms of gene expression in hamster peripheral organs: effects of transplanting the pacemaker. *J Neurosci* **26,** 6406–6412.

Guo Y-F & Stein PK (2003). Circadian rhythm in the cardiovascular system: chronocardiology. *Am Heart J* **145,** 779–786.

Halimi F, Piot O, Guize L & Le Heuzey JY (1997). Electrophysiological effects of vasoactive intestinal peptide in rabbit atrium: a modulation of acetylcholine activity. *J Mol Cell Cardiol* **29,** 37–44.

Hara R, Wan K, Wakamatsu H, Aida R, Moriya T, Akiyama M & Shibata S (2001). Restricted feeding entrains liver clock without participation of the suprachiasmatic nucleus. *Genes Cells* **6,** 269–278.

Hastings MH, Reddy AB & Maywood ES (2003). A clockwork web: circadian timing in brain and periphery, in health and disease. *Nat Rev Neurosci* **4,** 649–661.

Hawkes CH, Del Tredici K & Braak H (2007). Parkinson's disease: a dual-hit hypothesis. *Neuropathol Appl Neurobiol* **33,** 599–614.

Houben T, Deboer T, van Oosterhout F & Meijer JH (2009). Correlation with behavioral activity and rest implies circadian regulation by SCN neuronal activity levels. *J Biol Rhythms* **24,** 477–487.

Hu K, Ivanov PC, Hilton MF, Chen Z, Ayers RT, Stanley HE & Shea SA (2004). Endogenous circadian rhythm in an index of cardiac vulnerability independent of changes in behavior. *Proc Natl Acad Sci USA* **101,** 18223–18227.

Hurelbrink CB, Lewis SJG & Barker RA (2005). The use of the Actiwatch-Neurologica system to objectively assess the involuntary movements and sleep-wake activity in patients with mild-moderate Huntington's disease. *J Neurol* **252,** 642–647.

Iemitsu M, Miyauchi T, Maeda S, Sakai S, Kobayashi T, Fujii N, Miyazaki H, Matsuda M & Yamaguchi I (2001). Physiological and Pathological Cardiac Hypertrophy Induce Different Molecular Phenotypes in the Rat. *Am J Physiol Regul Integr Comp Physiol* **281,** R2029–R2036.

Ikeda H, Yong Q, Kurose T, Todo T, Mizunoya W, Fushiki T, Seino Y & Yamada Y (2007). Clock gene defect disrupts light-dependency of autonomic nerve activity. *Biochem Biophys Res Commun* **364,** 457–463.

Jeyaraj D *et al.* (2012). Circadian rhythms govern cardiac repolarization and arrhythmogenesis. *Nature* **483,** 96–99.

Kalsbeek A, Palm IF, La Fleur SE, Scheer FAJL, Perreau-Lenz S, Ruiter M, Kreier F, Cailotto C & Buijs RM (2006). SCN outputs and the hypothalamic balance of life. *J Biol Rhythms* **21,** 458–469.

Knutsson A, Akerstedt T, Jonsson BG & Orth-Gomer K (1986). Increased risk of ischaemic heart disease in shift workers. *Lancet* **2,** 89–92.

Ko CH & Takahashi JS (2006). Molecular components of the mammalian circadian clock. *Hum Mol Genet* **15 Spec No 2,** R271–277.

Ko ML, Shi L, Tsai J-Y, Young ME, Neuendorff N, Earnest DJ & Ko GY-P (2011). Cardiac-Specific Mutation of Clock Alters the Quantitative Measurements of Physical Activities without Changing Behavioral Circadian Rhythms. *J Biol Rhythms* **26,** 412–422.

Kobal J, Meglic B, Mesec A & Peterlin B (2004). Early sympathetic hyperactivity in Huntington's disease. *Eur J Neurol* **11,** 842–848.

Kobal J, Melik Z, Cankar K, Bajrovic FF, Meglic B, Peterlin B & Zaletel M (2010). Autonomic dysfunction in presymptomatic and early symptomatic Huntington's disease. *Acta Neurol Scand* **121,** 392–399.

Kuhlman SJ & McMahon DG (2006). Encoding the ins and outs of circadian pacemaking. *J Biol Rhythms* **21,** 470–481.

Lanska DJ, Lanska MJ, Lavine L & Schoenberg BS (1988). Conditions associated with Huntington's disease at death. A case-control study. *Arch Neurol* **45,** 878–880.

Larsen PJ (1999). Tracing autonomic innervation of the rat pineal gland using viral transneuronal tracing. *Microsc Res Tech* **46,** 296–304.

Lehman MN, Silver R, Gladstone WR, Kahn RM, Gibson M & Bittman EL (1987). Circadian rhythmicity restored by neural transplant. Immunocytochemical characterization of the graft and its integration with the host brain. *J Neurosci* **7,** 1626–1638.

Loh DH, Dragich JM, Kudo T, Schroeder AM, Nakamura TJ, Waschek JA, Block GD & Colwell CS (2011). Effects of vasoactive intestinal peptide genotype on circadian gene expression in the suprachiasmatic nucleus and peripheral organs. *J Biol Rhythms* **26,** 200–209.

Margolis RL & Ross CA (2003). Diagnosis of Huntington disease. *Clin Chem* **49,** 1726–1732.

Martino T, Arab S, Straume M, Belsham DD, Tata N, Cai F, Liu P, Trivieri M, Ralph M & Sole MJ (2004). Day/night rhythms in gene expression of the normal murine heart. *J Mol Med* **82,** 256–264.

Martino TA, Oudit GY, Herzenberg AM, Tata N, Koletar MM, Kabir GM, Belsham DD, Backx PH, Ralph MR & Sole MJ (2008). Circadian rhythm disorganization produces profound cardiovascular and renal disease in hamsters. *Am J Physiol Regul Integr Comp Physiol* **294,** R1675–1683.

Martino TA, Tata N, Belsham DD, Chalmers J, Straume M, Lee P, Pribiag H, Khaper N, Liu PP, Dawood F, Backx PH, Ralph MR & Sole MJ (2007). Disturbed diurnal rhythm alters gene expression and exacerbates cardiovascular disease with rescue by resynchronization. *Hypertension* **49,** 1104–1113.

Maywood ES, Mrosovsky N, Field MD & Hastings MH (1999). Rapid down-regulation of mammalian period genes during behavioral resetting of the circadian clock. *Proc Natl Acad Sci USA* **96,** 15211–15216.

Mihm MJ, Amann DM, Schanbacher BL, Altschuld RA, Bauer JA & Hoyt KR (2007). Cardiac dysfunction in the R6/2 mouse model of Huntington's disease. *Neurobiol Dis* **25,** 297–308.

Moga MM & Moore RY (1997). Organization of neural inputs to the suprachiasmatic nucleus in the rat. *J Comp Neurol* **389,** 508–534.

Moore RY & Eichler VB (1972). Loss of a circadian adrenal corticosterone rhythm following suprachiasmatic lesions in the rat. *Brain Res* **42,** 201–206.

Morton AJ, Wood NI, Hastings MH, Hurelbrink C, Barker RA & Maywood ES (2005). Disintegration of the Sleep-Wake Cycle and Circadian Timing in Huntington's Disease. *J Neurosci* **25,** 157–163.

Mrosovsky N (1996). Locomotor Activity and Non‐photic Influences on Circadian Clocks. *Biological Reviews* **71,** 343–372.

Mrosovsky N & Salmon PA (1987). A behavioural method for accelerating re-entrainment of rhythms to new light|[mdash]|dark cycles. *, Published online: 26 November 1987; | doi:101038/330372a0* **330,** 372–373.

Muller JE, Stone PH, Turi ZG, Rutherford JD, Czeisler CA, Parker C, Poole WK, Passamani E, Roberts R & Robertson T (1985). Circadian variation in the frequency of onset of acute myocardial infarction. *N Engl J Med* **313,** 1315–1322.

Muller JE, Tofler GH & Edelman E (1989). Probable triggers of onset of acute myocardial infarction. *Clin Cardiol* **12,** 473–475.

Neubauer S (2007). The failing heart--an engine out of fuel. *N Engl J Med* **356,** 1140–1151.

Nováková M, Polidarová L, Sládek M & Sumová A (n.d.). Restricted feeding regime affects clock gene expression profiles in the suprachiasmatic nucleus of rats exposed to constant light. *Neuroscience*; DOI: 10.1016/j.neuroscience.2011.09.028.

Oishi K, Sakamoto K, Okada T, Nagase T & Ishida N (1998). Antiphase circadian expression between BMAL1 and period homologue mRNA in the suprachiasmatic nucleus and peripheral tissues of rats. *Biochem Biophys Res Commun* **253,** 199–203.

Penev PD, Kolker DE, Zee PC & Turek FW (1998). Chronic circadian desynchronization decreases the survival of animals with cardiomyopathic heart disease. *Am J Physiol* **275,** H2334–2337.

Reebs SG & Mrosovsky N (1989). Effects of induced wheel running on the circadian activity rhythms of Syrian hamsters: entrainment and phase response curve. *J Biol Rhythms* **4,** 39–48.

Reilly DF, Curtis AM, Cheng Y, Westgate EJ, Rudic RD, Paschos G, Morris J, Ouyang M, Thomas SA & FitzGerald GA (2008). Peripheral circadian clock rhythmicity is retained in the absence of adrenergic signaling. *Arterioscler Thromb Vasc Biol* **28,** 121–126.

Rudic RD, McNamara P, Reilly D, Grosser T, Curtis A-M, Price TS, Panda S, Hogenesch JB & FitzGerald GA (2005). Bioinformatic analysis of circadian gene oscillation in mouse aorta. *Circulation* **112,** 2716–2724.

Sakamoto K & Ishida N (2000). Light-induced phase-shifts in the circadian expression rhythm of mammalian period genes in the mouse heart. *Eur J Neurosci* **12,** 4003–4006.

Sano H, Hayashi H, Makino M, Takezawa H, Hirai M, Saito H & Ebihara S (1995). Effects of suprachiasmatic lesions on circadian rhythms of blood pressure, heart rate and locomotor activity in the rat. *Jpn Circ J* **59,** 565–573.

Schaap J & Meijer JH (2001). Opposing effects of behavioural activity and light on neurons of the suprachiasmatic nucleus. *Eur J Neurosci* **13,** 1955–1962.

Scheer FA, Ter Horst GJ, van Der Vliet J & Buijs RM (2001). Physiological and anatomic evidence for regulation of the heart by suprachiasmatic nucleus in rats. *Am J Physiol Heart Circ Physiol* **280,** H1391–1399.

Scheer FAJL, Van Doornen LJP & Buijs RM (2004). Light and diurnal cycle affect autonomic cardiac balance in human; possible role for the biological clock. *Auton Neurosci* **110,** 44–48.

Scheer FAJL, Hilton MF, Mantzoros CS & Shea SA (2009). Adverse metabolic and cardiovascular consequences of circadian misalignment. *Proc Natl Acad Sci USA* **106,** 4453–4458.

Sei H, Oishi K, Chikahisa S, Kitaoka K, Takeda E & Ishida N (2008). Diurnal amplitudes of arterial pressure and heart rate are dampened in Clock mutant mice and adrenalectomized mice. *Endocrinology* **149,** 3576–3580.

Sharma KR, Romano JG, Ayyar DR, Rotta FT, Facca A & Sanchez-Ramos J (1999). Sympathetic skin response and heart rate variability in patients with Huntington disease. *Arch Neurol* **56,** 1248–1252.

Sheward WJ, Maywood ES, French KL, Horn JM, Hastings MH, Seckl JR, Holmes MC & Harmar AJ (2007). Entrainment to feeding but not to light: circadian phenotype of VPAC2 receptor-null mice. *J Neurosci* **27,** 4351–4358.

Stephan FK & Zucker I (1972). Circadian rhythms in drinking behavior and locomotor activity of rats are eliminated by hypothalamic lesions. *Proc Natl Acad Sci USA* **69,** 1583–1586.

Storch K-F, Lipan O, Leykin I, Viswanathan N, Davis FC, Wong WH & Weitz CJ (2002). Extensive and divergent circadian gene expression in liver and heart. *Nature* **417,** 78–83.

Takahashi JS, Hong H-K, Ko CH & McDearmon EL (2008). The genetics of mammalian circadian order and disorder: implications for physiology and disease. *Nat Rev Genet* **9,** 764–775.

Teclemariam-Mesbah R, Kalsbeek A, Pevet P & Buijs RM (1997). Direct vasoactive intestinal polypeptide-containing projection from the suprachiasmatic nucleus to spinal projecting hypothalamic paraventricular neurons. *Brain Res* **748,** 71–76.

Teclemariam-Mesbah R, Ter Horst GJ, Postema F, Wortel J & Buijs RM (1999). Anatomical demonstration of the suprachiasmatic nucleus-pineal pathway. *J Comp Neurol* **406,** 171–182.

Tüchsen F (1993). Working hours and ischaemic heart disease in Danish men: a 4-year cohort study of hospitalization. *Int J Epidemiol* **22,** 215–221.

Vosko AM, Schroeder A, Loh DH & Colwell CS (2007). Vasoactive intestinal peptide and the mammalian circadian system. *Gen Comp Endocrinol* **152,** 165–175.

Vukolic A, Antic V, Van Vliet BN, Yang Z, Albrecht U & Montani J-P (2010). Role of mutation of the circadian clock gene Per2 in cardiovascular circadian rhythms. *Am J Physiol Regul Integr Comp Physiol* **298,** R627–634.

Wang Q, Maillard M, Schibler U, Burnier M & Gachon F (2010). Cardiac hypertrophy, low blood pressure, and low aldosterone levels in mice devoid of the three circadian PAR bZip transcription factors DBP, HLF, and TEF. *Am J Physiol Regul Integr Comp Physiol* **299,** R1013–1019.

Warren WS, Champney TH & Cassone VM (1994). The suprachiasmatic nucleus controls the circadian rhythm of heart rate via the sympathetic nervous system. *Physiol Behav* **55,** 1091–1099.

Wu X, Liu Z, Shi G, Xing L, Wang X, Gu X, Qu Z, Dong Z, Xiong J, Gao X, Zhang C & Xu Y (2011). The circadian clock influences heart performance. *J Biol Rhythms* **26,** 402–411.

Wulff K, Gatti S, Wettstein JG & Foster RG (2010). Sleep and circadian rhythm disruption in psychiatric and neurodegenerative disease. *Nature Reviews Neuroscience* **11,** 589–599.

Yamanaka Y, Honma K, Hashimoto S, Takasu N, Miyazaki T & Honma S (2006). Effects of physical exercise on human circadian rhythms. *Sleep and Biological Rhythms* **4,** 199–206.

Yamashita T, Sekiguchi A, Iwasaki Y, Sagara K, Iinuma H, Hatano S, Fu L-T & Watanabe H (2003). Circadian variation of cardiac K+ channel gene expression. *Circulation* **107,** 1917–1922.

Yamazaki S, Numano R, Abe M, Hida A, Takahashi R-I, Ueda M, Block GD, Sakaki Y, Menaker M & Tei H (2000). Resetting Central and Peripheral Circadian Oscillators in Transgenic Rats. *Science* **288,** 682–685.

Yannielli PC, McKinley Brewer J & Harrington ME (2002). Is novel wheel inhibition of per1 and per2 expression linked to phase shift occurrence? *Neuroscience* **112,** 677–685.

Yoo S-H, Yamazaki S, Lowrey PL, Shimomura K, Ko CH, Buhr ED, Siepka SM, Hong H-K, Oh WJ, Yoo OJ, Menaker M & Takahashi JS (2004). PERIOD2::LUCIFERASE real-time reporting of circadian dynamics reveals persistent circadian oscillations in mouse peripheral tissues. *Proc Natl Acad Sci USA* **101,** 5339–5346.

Young ME (2006). The circadian clock within the heart: potential influence on myocardial gene expression, metabolism, and function. *Am J Physiol Heart Circ Physiol* **290,** H1–16.

Young ME, Razeghi P, Cedars AM, Guthrie PH & Taegtmeyer H (2001). Intrinsic diurnal variations in cardiac metabolism and contractile function. *Circ Res* **89,** 1199–1208.

CHAPTER 2

i. Introduction

The published paper entitled "Dysfunctions in circadian behavior and physiology in mouse models of Huntington's disease" by Kudo et al. 2011, contains my work examining daily and circadian rhythms of heart rate, heart rate variability, body temperature as well as ECG parameters in BACHD mice. All these circadian regulated outputs were disrupted in BACHD mice. Heart rate variability measurements indicated that BACHD mice had a dysfunctional autonomic nervous system.

The published paper entitled "Baroreceptor reflex dysfunction in the BACHD mouse model of Huntington's disease" by Schroeder et al. 2011, contains results from follow-up examination of the cardiovascular phenotype in BACHD mice. Measurement of BP in mildly anesthetized BACHD mice during the light phase suggests these mice have significantly increased blood pressure. The baroreceptor responses to pressor and vasoactive drugs were blunted in BACHD mice. We also detected increased heart weight/tibia length ratios in BACHD mice suggesting cardiac remodeling however, echocardiography found no significant differences in heart function in BACHD mice.

ii. Dysfunctions in Circadian Behavior and Physiology in Mouse Models of Huntington's Disease.

Abstract

Many patients with Huntington's disease (HD) exhibit disturbances in their daily cycle of sleep and wake as part of their symptoms. These patients have difficulty sleeping at night and staying awake during the day, which has a profound impact on the quality of life of the patients and their care-givers. In the present study, we examined diurnal and circadian rhythms of four models of HD including the BACHD, CAG 140 knock-in and R6/2 CAG 140 and R6/2 CAG 250 lines of mice. The BACHD and both R6/2 lines showed profound circadian phenotypes as measured by wheel-running activity. Focusing on the BACHD line for further analysis, the amplitude of the rhythms in the BACHD mice declined progressively with age. In addition, the circadian regulation of heart rate and body temperature in freely behaving BACHD mice were also disrupted. Furthermore, the distribution of sleep as well as the autonomic regulation of heart rate was disrupted in this HD model. To better understand the mechanistic underpinnings of the circadian disruption, we used electrophysiological tools to record from neurons within the central clock in the suprachiasmatic nucleus (SCN). The BACHD mice exhibit reduced rhythms in spontaneous electrical activity in SCN neurons. Interestingly, the expression of the clock gene PERIOD2 was not altered in the SCN of the BACHD line. Together, this data is consistent with the hypothesis that the HD mutations interfere with the expression of robust circadian rhythms in behavior and physiology. The data raise the possibility that the electrical activity within the central clock itself may be altered in this disease.

Introduction

Many patients with Huntington's disease (HD) exhibit disturbances in their daily cycle of sleep and wake as part of their symptoms. These patients have difficulty sleeping at night and staying awake during the day. This dysfunction in timing may not be causal to their disorder, yet these symptoms have a major impact on the quality of life of the patient population and on the family members who care for the HD patients. Previous work has found that a mouse model of HD (R6/2 CAG 245) exhibits a progressive breakdown of their circadian rest/ activity cycle that mimics the condition of human patients typified by: loss of consolidated sleep, increased wakeful activity during the sleep phase, and greater sleep during the active, waking phase (Morton *et al.*, 2005; Pallier *et al.*, 2007). This behavioral impairment in the mice is accompanied by disordered expression of circadian clock genes *in vivo* in the master circadian pacemaker in the hypothalamus: the suprachiasmatic nucleus (SCN), and in the motor control regions of the brain, including the striatum. Importantly, the use of hypnotics or scheduled feeding can improve the performance of the R6/2 mice (Pallier *et al.*, 2007; Maywood *et al.*, 2010). This work raises the possibility that targeted interventions to improve daily rhythms in patients may improve clinical symptoms of HD. HD is caused by an expanded CAG repeat in the huntingtin (HTT) protein (The Huntington's Disease Collaborative Research Group, 1993). There are 3 general types of mouse models of HD, including transgenic mice expressing the entire human *HTT* gene with 97 mixed CAA-CAG repeats (BACHD), as well as models expressing the first exon of the *HTT* gene with varying lengths of the CAG repeats (R6/2). Finally, there are knock-in mice generated by inserting a 140 CAG repeat expansion into the mouse *Htt* gene (CAG 140 knock-in). No single mouse model can be expected to recapitulate all aspects of the human disease, and we

hence felt that it was important to explore possible circadian dysfunction in different mouse models of HD.

In the present study, we first sought to determine whether circadian rhythms in wheel running activity are disrupted in four mouse models of HD: BACHD (Gray *et al.*, 2008), CAG 140 knock-in (Menalled *et al.*, 2009), R6/2 with 140 CAG repeats, and R6/2 with 250 CAG repeats (Mangiarini *et al.*, 1996) lines of mice. These mouse lines were screened by monitoring daily rhythms of wheel-running activity. This simple and automated assay is the method of choice for screening mutations that influence the circadian system of mammals. Due to the relatively short lifespan of the two R6/2 lines, we focused on the BACHD line for further long-term analysis using radiotelemetry in order to examine rhythms in heart rate and body temperature from freely behaving mice. We also specifically evaluated the possibility of alterations in autonomic regulation of heart rate in the BACHD model. Next, we sought to determine whether the BACHD mice exhibit reduced rhythms in spontaneous electrical firing in the SCN. Finally, we examined the daily rhythms of clock gene expression in the SCN of the BACHD mice. Together, these experiments examine the impact of the mutations causing HD on circadian behavior and provide the beginnings of a mechanistic understanding of how the HD mutation alters the physiological properties of the circadian timing system.

Material and methods

Animals

The experimental protocols used in this study were approved by the UCLA Animal Research Committee and all recommendations for animal use and welfare, as dictated by the

UCLA Division of Laboratory Animals and the guidelines from the National Institutes of Health, were followed. We used four lines of mice in this study: BACHD on the C57BL6/J background(Gray *et al.*, 2008), CAG 140 knock-in (KI) originally on a C57BL/6J x 129/Sv background, now N2-N3 on the C57BL/6J background (Hickey *et al.*, 2008; Menalled *et al.*, 2009), and the R6/2 CAG 140 and R6/2 CAG 250 on the C57BL/6J background (Mangiarini *et al.*, 1996). The transgene insertion site for the R6/2 and BACHD lines have not been characterized, and potential positional effects cannot currently be ruled out. The BACHD and both R6/2 lines were fully backcrossed into the C57BL/6J strain. Mutants and littermate wild-type (WT) controls were obtained from the mouse mutant resource at JAX (The Jackson Laboratory, Bar Harbor, Maine) in a colony maintained by the CHDI Foundation. For each line, we studied littermate mutants and WT controls in parallel. Genotype was determined at 15 days of age by PCR of tail snips. For the R6/2 and CAG 140 KI lines, the CAG repeat lengths were measured by Laragen (Los Angeles, CA). The mice were inspected daily for signs of ill health and euthanized if necessary.

Behavioral analysis

Methods employed were similar to those described previously (Colwell *et al.*, 2003, 2004). Male mice, at least 1 month (mo) of age, were housed individually and their wheel-running activity recorded as revolutions (rev) per 3 min interval. The running wheels and data acquisition system were obtained from Mini Mitter Co. (Bend, OR). The animals were exposed to a 12:12 light-dark cycle (LD; light intensity 300 Lux) for two weeks. For some mice, the LD cycle was shifted 6 hrs earlier or 6 hrs later and the number of cycle required for re-

synchronization measured. The animals were then placed into constant darkness (DD) to assess their free-running activity pattern. The locomotor activity rhythms of mice were analyzed by periodogram analysis combined with the χ^2 test with $P = 0.05$ significance level (El Temps, Barcelona, Spain) on the raw data. The periodogram shows the amplitude (referred to as "power") of periodicities in the time series for all periods of interest (between 20 and 31 h in 3 min steps). The power values were normalized to the percentage of variance derived from the Qp values of the periodogram (Qp x 100/N; N = total number of data points) according to the calculated $P = 0.05$ significance level. Slopes of an eye-fitted line through the onsets were also used to confirm period estimates made with the periodogram analysis. The average pattern of activity (i.e. the waveform estimate) was also determined at modulo-period for each animal in DD for 15 cycles. Some mice in DD were exposed to a brief light treatment at circadian time (CT) 16 with CT 12 defined by the locomotor activity onset. Following each treatment, the animals were allowed to free-run undisturbed in DD for 14 days. The light stimulus that was used to induce phase shifts was an exposure to white light (100 Lux, 10 min). Phase shifts in the activity rhythm were determined by measuring the phase difference between eye-fitted lines connecting the onset of activity for a period of 10 days before and 10 days after an experimental manipulation. Measurements were made by investigators "blind" to the experimental group. In order to estimate the steady state phase delays produced, one day of data after treatments were excluded from the analysis. Stimulus intensity (Lux) was measured with a light meter (BK precision, Yorba Linda, CA). All handling of animals was carried out either in the light portion of the LD cycle or in DD with the aid of night vision goggles (FJW Industries, Palatine, IL).

Sleep measurements

BACHD mutants and their WT littermates were first entrained to a 12:12 LD cycle for at least 2 weeks. The mice were housed individually in the absence of wheels and recorded using a video surveillance camera system (Gadspot, GS-335C, City of Industry, CA). The sleep state is marked by several easily observed behaviors, including adoption of a species-specific sleep posture with the eyes closed (Campbell and Tobler, 1984). We scored a mouse as being asleep only when its eyes were closed as it lay on its side, or if it was curled up with its head tucked into its body, or if the mouse did not make any movements other than brief transitional changes in posture for durations of at least 40 sec. We and others have previously employed this method to determine the basic temporal distribution of behavioral sleep across a 24-h period (Schwartz & Smale, 2005; Pack *et al.*, 2007; Loh *et al.*, 2010). Sleep/wake behavior was scored visually in 5 min intervals, which were summed and averaged to determine day and night percentages of time spent in sleep. Consolidation was determined by counting the number of consecutive bins of sleep that exceeded 20 min in duration.

Telemetry Measurements

Methods employed were similar to those described previously (Schroeder, et al., 2010). WT and BACHD mice (4-5 mo) were surgically implanted with a wireless radio-frequency transmitter (ETA-F20, Data Sciences International, St. Paul, MN). Mice were housed in individual cages in the absence of a running wheel. Cages were placed atop telemetry receivers (Data Sciences International) in a light and temperature-controlled chamber. Standard rodent chow was provided *ad libitum*. Data collection began 2 weeks post-surgery, to allow mice to

recover in the 12:12 LD cycle. We recorded 20 sec of electrocardiogram (ECG) and measured average body temperature and cage activity every 10 min for approximately 15 days. Similar to our collection of wheel-running behavior, we then shifted the mice into DD and continued the measurements for another 15-20 days. Heart rate (HR) is extrapolated from ECG waveforms using the RR interval.

ECG interval measurements (RR, PR, QRS, QT and QTc) were calculated using Ponemah Analysis Software (Data Sciences International) at time points zeitgeber time (ZT) 2-4 and ZT 14-16 (LD conditions). A 20-sec ECG recording every hr was used to calculate Heart Rate Variability (HRV) in the time-domain (standard deviation of all normal R-R intervals, SDNN) using analysis software (Data Science International). Circadian rhythms of HR and body temperature were analyzed by periodogram analysis combined with a χ^2 test (El Temps software, Barcelona, Spain). The strongest amplitude (or power) of periodicities (within 20 and 31 hr limits) was compared between WT and BACHD deficient mice. The amplitude of the χ^2 test determines the period of a rhythm and its robustness.

Whole cell patch-clamp electrophysiology

Methods used were similar to those described previously (Itri *et al.*, 2005, 2010). 300 µm coronal slices of the mid-SCN were collected by vibratome dissection of brains from mice between 2 and 3 months of age. Slices were placed in a recording chamber (PH-1, Warner Instruments, Hamden, CT) attached to the stage of a fixed-stage upright DIC microscope (OLYMPUS, Tokyo, Japan). The slices were superfused continuously (2 ml/min) with artificial cerebrospinal fluid (ACSF) aerated with 95 % O_2/ 5 % CO_2. The whole cell patch clamp recordings from the SCN were taken with recording electrodes. These micropipettes (typically

4–7 MΩ) were pulled from glass capillaries (WPI, Sarasota, FL) on a multistage puller (Sutter P-97, Novato, CA) and filled with the standard solution. The standard solution contained (in mM): K-gluconate, 112.5; EGTA, 1; Hepes, 10; MgATP, 5; GTP, 1; leupeptin, 0.1; phosphocreatine, 10; NaCl, 4; KCl, 17.5; CaCl2, 0.5; and MgCl2, 1. The pH was adjusted to 7.25-7.3 and the osmolality was adjusted between 290-300 mOsm. Recordings were obtained with AXOPATCH 200B amplifier (Molecular Devices, Sunnyvale, CA) and monitored on-line with pCLAMP (Ver 9.2, Molecular Devices). To minimize changes in offset potentials with changing ionic conditions, the ground path used a KCl agar bridge. Each of the cells was determined to be within the SCN by directly visualizing the cell's location with DIC microscopy. Cells were approached with slight positive pressure (2–3 cm H_2O). The pipette was lowered to the vicinity of the membrane while maintaining positive pressure. After forming a high-resistance seal (2–10 GΩ) by applying negative pressure, a second pulse of negative pressure was used to break the membrane. The access resistance of these cells ranged from 15-35 MΩ in the whole cell voltage-clamp configuration while the cell capacitance was typically between 6-18 pF. Data were not collected if access resistance was greater than 40 MΩ or if the value changed significantly (>20%) during the course of the experiment. In these studies, we used a 70% compensation using positive feedback correction. The junction potentials between the pipette and the extracellular solution were cancelled by the voltage-offset of the amplifier before establishing a seal and were not further corrected. Series and input resistance were monitored repeatedly by checking the response to small pulses in a passive potential range. The standard extracellular solution used for all experiments was ACSF. Drug treatments were performed by dissolving pharmacological agents in the ACSF used to bathe the slices during recording.

Solution exchanges within the slice were achieved by a rapid gravity feed delivery system. Spontaneous firing rates (SFR) were recorded with pCLAMP for 1 min using current-clamp in the whole cell patch configuration. No current was injected during recording.

Immunohistochemistry (IHC)

The methods employed were similar to those previously described (Wang *et al.*, 2009; Dragich *et al.*, 2010). BACHD and WT littermates of 12 mo of age were used. Mice were anaesthetized by Isoflurane (Phoenix Pharmaceutical, Burlingame, CA) and perfused with phosphate-buffered saline (PBS, pH 7.4) with heparin (2 units/ml, Henry Schein, Melville, NY) followed by 4% (w/v) paraformaldehyde (Sigma-Aldrich) in PBS (pH 7.4). Brains were dissected, post-fixed at 4 °C overnight, and cryoprotected in 20 % sucrose in PBS (pH 7.4). IHC was performed on free-floating 20 µm cryostat (Thermo Fisher Scientific, Waltham, MA) coronal brain sections from the middle of the rostral-caudal axis. Sections were washed for 5 min with PBS (pH 7.4, three times), and then endogenous peroxidase activity was quenched with PBS (3 % H_2O_2, 10 % Methanol, 10 min). Sections were then washed again in PBS (three times), dipped in 3 % normal goat serum in PBS with 0.1 % Triton X-100 for 1 hr, and then incubated with a rabbit anti-PER2 (1:1,000; Alpha Diagnostics, San Antonio, TX) in PBS (3 % normal goat serum, 0.1 % Triton X-100) at 4 °C overnight. Sections were washed in PBS (three times), then incubated with biotinylated goat anti-rabbit antibody (1:200) for 2 hr. Sections were washed again for 5 min in PBS (five times) and dipped in AB solution (Vector Laboratories, Burlingame, CA) for 45 min, washed again in PBS (three times), then placed in filtered 0.05 % 3,3'-diaminobenzidine in Tris-buffered saline (TBS) containing a 1:800 dilution of 1.3 % H_2O_2.

After sufficient color reaction (5-6 min), sections were washed with TBS and mounted on slides immediately. Sections were then dried overnight, dehydrated with ascending concentrations of ethanol, and cover-slipped. Images were captured with Axio Vision camera systems (Carl Zeiss, Thornwood, NY). Control experiments in which the primary antibody was not added did not exhibit any positive staining. In addition, blocking experiments, performed by adding the PER2 peptide (1 mg/ml in PBS, pH 7.4, diluted 1:500) to the primary incubation solution, prevented PER2 staining. In previous work using the same protocol, we could not detect any positive staining in PER2 KO mouse (Wang *et al.*, 2009).

Statistical measurements

The data sets were analyzed by a two-way analysis of variance (ANOVA) or a one-way ANOVA. If significant group differences were detected ($P < 0.05$) by the ANOVA, then the post hoc analysis was applied. If the data passed an equal variance test, Tukey's method was applied and if the data failed an equal variance test, Holm-Sidak method was applied. For all tests, values were considered significantly different if $P < 0.05$. All tests were performed using SigmaStat (version 3.5, SYSTAT Software, San Jose, CA). Values were shown as mean ± standard error of the mean (S.E.M.).

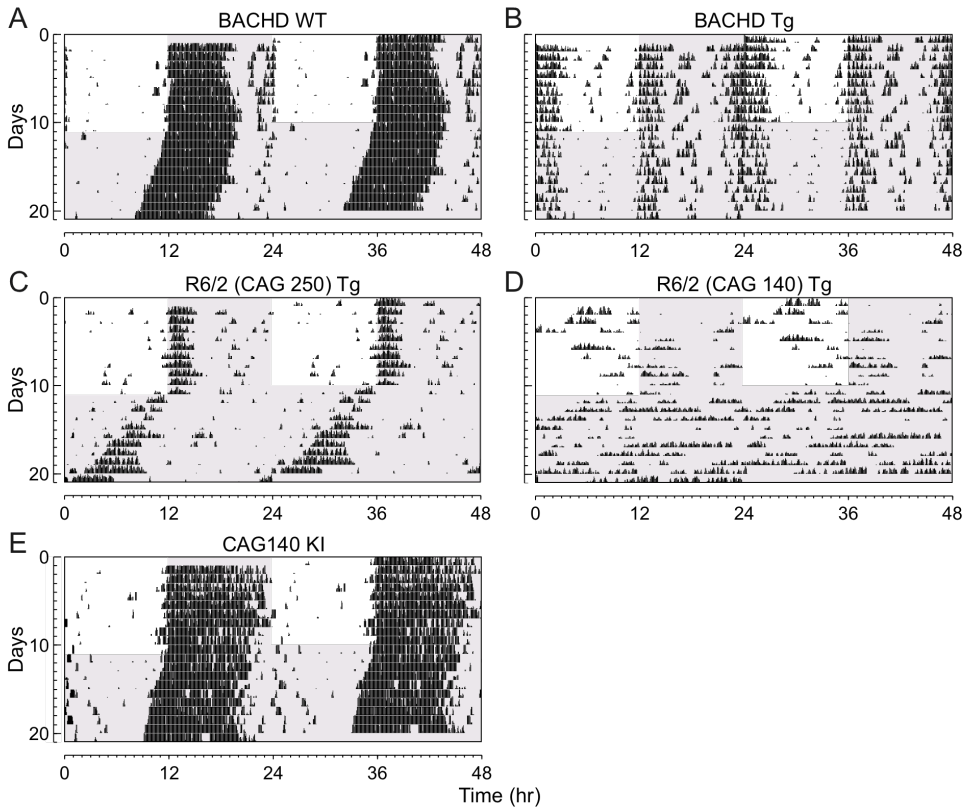

Figure 2-1: *Circadian dysfunction is a common feature of mouse models of HD. Mice were placed individually in cages with running wheels, and locomotor activity was recorded under different lighting conditions. Each horizontal row represents an activity record for a 24-hr day. Successive days are plotted from top to bottom. The grey shading represents darkness. Mice were initially held in LD (12:12) and then released into DD. Panels show examples of the wheel-running activity recorded from WT (A), BACHD (B), R6/2 CAG 250 (C), R6/2 CAG 140 (D), and CAG 140 (E). The mice were all 2-3 mo of age. See Table 2-1 for detailed analysis.*

Results

Diurnal and circadian rhythms of wheel running behavior are disrupted in R6/2 and BACHD mouse models of HD.

We used wheel-running activity to determine the impact of the insertion of the different *Htt/HTT* mutations on diurnal and circadian rhythms of behavior (**Fig. 2-1**). In these studies, we compared locomotor activity rhythms in WT mice to locomotor activity measured in littermate

BACHD (n = 8), R6/2 CAG 250 (n = 5), R6/2 CAG 140 (n = 7), and CAG 140 KI (n = 8) lines of mice at 2 to 3 mo of age. As has been previously described (Morton *et al.*, 2005), under both LD and DD conditions, the majority of mice from the R6/2 lines were arrhythmic (**Table 2-1**). Due to mortality, we were not able to study the R6/2 lines past this time point. In contrast to the results obtained with the R6/2 lines, the CAG 140 KI remained robustly rhythmic at this age (~3 mo). In fact, this line showed no significant deficits in the key circadian parameters of period or amplitude even when we extended our analysis up to 12 mo of age (data not shown). The BACHD mice (8 out of 8) exhibited low amplitude, fragmented rhythms in wheel running behavior with a long free-running period (**Table 2-1**). In addition, most of the BACHD mice exhibited a bimodal activity pattern (75%). These circadian deficits were seen throughout the first year of life of these mice (**Fig. 2-2**). The amplitude of the rhythms in both LD and DD progressively declined over the life of the mice (**Table 2-2**). For example, analysis of activity in DD by two-way ANOVA for age and genotype revealed a significant effect of both age ($F_{3,40}$ = 3.48, P = 0.02) and genotype ($F_{1,40}$ = 43.38, $P < 0.001$) with a post hoc Tukey's test indicating a significant effect of the BACHD mutation in all age groups. Together, our behavioral analysis demonstrates that by three mo of age (young adult), three mouse models of HD (BACHD, R6/2 CAG 250, & R6/2 CAG 140) exhibit disrupted daily and circadian rhythms in wheel-running activity.

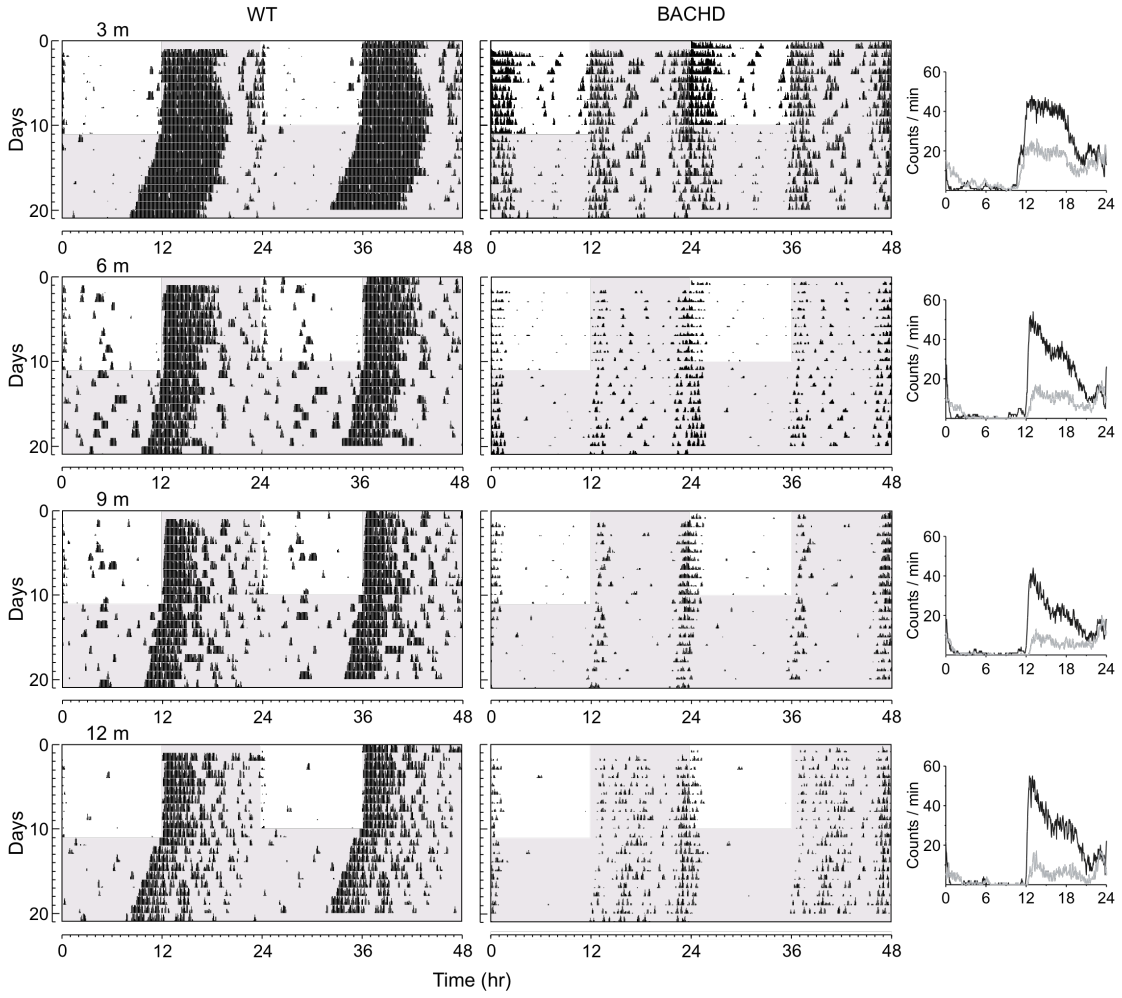

Figure 2-2: *BACHD mice show an age-related decline in activity levels. Panels show examples of wheel-running activity measured from WT (left panels) and littermate BACHD (middle panels) measured at ~3, 6, 9, and 12 mo of age. The average waveform of activity for each genotype (black line =WT; grey line = BACHD) as measured over 10-days in LD is also shown (right panels). Activity and power showed progressive declines under both LD and DD conditions. See Table 2-2 for detailed analysis.*

The light-response of the circadian system is altered in BACHD mice

As nocturnal animals, WT mice restrict most of their wheel running activity to the night (93% of total activity). In contrast, the BACHD mice exhibited a significant amount of wheel running activity in the light (24%; $t_{14} = -3.54$, $P < 0.001$). One possible explanation is that the

BACHD line may have deficits in the light-response of the circadian system and we carried out two additional experiments to test this possibility. First, we examined the ability of the BACHD mice to re-synchronize to 6 hr shifts in the LD cycle (**Fig. 2-3A**). We found that the BACHD mice took longer to resynchronize to both the 6 hr delay (t_{13} = -2.25, $P < 0.05$) and advance (t_{13} = -3.11, $P < 0.01$) in the LD cycle than their WT littermates. In addition, to directly assess the effects of light on the circadian system, the phase shifts induced by single, discrete light treatments were examined (**Fig. 2-3B**). Whereas WT littermates exposed to white light at CT 16 (100 lux, 10 min duration) showed a 113 ± 5 min (n = 8) phase delay, the BACHD mice had a 55% reduction in magnitude of phase delay after the same light treatment (51 ± 10 min, n = 8; t_{15} = 5.53, $P < 0.01$). Therefore, the circadian system of the BACHD mice shows a reduced sensitivity to the phase-shifting effect of light.

Genotype	WT	BACHD	R6/2 250	R6/2 140	CAG140 KI
LD					
Arrhythmic (%)	0%	0%	50%	75%	0%
Power (% variation)	59.5 ± 2.7	34.5 ± 3.7**	na	na	52.9 ± 4.6
Activity (rev/h)	981 ± 70	628 ± 99**	104 ± 39**	195 ± 125*	835 ± 99
DD					
Arrhythmic (%)	0%	0%	50%	75%	0%
Tau (hrs)	23.69 ± 0.05	24.07 ± 0.04*	na	na	23.82 ± 0.04
Power (% variation)	50.8 ± 5.5	31.0 ± 4.3**	na	na	54.6 ± 4.3
Activity (rev/h)	1050 ± 34	543 ± 121**	98 ± 50**	195 ± 98*	711 ± 144

Table 2-1: *Key circadian parameters in 4 mouse models of HD. Rhythms in wheel-running activity of young male mice were examined using periodogram analysis (2-3 mo of age; n = 4-8 per genotype). Results from littermate WT and mutant mice were compared with a Student's t-Test with *= P < 0.05 and **= P < 0.01. In the R6/2 lines, the number of rhythmic animals was too low toaccurately describe the circadian parameters. These parameters are labeled as not available (na).*

Genotype		WT	BACHD
LD			
	Power (% variation)		
	3 mo	59.5 ± 2.7	34.5 ± 3.7*
	6 mo	55.1 ± 3.3	42.4 ± 2.9*
	9 mo	54.3 ± 3.3	32.9 ± 3.6*
	12 mo	55.0 ± 2.0	32.8 ± 3.5*
	Activity (rev/h)		
	3 mo	981 ± 70	628 ± 99*
	6 mo	713 ± 73	297 ± 52*#
	9 mo	760 ± 127	277 ± 47*#
	12 mo	734 ± 118	233 ± 58*#
DD			
	Tau (hrs)		
	3 mo	23.69 ± 0.05	24.07 ± 0.04*
	6 mo	23.61 ± 0.12	24.05 ± 0.04*
	9 mo	23.54 ± 0.08	24.12 ± 0.06*
	12 mo	23.69 ± 0.06	23.96 ± 0.02*
	Power (% variation)		
	3 mo	50.8 ± 5.5	31.0 ± 4.3*
	6 mo	51.2 ± 4.8	34.7 ± 2.9*
	9 mo	45.8 ± 3.8	31.2 ± 2.1*
	12 mo	45.1 ± 2.4	27.5 ± 2.3*
	Activity (rev/hr)		
	3 mo	1050 ± 34	543 ± 121*
	6 mo	872 ± 149	265 ± 50*
	9 mo	749 ± 165	229 ± 49*
	12 mo	762 ± 98	190 ± 19*#
	Fragmentation (bouts/day)		
	3 mo	4.4 ± 0.4	7.4 ± 0.8*
	6 mo	4.5 ± 0.9	7.3 ± 0.8*
	9 mo	5.1 ± 0.6	7.2 ± 0.8*
	12 mo	5.0 ± 0.2	8.1 ± 0.4*
	Bimodal (%)		
	3 mo	0%	37.5%
	6 mo	0%	62.5%
	9 mo	0%	66.7%
	12 mo	0%	50%

Table 2-2*: Age-related decline in amplitude of wheel-running activity rhythms in BACHD mice. Rhythms in wheel-running activity in male mice (*n *= 4–8 per age-group) were examined using periodogram analysis. Comparisons between age and genotype were made between littermate WT and mutant mice with a 2-way ANOVA followed by Tukey's post hoc analysis with * indicating a significant difference at* $P < 0.05$ *between genotypes within age and* $^{\#}$ *indicating* $P < 0.05$ *between ages within genotype.*

The distribution of behavioral sleep is disrupted in BACHD mice.

To examine the sleep/wake temporal distribution, we measured behavioral sleep in young adult (3 mo) and middle aged (12 mo) BACHD mutants and their WT littermates (**Table 2-3**). Both mutants and WT mice showed significantly more daytime sleep at 12 mo than at 3 mo (two way ANOVA $F_{1,29} = 18.44$, $P < 0.001$), and the post-hoc Tukey's *t*-test revealed that the BACHD mutants had significantly less daytime sleep than WT at 3 mo of age ($t_{20} = 2.07$, $P = 0.049$). Nighttime sleep was significantly greater in 12 mo old WT mice than their younger counterparts ($t_{14} = 4.43$, $P < 0.001$), but this age-related effect was not observed in the BACHD mutants ($t_{12} = 0.14$, $P = 0.89$). A higher resolution analysis of sleep distribution of the 3 mo old BACHD mutants pinpointed the early hours of the day as the time during which they displayed markedly less sleep than the WT littermates (**Supp. Fig. 2-1**; two way repeated measures ANOVA $F_{7,20} = 2.82$, $P = 0.009$). Post-hoc analysis by Tukey's *t*-tests revealed that the BACHD mutants spent significantly less time in sleep during the hours of ZT 0 to ZT 3 ($t_{20} = 2.99$, $P = 0.003$) as well as between ZT 3 and ZT 6 ($t_{20} = 2.36$, $P = 0.02$). Therefore, the BACHD mice exhibited significantly reduced sleep during the early day.

Genotype	WT	BACHD
Sleep in day (%)		
3 mo	66.67 ± 1.53	61.98 ± 1.68*
12 mo	74.48 ± 2.65#	72.98 ± 2.65#
Sleep in night (%)		
3 mo	26.53 ± 1.59	28.19 ± 1.74
12 mo	40.63 ± 2.76#	28.65 ± 2.76*
Sleep bouts in day		
3 mo	8.25 ± 0.36	8.03 ± 0.39
12 mo	9.13 ± 0.62	7.88 ± 0.62
Sleep bouts in night		
3 mo	3.65 ± 0.40	4.13 ± 0.44
12 mo	6.50 ± 0.70#	4.13 ± 0.70*

Table 2-3: *The distribution of behavioral sleep is altered in the BACHD mice. Behavioral measurements of sleep were carried out using video analysis on mice of 3 months (*n *= 12 per genotype) and 12 months of age (*n *= 4 per genotype). Comparisons between age and genotype were made between littermate WT and mutant mice with a 2-way ANOVA followed by Tukey's post hoc analysis. * indicates* $P < 0.05$ *between genotypes within age while # indicates* $P < 0.05$ *between ages within genotype.*

Circadian rhythms of heart rate and body temperature are severely disrupted in the BACHD mice.

Surgical implantation of a telemetric device into the abdomen of mice allows for continuous recording of ECG waveforms and body temperature in freely-moving WT and BACHD mice. We compared and analyzed a number of ECG features (RR, PR, QRS, QT, QTc intervals) between WT and BACHD mice under LD conditions to detect any diurnal and genotypic differences. Both the WT and BACHD mice displayed significant day/night differences in the RR, PR, and QRS (**Table 2-4**). Interestingly, the BACHD mice showed a significant increase in the PR interval during the night and a loss of diurnal rhythmicity in this parameter.

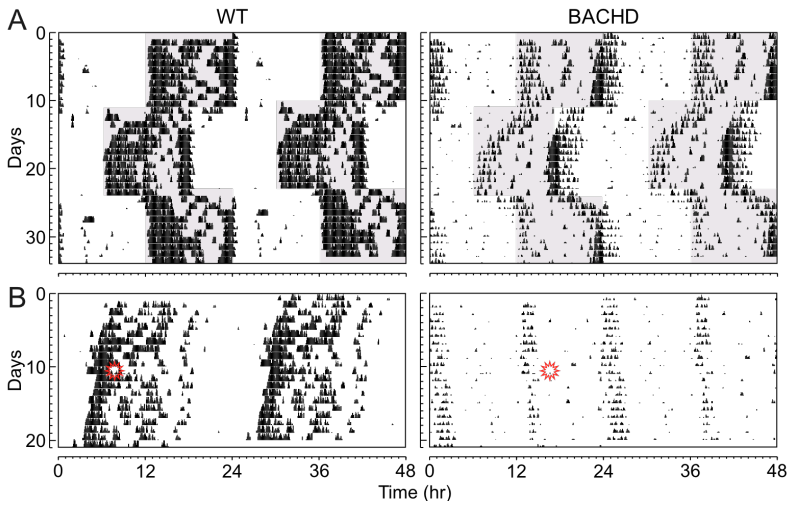

***Figure 2-3**: BACHD mice show a decreased circadian response to light. (A) Examples of the response to 6 hr shifts in the LD cycle for WT and BACHD mice at ~6 mo of age. (B) Examples of light-induced phase shifts for WT and BACHD mice at ~6 mo of age in DD. Mice in DD were exposed to light (100 lux, 10 min duration) at CT 16 (indicated by symbol) and the resulting phase delay measured.*

In order to examine the circadian component of HR and body temperature, we plotted the raw data to produce graphs similar to the actogram (**Fig. 2-4**) used for wheel-running activity analysis. We also analyzed the raw data of individual mice by periodogram analysis (**Table 2-5**) and used the amplitude as an index of rhythm strength. Under LD conditions, WT mice exhibited robust daily rhythms of HR and body temperature that were synchronized to the LD cycle. Significant diurnal differences in HR (t_6=-11.54, $P < 0.001$, $n = 7$) and body temperature (t_6=-8.693, $P < 0.001$, $n = 7$) were detected by *t*-tests (**Table 2-5**). When WT mice were placed in DD, circadian rhythms of HR and body temperature remained robust with a free-running period of 23.7 hrs (**Fig. 2-4, Table 2-5**). Circadian differences in average HR (t_6=9.085, $P < 0.001$, $n = 7$) and body temperature (t_6=-19.684, $P < 0.001$, $n = 7$) remained significant (**Table 2-5**). The BACHD mice displayed weak diurnal rhythms in HR and body temperature (**Fig. 2-4**). The mutant mice exhibited increased HR and temperature during the day compared to WT (**Table 2-5**). Furthermore, under DD conditions, we detected significant circadian differences in body temperature (t_7=-6.693, $P < 0.001$, $n = 8$) and HR (t_7=-3.636, $P = 0.008$, $n = 8$; **Table 2-5**). Under DD conditions, the average HR and body temperature was higher in the BACHD mice than in WT (**Table 2-5**). These data indicate that the amplitude of the temporal patterning of HR and body temperature is reduced in the BACHD mice due to a higher HR and body temperature during the day.

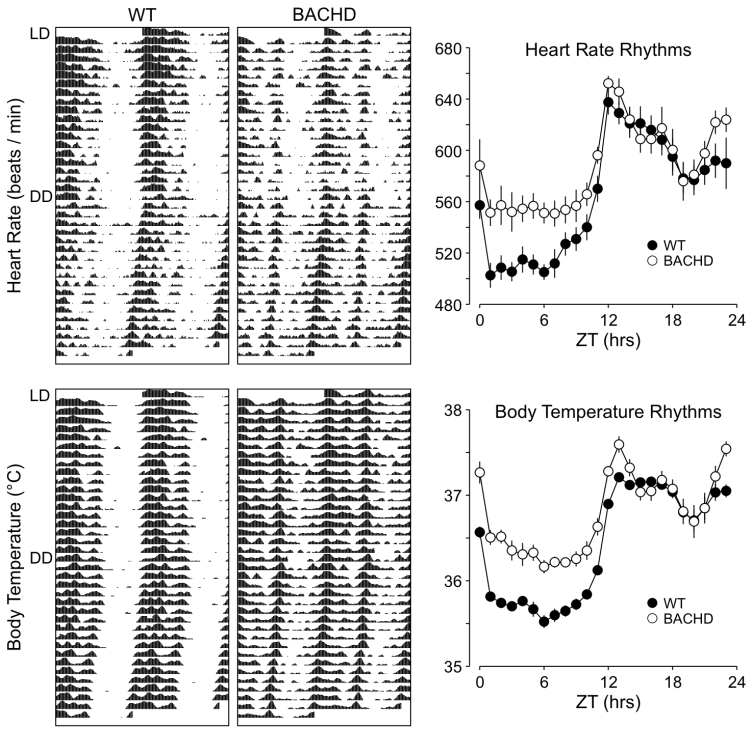

Figure 2-4*: BACHD mice exhibit a breakdown in circadian rhythms as measured by telemetry. Examples of heart rate and body temperature measured from WT (left panels) and littermate BACHD (right panels) mice at ~6 mo of age are shown. Each horizontal row represents an activity record for a 24-hr day. Activity double plotted to aid detection of activity patterns. Successive days are plotted from top to bottom. The average waveform of activity for each genotype as measured over 10-days in LD is also shown (right panels).*

Rhythms of HRV are disrupted in the BACHD mice

HRV is an index of the balance of sympathovagal signals to the heart and measures the variability of the time between individual heartbeats (Massin *et al.*, 2000). We assessed the temporal patterning of neural signals to the heart by calculating HRV from WT and BACHD mice under LD and DD conditions (**Fig. 2-5**). WT mice exhibited significant diurnal differences in HRV under LD (WT: t_4=3.00, P = 0.04) and significant circadian differences under DD conditions (t_4=3.582, P = 0.023). BACHD mice did not exhibit a diurnal difference in HRV under LD conditions (t_5=1.414, P = 0.216) or DD conditions (t_5=3.542, P = 0.14). The average

HRV (measured over 24 hrs) was significantly lower in the BACHD group ($t_{10} = 2.511$, $P = 0.031$, **Fig. 2-5**). Overall our data suggest that the autonomic system is still functioning but the temporal patterning is altered, with particular deficits in the daytime or rest phase. These results suggest that temporal patterning as well as the overall level of autonomic regulation of the cardiovascular system is compromised in the BACHD mice.

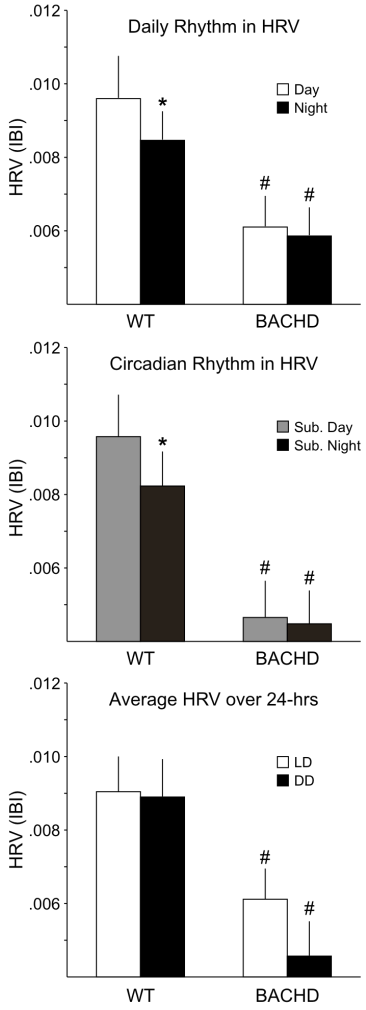

Figure 2-5*: BACHD mice exhibit a loss of their circadian rhythm in HRV. HRV is determined by calculating the variance of the time between individual beats, and is also known as the inter-beat-interval (IBI). Top panel shows the average HRV as measured in the day and in the night when mice are maintained on an LD cycle. The middle panel shows the average HRV as measured in the subjective day and night under DD conditions. The bottom panel shows that the overall HRV was significantly reduced in the BACHD mice. The * indicates significance difference in the HRV at the level of P < 0.05 as analyzed by one-way ANOVA followed by Tukey's post-hoc comparison.*

Daytime excitability of SCN neurons is reduced in the BACHD mice

Using the current-clamp recording technique in the whole-cell patch clamp configuration (**Fig. 2-6**), we measured the SFR in dorsal SCN neurons from WT (n = 25) and BACHD (n = 26) mice. Recordings (1 min) were made during the day (ZT 4-6) and night (ZT 14-16) and the resulting data analyzed by two-way ANOVA. This analysis revealed a significant effect of time of day ($F_{1,50}$ = 94.23, $P < 0.05$). As expected, the SFR of WT mice was significantly (t = 4.395, P <0.05) higher during the day (6.7 ± 1.5 Hz, n = 13) than during the night (2.1 ± 0.7 Hz, n = 12). In contrast, in the BACHD mice, there were no significant (t = 0.836, P = 0.557) differences between SFR during the day (3.1 ± 0.8 Hz, n = 14) and night (2.3 ± 1.0 Hz, n = 12). The daytime SFR was significantly reduced (t = 3.575, P = 0.015) in the BACHD mice compared to WT mice. So the insertion of the human HD gene appeared to eliminate the day/night difference in spontaneous activity in the mouse SCN by reducing the firing rate during the day.

Genotype		WT	BACHD
RR (ms)			
	Day	125 ± 4	122 ± 7
	Night	99 ± 2.3*	107 ± 5*
PR (ms)			
	Day	38.1 ± 0.9	37.5 ± 0.6
	Night	34.8 ± 0.6*	36.9 ± 0.6$^{\#}$
QRS (ms)			
	Day	13.9 ± 0.3	13.7 ± 0.3
	Night	12.9 ± 0.4*	13.5 ± 0.3*
QT (ms)			
	Day	51.9 ± 1.1	51.9 ± 2.8
	Night	44.8 ± 1.9	46.6 ± 2.2*
QTc (ms)			
	Day	128 ± 1	128 ± 3
	Night	123 ± 2*	124 ± 2*

Table 2-4: *Average duration of ECG features (RR, PR, QRS, QT and QTc intervals) in WT and BACHD mice under LD conditions. ECG intervals at two time points: day (ZT 2–4) and night (ZT 14–16) were calculated and averaged over 8 days.* * *indicates significant difference in intervals between day and night (*P *< 0.05), which was analyzed by a paired Student's* t*-test.* # *indicates significant difference in intervals between WT and BACHD mice (*P *< 0.05) and was analyzed using an unpaired Student's* t*-test.*

PER2 expression is not altered in the SCN of BACHD mice.

To determine if the molecular machinery necessary to generate circadian oscillations was affected by the insertion of the HD gene, we used IHC to examine PER2 protein expression within the SCN. The wheel running activity of WT and BACHD mice in LD was monitored and the mice were placed in DD for 3 days. Mice (n = 3-4 per time point) from each genotype were sampled at 2 different points in the daily cycle (CT 2 and 14). PER2 was strongly expressed in the SCN of both WT and BACHD mice (**Fig. 2-7**) with immuno-reactivity seen throughout the SCN. The mean number of immuno-positive neurons per SCN section varied with time of day (**Fig. 2-7**) with peak counts found at early subjective night (CT 14) and low counts measured in the early subjective day (CT 2). As measured by the PER2 rhythm, we do not see any evidence for gross disruption of the molecular clockwork in the BACHD mutant mice.

Heart rate		
Genotype	WT	BACHD
Arrhythmic (%)	0%	0%
Tau (hrs)	23.83 ± 0.04	23.85 ± 0.03
Power (%)	28.0 ± 1	26.3 ± 3
Average (24 h)	561 ± 7	586 ± 8*
Sub. Day (average)	520 ± 7	554 ± 9*
Sub. Night (average)	595 ± 7	611 ± 8
Body temperature		
Genotype	WT	BACHD
Arrhythmic (%)	0%	0%
Tau (hrs)	23.83 ± 0.03	23.85 ± 0.02
Power (%)	69.2 ± 2	64.2 ± 4
Average (24 h)	36.3 ± 0.04	36.6 ± 0.09*
Sub. Day (average)	35.6 ± 0.07	35.9 ± 0.14*
Sub. Night (average)	36.9 ± 0.03	37.0 ± 0.11

Table 2-5: *Key circadian parameters in heart rate and body temperature measured in freely moving mice maintained in constant darkness. The mice (*n *= 6–8 per group) were all young adult (6 months of age) males. Rhythms in HR and body temperature were measured using telemetry and examined using periodogram analysis. Comparisons were made between littermate WT and mutant mice with a Student's* t*-test, with * indicating a significant difference at* P *< 0.05 and ** indicating a significant difference at* P *< 0.01.*

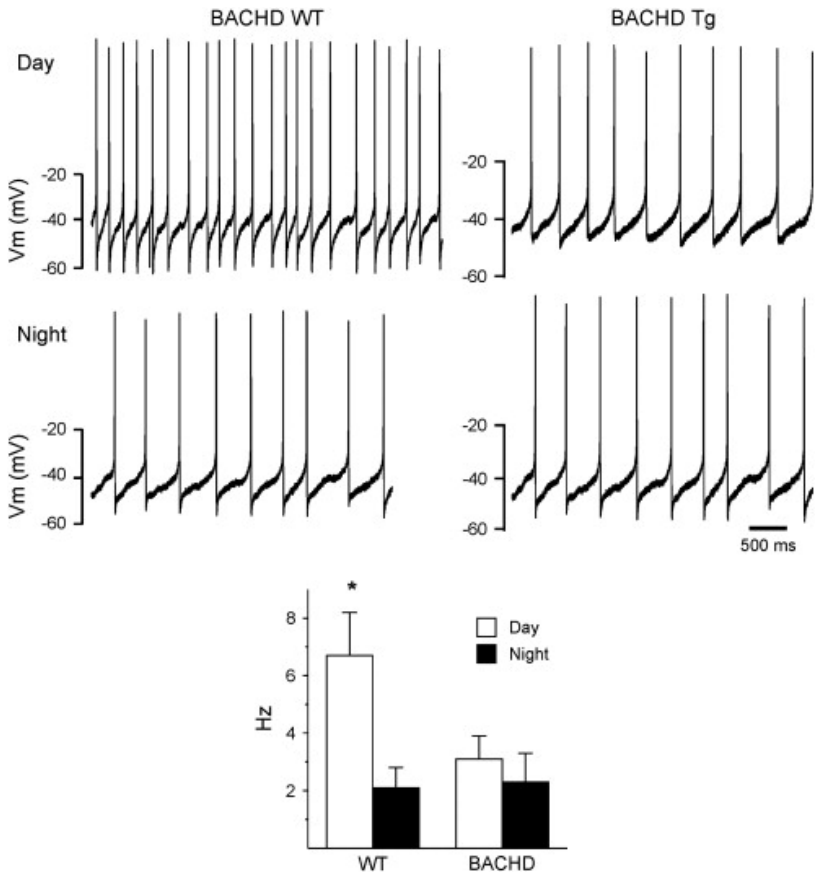

Figure 2-6: *Daytime spontaneous neural activity is reduced in the SCN of BACHD mice. Using the current-clamp recording technique in the cell-attached configuration, we measured the spontaneous firing rate (SFR) in dorsal SCN neurons during the day (ZT 4-6; n = 13-14 per genotype) and night (ZT 16-18; n = 12 per genotype). The top panels show representative examples of firing rate recorded from the WT and BACHD mice at each time point. The bottom panel shows plots of average firing rate for each genotype. Data is shown at means ± SEM. The * indicates significance difference between SFR at the level of P < 0.05 as analyzed by two-way ANOVA followed by Tukey's post-hoc comparison.*

Discussion

There are 3 general types of mouse models of HD (Levine *et al.*, 2004; Menalled *et al.*, 2009; Cepeda *et al.*, 2010) including: transgenic mice expressing the entire human HD gene (BACHD), transgenic mice expressing the first exon of the HD gene (R6/2), and knock-in mice

generated by inserting the expanded CAG repeats into the mouse HD gene (CAG 140). No single mouse model can be expected to recapitulate all aspects of the human disease; therefore, we felt that it was important to explore possible circadian dysfunction in different mouse models of HD. First, we confirmed the dramatic loss of daily and circadian rhythms in the R6/2 line (CAG 240, and CAG 140) as has been reported by Dr. Morton and colleagues (**Fig. 2-1**; Morton *et al.*, 2005; Pallier *et al.*, 2007) . Both of the R6/2 lines of mice quickly progressed from pre-symptomatic (4-6 weeks) to disrupted circadian rhythms and death (8-12 weeks). This rapid progression makes the R6/2 lines excellent models for many aspects of HD but also made examination of the circadian phenotype difficult. Many of the behavioral tests used to measure circadian parameters last longer than the short lifespan of the R6/2 mice. In contrast, the CAG 140 KI mice did not show a circadian phenotype at 3 mo of age (**Fig. 2-1**). At the older ages, the CAG 140 KI showed reduced amplitude locomotor activity rhythms (10-20%, $P > 0.05$) and increased time to re-entrain to a shift in the LD cycle (data not shown). However, the circadian effects were mild compared to that seen in the other models and we stopped collecting data when the mice were 12 mo of age. The mice line that we used was not fully back-crossed onto the C57 background, so the genetic background may have contributed to the mild circadian phenotype. Of course, the mice may well have developed a more significant circadian phenotype at an older age.

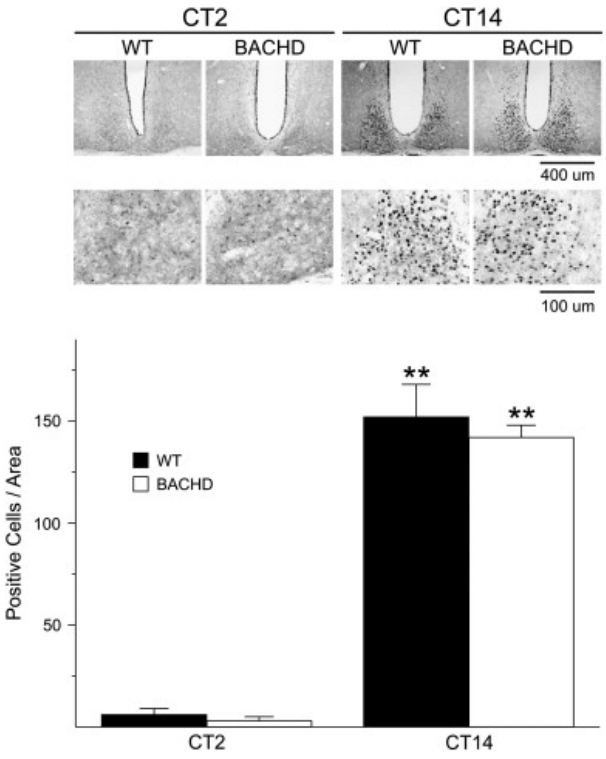

Figure 2-7: *PER2 rhythm within the SCN did not appear to be disrupted even in aged BACHD mice. Mice were held in DD and wheel running activity measured to determine circadian phase. IHC was used to measure PER2 immunoreactivity in the SCN (n = 3-4 per group) of BACHD and WT controls. Tissue was collected in subjective day (CT 2) or subjective night (CT 14). (top panels) Photomicrographs of SCN tissue of each genotype in low (10X) and higher (40X) magnification. (bottom panel) Numbers of PER2 immuno-positive cells in the SCN varied as a function of time of day with highest count in early night. No differences were found between the genotypes. Tukey's post-hoc comparison, **P<0.01 (vs. CT2).*

The BACHD line exhibited clear diurnal and circadian deficits in wheel running activity at 3 mo of age (**Fig. 2-1**), a time at which motor deficits associated with the HD phenotype are first seen in this mouse model, but prior to development of neurodegeneration (Gray *et al.*, 2008). There was a clear age-related progression to the disease with the amplitude of the rhythms declining with age (**Fig. 2-2**). The central clock driving circadian rhythms is located in the SCN in the hypothalamus. While many of the symptoms of HD appear to be the result of pathology within the basal ganglia, there has long been evidence that hypothalamic dysfunction

is also involved (Lavin *et al.*, 1981; Kremer *et al.*, 1990; Petersén *et al.*, 2005; Wood *et al.*, 2008). In humans, many of the non-motor symptoms of HD begin before the onset of motor symptoms, and include dysfunctions in hypothalamic-driven function, such as sleep, emotional state and metabolism (Julien *et al.*, 2007; Duff *et al.*, 2007; Soneson *et al.*, 2010). The early onset of the circadian disorders described in the present study (3 mo or young adult) fits with the clinical disease progression seen in humans. Besides a clear deficit in the behavioral output, we were also able to document a compromised light response of the BACHD mice (**Fig. 2-3**). The mice had difficulty adjusting to changes in the LD cycle, possibly due to the decreased magnitude of the phase shifting effects of light. One likely consequence of these entrainment deficits is that the BACHD mice exhibit more activity during the time of the daily LD cycle when they should be sleeping. In HD patients, sleep disturbances are a common clinical complaint that impairs the quality of life (Goodman & Barker, 2010). To explore the sleep/wake patterns of the BACHD, we turned to behavioral measures of sleep (Campbell & Tobler, 1984; Schwartz & Smale, 2005; Loh *et al.*, 2010). We measured the patterns of sleep/wake in BACHD and WT littermates using video analysis. The results (**Table 2-3**) clearly show that the mice exhibited a reduction of sleep early in their sleep cycle. This observation with the BACHD mice parallels clinical observations of a prolonged sleep latency in the HD patients (Cuturic *et al.*, 2009; Aziz *et al.*, 2010; Goodman & Barker, 2010). Future work using EEG recordings will be necessary to specifically examine if the BACHD mice show any change in sleep states or in the depth of sleep.

In HD patients, there is the suggestion of cardiac dysfunction with the best evidence indicating that HD alters the autonomic tone in cardiac tissue (e.g. Andrich *et al.*, 2002; Kobal *et*

al., 2004; Bär *et al.*, 2008). The telemetry system enabled us to record ECG waveforms (**Supplemental Fig. 2-2**) and calculate HRV from WT and BACHD mice under LD and DD conditions. HRV is a measure of the variation in the beat-to-beat (R-R) interval, and reflects the balance of sympathetic and parasympathetic input to the heart. We found an overall decrease in HRV in BACHD mice compared to WT mice, indicating autonomic dysfunction in the BACHD mice (**Fig. 2-5**). A decrease in HRV has been previously reported in patients in the early presymptomatic and middle stages of HD progression (Andrich *et al.*, 2002; Kobal *et al.*, 2010). As both HR and body temperature are regulated by the autonomic nervous system (ANS), the increase in average HR and body temperature observed in BACHD mice compared to WT mice is further evidence for dysfunction of the ANS. It is interesting to consider that the telemetry recordings were carried out without the presence of a running wheel, which can alter overall activity levels in mice. Reduced HRV is generally considered an indication of poor cardiovascular health and has been shown to be a predictor for cardiovascular disease and mortality (Bigger *et al.*, 1992; Buccelletti *et al.*, 2009; Thayer *et al.*, 2010). In this regard, it is worth considering that the autonomic imbalance may be promoting cardiac failure, which is a leading cause of death among HD patients (Chiu & Alexander, 1982; Lanska *et al.*, 1988). In addition to the overall decrease of HRV, the diurnal and circadian rhythms of HRV were also lost in BACHD mice. The loss of rhythms in autonomic output and the shift in autonomic balance may be driving the damped rhythms of HR and body temperature in BACHD mice. We also compared various ECG parameters between WT and BACHD mice under LD conditions (**Table 2-4**). While most parameters were not different between the two genotypes and displayed significant day/night differences, we did not detect a day/night difference in the PR

interval in the BACHD mice and the night-time value was increased compared to WT. The PR interval reflects the time the electrical impulse takes to travel from the sinus node through the atrioventricular node, the electrical pathway that connects the top chambers to the bottom chambers of the heart. Regulation of this interval is dependent upon a number of factors, one being input from the autonomic system, whereby the PR interval elongates with increased parasympathetic tone, and shortens with increased sympathetic tone (Wallick *et al.*, 1982; Carruthers *et al.*, 1987). Thus, the loss of day/night difference in the PR interval seen in the BACHD mice is further evidence for a dysfunction in ANS regulation. Overall, the dramatic decrease in HRV, increase in HR and body temperature, loss of day/night differences in the PR interval, as well as the decrease in the amplitude of rhythmicity in HR and body temperature suggests that the function of the ANS is compromised in the BACHD mice.

SCN neurons are spontaneously active neurons that generate AP with a peak frequency of around 10-12 Hz during the day (Kuhlman & McMahon, 2006; Ko *et al.*, 2009). During the night, SCN neurons are normally quiescent. In the present study, we examined the impact of the BACHD on the level of spontaneous activity during the day and night (**Fig. 2-6**). In the daytime, we found that the excitability of SCN neurons was significantly reduced in the BACHD mice. Neurons in the SCN are well positioned to drive the rhythms in cardiac output through the regulation of the ANS (Buijs *et al.*, 2003; Kalsbeek *et al.*, 2006). Previous anatomical studies have shown that VIP is expressed in SCN efferents projecting onto pre-autonomic neurons of the paraventricular nucleus (Teclemariam-Mesbah *et al.*, 1997). Both VIP message and protein are reduced in the SCN of R6/2 mice (Fahrenkrug *et al.*, 2007) suggesting a mechanism through which cardiac output may be altered in this line of mice. The decrease in the daytime electrical

activity in the SCN could well weaken the temporal patterning of the ANS. The rhythms in both HR and body temperature were reduced in the BACHD mice due to deficits in the inhibition of these parameters in the day. Similarly, the induction of sleep was significantly reduced early in the day. These observations are all consistent with the hypothesis that the weakening of electrical output from the SCN could underlie a number of the phenotypes observed in the BACHD mice. These physiological results provide important support for the hypothesis that the HD mutation alters the generation of the daily rhythms in firing rate that are a hallmark feature of SCN neurons.

Interacting molecular feedback loops driving rhythmic transcription and translation of key clock genes such as *Period* (e.g. Hastings *et al.*, 2003), are at the core of the oscillatory mechanism responsible for driving circadian oscillation. As a first screen for possible deficits in this molecular clockwork, we looked at PER2 expression in the peak and trough of the rhythm (**Fig. 2-7**). By this measure, we do not see any evidence that the molecular clockwork is disrupted in the SCN of BACHD mutant mice. However, in light of the differential loss of rhythms in the core clock genes Cry1 and Dbp, but not of Bmal1 and Per2 in the liver of R6/2 mice (Maywood *et al.*, 2010), further work is required for a definitive answer as to whether rhythms in gene expression are altered in the SCN of BACHD mice. Prior work with the R6/2 line suggests that the behavioral impairment in the mice is accompanied by disordered expression of circadian clock genes *in vivo* in the hypothalamus (SCN) and in the motor controls regions of the brain including the striatum (Pallier *et al.*, 2007). The BACHD mice did show a lengthening of free-running period in DD (**Table 2-1**). Changes in the circadian period length are indicative of a disruption in the underlying circadian pacemaker system (Takahashi *et al.*,

2008). Therefore, our data with the BACHD mice suggest that these mice have deficits in all of the key elements of the circadian timing system including photic input, generation of oscillations, and outputs.

This disruption of circadian rhythms is likely to have profound consequences on the health of the HD patient (Hastings *et al.*, 2003; Takahashi *et al.*, 2008). It is becoming increasingly clear that robust daily rhythms of sleep & wake are essential to good health. A wide range of studies have demonstrated that disruption of the circadian system leads to a cluster of symptoms, including metabolic deficits (Turek *et al.*, 2005; Marcheva *et al.*, 2010), cardiovascular problems (Feng *et al.*, 2006; Bray & Young, 2008), difficulty sleeping (Wulff *et al.*, 2009; Reid & Zee, 2009) and cognitive deficits (Wang *et al.*, 2009; Gerstner *et al.*, 2009; Loh *et al.*, 2010). Many of these same symptoms are seen in HD patients prior to onset of motor symptoms. This brings up the question as to the extent that circadian perturbations exacerbate the non-motor symptoms of HD. Recent work suggests that interventions that may stabilize the deteriorating daily rhythms can help with the cognitive symptoms in the R6/2 line (Pallier *et al.*, 2007; Maywood *et al.*, 2010). We do not know yet if these interventions actually improve the circadian rhythms and if this type of treatment strategy can be effective in mouse models. Based on the present data, future work will need to focus on a better understanding of how the BACHD mutation alters the electrical activity within the SCN and on interventions that can improve these disruptions.

iii. Supplemental Data

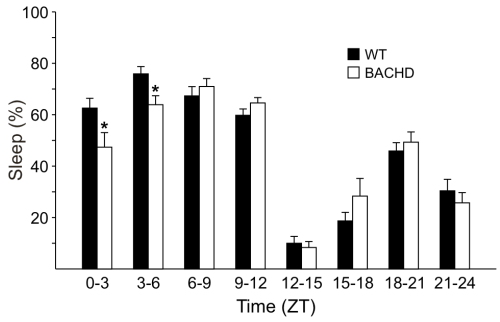

Supplemental Figure 2-1: *BACHD mice exhibit decreased sleep in the early day. Video analysis was used to measure sleep behavior in WT and BACHD mice. The bar graph shows the distribution of sleep as a function of time of day for each genotype. Sleep was significantly reduced in the first 6 hrs of the day but not at the other times. The * indicates significance difference in the % of sleep at the level of P < 0.05 as analyzed by two-way ANOVA followed by Tukey's post-hoc comparison.*

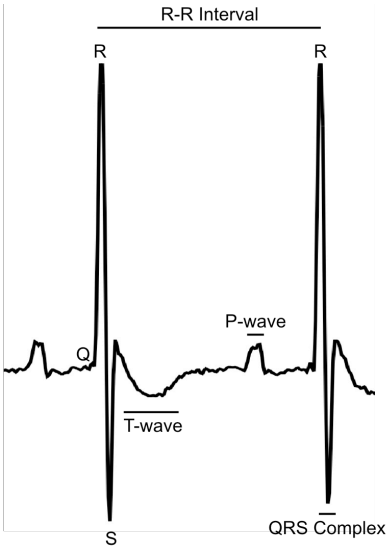

Supplemental Figure 2-2: *In vivo ECG recordings from freely-behaving mice. Representative example of In ECG tracing from a WT mouse labeled with features and intervals of the waveform. The PR interval was significantly increased in the BACHD mice (**Table 2-4**).*

iv. Bibliography

Andrich J, Schmitz T, Saft C, Postert T, Kraus P, Epplen JT, Przuntek H & Agelink MW (2002). Autonomic nervous system function in Huntington's disease. *J Neurol Neurosurg Psychiatr* **72,** 726–731.

Anon (1993). A novel gene containing a trinucleotide repeat that is expanded and unstable on Huntington's disease chromosomes. The Huntington's Disease Collaborative Research Group. *Cell* **72,** 971–983.

Aziz NA, Anguelova GV, Marinus J, Lammers GJ & Roos RAC (2010). Sleep and circadian rhythm alterations correlate with depression and cognitive impairment in Huntington's disease. *Parkinsonism & Related Disorders* **16,** 345–350.

Bär KJ, Boettger MK, Andrich J, Epplen JT, Fischer F, Cordes J, Koschke M & Agelink MW (2008). Cardiovagal modulation upon postural change is altered in Huntington's disease. *Eur J Neurol* **15,** 869–871.

Bigger JT Jr, Fleiss JL, Steinman RC, Rolnitzky LM, Kleiger RE & Rottman JN (1992). Frequency domain measures of heart period variability and mortality after myocardial infarction. *Circulation* **85,** 164–171.

Bray MS & Young ME (2008). Diurnal variations in myocardial metabolism. *Cardiovasc Res* **79,** 228–237.

Buccelletti E, Gilardi E, Scaini E, Galiuto L, Persiani R, Biondi A, Basile F & Silveri NG (2009). Heart rate variability and myocardial infarction: systematic literature review and metanalysis. *Eur Rev Med Pharmacol Sci* **13,** 299–307.

Buijs RM, la Fleur SE, Wortel J, Van Heyningen C, Zuiddam L, Mettenleiter TC, Kalsbeek A, Nagai K & Niijima A (2003). The suprachiasmatic nucleus balances sympathetic and parasympathetic output to peripheral organs through separate preautonomic neurons. *J Comp Neurol* **464,** 36–48.

Campbell SS & Tobler I (1984). Animal sleep: a review of sleep duration across phylogeny. *Neurosci Biobehav Rev* **8,** 269–300.

Carruthers SG, McCall B, Cordell BA & Wu R (1987). Relationships between heart rate and PR interval during physiological and pharmacological interventions. *Br J Clin Pharmacol* **23,** 259–265.

Cepeda C, Cummings DM, André VM, Holley SM & Levine MS (2010). Genetic mouse models of Huntington's disease: focus on electrophysiological mechanisms. *ASN Neuro* **2,** e00033.

Chiu E & Alexander L (1982). Causes of death in Huntington's disease. *Med J Aust* **1,** 153.

Colwell CS, Michel S, Itri J, Rodriguez W, Tam J, Lelievre V, Hu Z, Liu X & Waschek JA (2003). Disrupted circadian rhythms in VIP- and PHI-deficient mice. *Am J Physiol Regul Integr Comp Physiol* **285,** R939–949.

Colwell CS, Michel S, Itri J, Rodriguez W, Tam J, Lelièvre V, Hu Z & Waschek JA (2004). Selective deficits in the circadian light response in mice lacking PACAP. *Am J Physiol Regul Integr Comp Physiol* **287,** R1194–1201.

Cuturic M, Abramson RK, Vallini D, Frank EM & Shamsnia M (2009). Sleep patterns in patients with Huntington's disease and their unaffected first-degree relatives: a brief report. *Behav Sleep Med* **7,** 245–254.

Dragich JM, Loh DH, Wang LM, Vosko AM, Kudo T, Nakamura TJ, Odom IH, Tateyama S, Hagopian A, Waschek JA & Colwell CS (2010). The role of the neuropeptides PACAP and VIP in the photic regulation of gene expression in the suprachiasmatic nucleus. *Eur J Neurosci* **31,** 864–875.

Duff K, Paulsen JS, Beglinger LJ, Langbehn DR & Stout JC (2007). Psychiatric symptoms in Huntington's disease before diagnosis: the predict-HD study. *Biol Psychiatry* **62,** 1341–1346.

Fahrenkrug J, Popovic N, Georg B, Brundin P & Hannibal J (2007). Decreased VIP and VPAC2 receptor expression in the biological clock of the R6/2 Huntington's disease mouse. *J Mol Neurosci* **31,** 139–148.

Feng J-M, Hu YK, Xie L-H, Colwell CS, Shao XM, Sun X-P, Chen B, Tang H & Campagnoni AT (2006). Golli protein negatively regulates store depletion-induced calcium influx in T cells. *Immunity* **24,** 717–727.

Gerstner JR, Lyons LC, Wright KP Jr, Loh DH, Rawashdeh O, Eckel-Mahan KL & Roman GW (2009). Cycling behavior and memory formation. *J Neurosci* **29,** 12824–12830.

Goodman AOG & Barker RA (2010). How vital is sleep in Huntington's disease? *J Neurol* **257,** 882–897.

Gray M, Shirasaki DI, Cepeda C, André VM, Wilburn B, Lu X-H, Tao J, Yamazaki I, Li S-H, Sun YE, Li X-J, Levine MS & Yang XW (2008). Full-length human mutant huntingtin with a stable polyglutamine repeat can elicit progressive and selective neuropathogenesis in BACHD mice. *J Neurosci* **28,** 6182–6195.

Hastings MH, Reddy AB & Maywood ES (2003). A clockwork web: circadian timing in brain and periphery, in health and disease. *Nat Rev Neurosci* **4,** 649–661.

Hickey MA, Kosmalska A, Enayati J, Cohen R, Zeitlin S, Levine MS & Chesselet M-F (2008). Extensive early motor and non-motor behavioral deficits are followed by striatal neuronal loss in knock-in Huntington's disease mice. *Neuroscience* **157,** 280–295.

Itri JN, Michel S, Vansteensel MJ, Meijer JH & Colwell CS (2005). Fast delayed rectifier potassium current is required for circadian neural activity. *Nat Neurosci* **8,** 650–656.

Itri JN, Vosko AM, Schroeder A, Dragich JM, Michel S & Colwell CS (2010). Circadian regulation of a-type potassium currents in the suprachiasmatic nucleus. *J Neurophysiol* **103,** 632–640.

Julien CL, Thompson JC, Wild S, Yardumian P, Snowden JS, Turner G & Craufurd D (2007). Psychiatric disorders in preclinical Huntington's disease. *J Neurol Neurosurg Psychiatr* **78,** 939–943.

Kalsbeek A, Perreau-Lenz S & Buijs RM (2006). A network of (autonomic) clock outputs. *Chronobiol Int* **23,** 521–535.

Ko GY-P, Shi L & Ko ML (2009). Circadian regulation of ion channels and their functions. *J Neurochem* **110,** 1150–1169.

Kobal J, Meglic B, Mesec A & Peterlin B (2004). Early sympathetic hyperactivity in Huntington's disease. *Eur J Neurol* **11,** 842–848.

Kobal J, Melik Z, Cankar K, Bajrovic FF, Meglic B, Peterlin B & Zaletel M (2010). Autonomic dysfunction in presymptomatic and early symptomatic Huntington's disease. *Acta Neurol Scand* **121,** 392–399.

Kremer HP, Roos RA, Dingjan G, Marani E & Bots GT (1990). Atrophy of the hypothalamic lateral tuberal nucleus in Huntington's disease. *J Neuropathol Exp Neurol* **49,** 371–382.

Kuhlman SJ & McMahon DG (2006). Encoding the ins and outs of circadian pacemaking. *J Biol Rhythms* **21,** 470–481.

Lanska DJ, Lanska MJ, Lavine L & Schoenberg BS (1988). Conditions associated with Huntington's disease at death. A case-control study. *Arch Neurol* **45,** 878–880.

Lavin PJ, Bone I & Sheridan P (1981). Studies of hypothalamic function in Huntington's chorea. *J Neurol Neurosurg Psychiatr* **44,** 414–418.

Levine MS, Cepeda C, Hickey MA, Fleming SM & Chesselet M-F (2004). Genetic mouse models of Huntington's and Parkinson's diseases: illuminating but imperfect. *Trends Neurosci* **27,** 691–697.

Loh DH, Navarro J, Hagopian A, Wang LM, Deboer T & Colwell CS (2010). Rapid changes in the light/dark cycle disrupt memory of conditioned fear in mice. *PLoS ONE*; DOI: 10.1371/journal.pone.0012546.

Mangiarini L, Sathasivam K, Seller M, Cozens B, Harper A, Hetherington C, Lawton M, Trottier Y, Lehrach H, Davies SW & Bates GP (1996). Exon 1 of the HD gene with an expanded CAG repeat is sufficient to cause a progressive neurological phenotype in transgenic mice. *Cell* **87,** 493–506.

Marcheva B, Ramsey KM, Buhr ED, Kobayashi Y, Su H, Ko CH, Ivanova G, Omura C, Mo S, Vitaterna MH, Lopez JP, Philipson LH, Bradfield CA, Crosby SD, JeBailey L, Wang X, Takahashi JS & Bass J (2010). Disruption of the clock components CLOCK and BMAL1 leads to hypoinsulinaemia and diabetes. *Nature* **466,** 627–631.

Massin MM, Maeyns K, Withofs N, Ravet F & Gérard P (2000). Circadian rhythm of heart rate and heart rate variability. *Arch Dis Child* **83,** 179–182.

Maywood ES, Fraenkel E, McAllister CJ, Wood N, Reddy AB, Hastings MH & Morton AJ (2010). Disruption of peripheral circadian timekeeping in a mouse model of Huntington's disease and its restoration by temporally scheduled feeding. *J Neurosci* **30,** 10199–10204.

Menalled L, El-Khodor BF, Patry M, Suárez-Fariñas M, Orenstein SJ, Zahasky B, Leahy C, Wheeler V, Yang XW, MacDonald M, Morton AJ, Bates G, Leeds J, Park L, Howland D, Signer E, Tobin A & Brunner D (2009). Systematic behavioral evaluation of Huntington's disease transgenic and knock-in mouse models. *Neurobiol Dis* **35,** 319–336.

Morton AJ, Wood NI, Hastings MH, Hurelbrink C, Barker RA & Maywood ES (2005). Disintegration of the Sleep-Wake Cycle and Circadian Timing in Huntington's Disease. *J Neurosci* **25,** 157–163.

Pack AI, Galante RJ, Maislin G, Cater J, Metaxas D, Lu S, Zhang L, Von Smith R, Kay T, Lian J, Svenson K & Peters LL (2007). Novel method for high-throughput phenotyping of sleep in mice. *Physiol Genomics* **28,** 232–238.

Pallier PN, Maywood ES, Zheng Z, Chesham JE, Inyushkin AN, Dyball R, Hastings MH & Morton AJ (2007). Pharmacological imposition of sleep slows cognitive decline and reverses dysregulation of circadian gene expression in a transgenic mouse model of Huntington's disease. *J Neurosci* **27,** 7869–7878.

Petersén A, Gil J, Maat-Schieman MLC, Björkqvist M, Tanila H, Araújo IM, Smith R, Popovic N, Wierup N, Norlén P, Li J-Y, Roos RAC, Sundler F, Mulder H & Brundin P (2005). Orexin loss in Huntington's disease. *Hum Mol Genet* **14,** 39–47.

Reid KJ & Zee PC (2009). Circadian rhythm disorders. *Semin Neurol* **29,** 393–405.

Schwartz MD & Smale L (2005). Individual differences in rhythms of behavioral sleep and its neural substrates in Nile grass rats. *J Biol Rhythms* **20,** 526–537.

Soneson C, Fontes M, Zhou Y, Denisov V, Paulsen JS, Kirik D & Petersén A (2010). Early changes in the hypothalamic region in prodromal Huntington disease revealed by MRI analysis. *Neurobiol Dis* **40,** 531–543.

Takahashi JS, Hong H-K, Ko CH & McDearmon EL (2008). The genetics of mammalian circadian order and disorder: implications for physiology and disease. *Nat Rev Genet* **9,** 764–775.

Teclemariam-Mesbah R, Kalsbeek A, Pevet P & Buijs RM (1997). Direct vasoactive intestinal polypeptide-containing projection from the suprachiasmatic nucleus to spinal projecting hypothalamic paraventricular neurons. *Brain Res* **748,** 71–76.

Thayer JF, Yamamoto SS & Brosschot JF (2010). The relationship of autonomic imbalance, heart rate variability and cardiovascular disease risk factors. *Int J Cardiol* **141,** 122–131.

Turek FW, Joshu C, Kohsaka A, Lin E, Ivanova G, McDearmon E, Laposky A, Losee-Olson S, Easton A, Jensen DR, Eckel RH, Takahashi JS & Bass J (2005). Obesity and metabolic syndrome in circadian Clock mutant mice. *Science* **308,** 1043–1045.

Wallick DW, Martin PJ, Masuda Y & Levy MN (1982). Effects of autonomic activity and changes in heart rate on atrioventricular conduction. *Am J Physiol* **243,** H523–527.

Wang LM-C, Dragich JM, Kudo T, Odom IH, Welsh DK, O'Dell TJ & Colwell CS (2009). Expression of the circadian clock gene Period2 in the hippocampus: possible implications for synaptic plasticity and learned behaviour. *ASN Neuro*; DOI: 10.1042/AN20090020.

Wood NI, Goodman AOG, van der Burg JMM, Gazeau V, Brundin P, Björkqvist M, Petersén A, Tabrizi SJ, Barker RA & Morton AJ (2008). Increased thirst and drinking in Huntington's disease and the R6/2 mouse. *Brain Res Bull* **76,** 70–79.

Wulff K, Porcheret K, Cussans E & Foster RG (2009). Sleep and circadian rhythm disturbances: multiple genes and multiple phenotypes. *Curr Opin Genet Dev* **19,** 237–246.

v. Baroreceptor reflex dysfunction in the BACHD mouse model of Huntington's disease.

Abstract

Huntington's disease is a progressive, neurodegenerative disorder that presents with a triad of clinical symptoms, which include movement abnormalities, emotional disturbance and cognitive impairment. Recent studies reported dysfunction of the autonomic nervous system in Huntington's disease patients, which may contribute to the increased incidence of cardiovascular events in this patient population that often leads to death. We measured the baroreceptor reflex, a process dependent on proper autonomic function, in the BACHD mouse model of Huntington's disease. We found a blunted response of the baroreceptor reflex as well as significantly higher daytime blood pressure in BACHD mice compared to WT controls, which are both indications of autonomic dysfunction. BACHD mice had increased heart weight to tibia length ratios at 7 and 12 mo of age suggesting hypertrophic changes of the heart, which we speculate is a response to the increased blood pressure and aberrant baroreceptor reflex. Despite these structural changes, the hearts of BACHD mice continue to function normally as assessed by echocardiographic analysis. Studies of autonomic and cardiovascular function in BACHD mice may help elucidate the pathology of Huntington's disease and aid in the development of clinical strategies to offset the incidence of fatal cardiovascular events in the Huntington's disease patient population.

Introduction

Huntington's disease is an autosomal dominant neurodegenerative disorder characterized by apoptotic death of neurons in various brain regions that result in the progressive deterioration of movement, cognitive abilities and behavioral control (Margolis & Ross, 2003).

In addition, Huntington's disease patients are at increased risk for cardiovascular morbidity and are likely to succumb to cardiovascular events (Chiu & Alexander, 1982; Lanska *et al.*, 1988). Recent studies reported that individuals with Huntington's disease display aberrant changes in the autonomic nervous system (ANS) that are detected even before the onset of other Huntington's disease symptoms. Misregulation of both the sympathetic and parasympathetic branches of the ANS have been described, whereby the sympathetic nervous system (SNS) becomes hyperactive in presymptomatic Huntington's disease patients while the activity of the parasympathetic nervous system (PNS) progressively declines (Sharma *et al.*, 1999; Andrich *et al.*, 2002; Kobal *et al.*, 2004, 2010; Bär *et al.*, 2008; Aziz *et al.*, 2010*a*). These types of changes in the ANS are associated with poor prognosis for serious cardiovascular events that many times lead to death (Algra *et al.*, 1993; Tsuji *et al.*, 1994; Dekker *et al.*, 1997). Further study of the cardiovascular system as well as autonomic activity in Huntington's disease patients may help in better understanding disease pathology that may lead to clinical strategies to help curb the number of cardiovascular events in the patient population.

Many mouse models of Huntington's disease have been created to recapitulate the various characteristics of the disease to allow for mechanistic investigations. In some of the models, a cardiovascular phenotype has been documented (Mihm *et al.*, 2007; Pattison *et al.*, 2008; Sassone *et al.*, 2009; Kudo *et al.*, 2011). We are particularly interested in the BACHD model: a transgenic mouse that expresses the expanded form of the human *htt* gene that encode 97 stable glutamine repeats (Gray *et al.*, 2008). BACHD mice develop HTT aggregates similar to adult onset Huntington's disease and display progressive motor deficits. There is also evidence for circadian deficits along with indications that the ANS is affected as measured by heart rate variability (Kudo *et al.*, 2011). Further investigations of this mouse model may help

elucidate the autonomic and cardiovascular pathology in Huntington's disease.

In this study, we investigated the cardiovascular phenotype in BACHD mice and report echocardiography, heart morphometry and baroreceptor reflex properties in middle-aged mice. The baroreceptor reflex is responsible for the overall tone as well as the acute moment-to-moment regulation of blood pressure (BP) by modulating cardiac output and total peripheral resistance (Pilowsky & Goodchild, 2002; Benarroch, 2008). The central autonomic network, which includes the nucleus tractus solitarius (NTS) and other nuclei, receive and integrate BP information from baroreceptor cells located in the carotid artery and aortic arch. The system responds by modulating autonomic outflow to various tissues of the body such as the heart, blood vessels and adrenal glands, in order to adjust BP accordingly (Pilowsky & Goodchild, 2002). Dysregulation of this reflex in the long run, may lead to detrimental consequences on the cardiovascular system (Timmers *et al.*, 2003). Effects on the heart can be assessed using echocardiography and morphometry measurements, which look for changes in heart function and structure, respectively. In our study, we find evidence for abnormal heart morphometry, changes in baseline BP, as well as a dysfunctional baroreceptor reflex response that would suggest dysregulation by the ANS.

Methods

Animals

BACHD mice on the C57BL6/J background (Gray *et al.*, 2008) along with littermate wild-type (WT) controls were obtained from the mouse mutant resource at JAX (The Jackson Laboratory, Bar Harbor, Maine) in a colony maintained by the CHDI Foundation. In order to obtain a sufficient number of animals for the baroreceptor studies, we included data from non-

littermate (n=4/8) C57BL6/J WT mice. Animals were housed in a controlled environment with a 12 hr light and 12 hr dark lighting cycle where lights-on occurred at 7am. All the animals used in these studies were subject to all recommendations for animal use and welfare outlined by the UCLA Division of Laboratory Animals, as well as guidelines from the National Institutes of Health. The protocols for these studies were approved by the UCLA Animal Research Committee.

Baseline Measurements and Baroreceptor Reflex

The administration of Angiotensin II (ATII) or Nitroprusside (NP) leads to episodes of hypertension or hypotension, respectively. Changes in BP as a result of drug administration should elicit a compensatory response of heart rate (HR) via the baroreceptor reflex in order to normalize BP levels. Differences in the ratio of change in HR to BP ($\Delta HR/\Delta BP$) may indicate aberrant signaling to the heart by the ANS. Baroreceptor function was examined in WT (n=8) and BACHD (n=6) mice (7-9 mo of age) between the times of 11am (zeitgeber time, ZT 4) and 4pm (ZT 9). During the experiment, HR was determined from the R-R interval of the electrocardiogram (EKG). Mice were anesthetized and both femoral arteries were catheterized, whereby BP measurements were collected from one artery and drugs were administered through the other artery. Following catheterization, isoflurane levels were decreased to between 1-1.5% and the mice were allowed to rest for at least 10 minutes. Baseline BP and HR were then recorded. Increasing concentrations of AT II (Low Dose (LD): 0.5, Mid Dose (MD): 1.0, High Dose (HD): 4.0 μg/kg) were administered, and each dose was followed by a flush of saline (+heparin 3U/mL) to ensure full delivery of the drugs. Increasing concentrations of NP (LD: 10, MD: 20, HD: 40 μg/kg) were then administered similarly. We spaced each drug infusion leaving

at least 10-15 minutes between administrations to allow BP and HR to return to baseline levels. As a control, we blocked both the muscarinic (75μg/kg glycopyrrolate) and β-adrenergic (750μg/kg propranolol) receptors before administering another HD dose of ATII and NP. We calculated the absolute value of the maximum change in BP as well as the subsequent directional change in HR. Ratios of these two values (ΔHR/ΔBP) reflect the magnitude HR change relative to the change in BP that characterizes the sensitivity of the baroreceptor response.

Echocardiography and Heart Morphometry

In order to assess cardiac function, WT (n=6) and BACHD (n=5) mice (11-12 mo) were subject to a two-dimensional, M-mode echocardiography and spectral Doppler images acquired by a Siemens Acuson Sequoia C256 equipped with a 15L8 15MHz probe (Siemens Medical Solutions, Mountain View, CA) as previously described (Jordan *et al.*, 2010). Mice were lightly anesthetized with 1% isoflurane vaporized in oxygen (Summit Anesthesia Solutions, Bend, OR). The HR was determined from the R-R intervals of their EKG and was maintained at physiological levels (between 450 and 650 bpm) during the procedure. Parameters measured include: Ventricular Septal Thickness (VST), End Diastolic Diameter (EDD), Posterior Wall Thickness (PWT), End Systolic Diameter (ESD), Aortic Ejection Time (Ao-ET), Left Ventricular percent Fractional Shortening (LV%FS), Left Ventricular Ejection Fraction (LvEF), Left Ventricular Mass (LVmass), and Early Diastole/Atrial contraction ratio (E/A).

Body weight (BW), heart weight (HW) and tibia length (TL) were measured from 7-8 mo (WT: n=5; BACHD: n=7) and 12 mo old (WT: n=6; BACHD: n=5) mice. HW/TL or HW/BW ratios were calculated to determine if there are differences in heart morphometry.

Statistics

Baseline BP, HR as well as echocardiogram parameters were compared using a Student's t-test. A two-way repeated measures ANOVA was used to analyze the Baroreceptor data (genotype x drug concentration) and a two-way ANOVA was used to analyze the morphometry data (genotype x age).

Results

Baseline BP and HR in anesthetized mice

To begin to determine whether BACHD mice show dysfunction in the cardiovascular system, we measured baseline BP and HR in lightly anesthetized WT (n=8) and BACHD mice (n=6; 7-9 mo of age). Systolic BP was significantly higher in BACHD mice (108.0 ± 6.9 mmHg) compared to WT controls (86.1 ± 3.2 mmHg*;* t_{12}=-3.13, P=0.009) although BP levels were still considered to be within the normal range. BACHD mice also displayed increased HRs (615 ± 23 bpm) compared to WTs (537 ± 21 bpm; T=61.0, P=0.043). The increased BP and HR measured in BACHD mice reflect a change in the regulation of the cardiovascular system. Although the BP levels are still normal, the increase may be indicative of future susceptibility for cardiovascular events.

Baroreceptor Reflex

There is evidence that the ANS is dysfunctional in patients with Huntington's disease. It has also been reported that BACHD mice have significantly decreased HRV indicative of abnormal signal input to the heart by the ANS (Kudo *et al.*, 2011). We measured the baroreceptor reflex of BACHD and WT mice to determine whether this feedback mechanism of

regulating BP, which is mediated by the ANS, is also disrupted. Changes in the ratios between the magnitude change in BP and HR after ATII (vasoconstrictor) or NP (vasodilator) administration, may indicate aberrant signaling to the heart by the ANS.

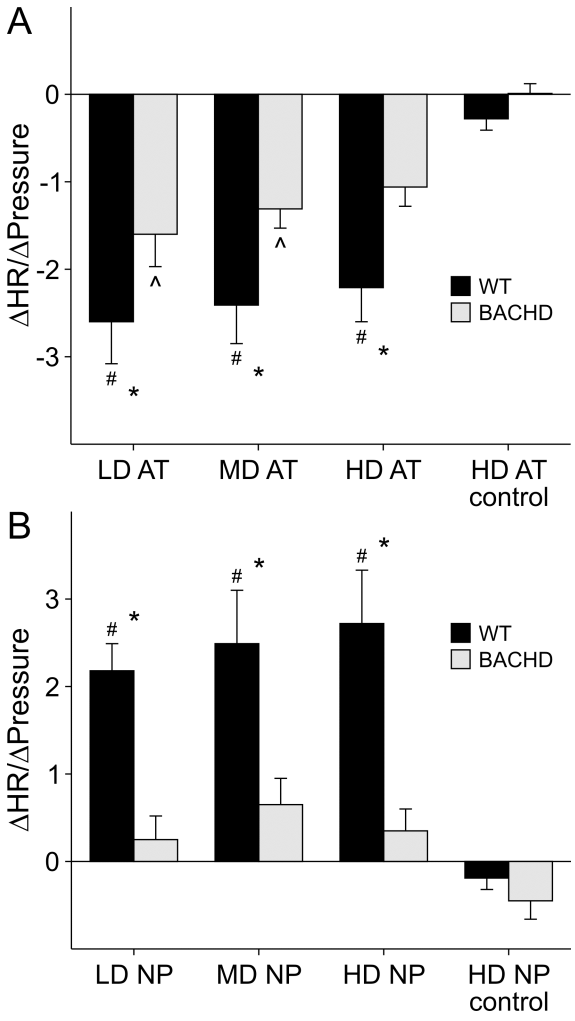

Figure 2-8: *Baroreceptor Reflex in WT and BACHD mice. Mice were administered increasing concentrations of ATII (A) and NP (B). For control conditions, mice were primed with muscarinic and β-blockers before administration of the HD of ATII and NP. The maximum change in HR (ΔHR) and the absolute value of the maximum change in BP (ΔBP) following drug administration was measured. We compared ΔHR/ΔBP among the different groups using a 2-way repeated measures ANOVA. # significant response compared to control conditions in WT mice. ^ significant response compared to control conditions in BACHD mice. * significant difference between WT and BACHD mice.*

Increasing concentrations of ATII (LD-0.5, MD-1.0, HD-4.0 μg/kg) were administered to mildly anesthetized WT and BACHD mice. By 2-way repeated measures ANOVA, we detected

significant variation between genotype ($F_{1,55}$=7.28, P=0.019) and concentration of ATII drug ($F_{3,55}$=16.94, P<0.001), but no significant interaction between genotype and drug concentration ($F_{3,55}$=0.88, P=0.46; **Fig. 2-8A**). Post *hoc* analysis indicate significant responses to all concentrations of AT II in WT mice when compared to the control conditions where the β- and muscarinic receptors were respectively blocked with propranolol and glycopyrrolate before administration of a HD of ATII (control vs. LD: t_{14}= 2.32, P<0.01; control vs. MD: t_{14}= 2.13, P<0.001; control vs. HD: t_{14}= 1.50, P<0.001). Compared to controls, BACHD mice showed a significant difference in ΔHR/ΔBP ratio when administered the LD and MD of ATII, but did not have a significant response to the HD (control vs. LD: t_{10}= 3.49, P=0.008; control vs. MD: t_{10}= 2.87, P=0.041; control vs. HD: t_{10}= 2.31, P=0.16). For each of the doses of ATII, the HR of BACHD mice responded with less magnitude compared to WT mice (LD: t_{12}= 2.03, p=0.049; MD: t_{12}= 2.21, p=0.033; HD: t_{12}= 2.33, P=0.025). There was no difference in the ΔHR/ΔBP ratios between WT and BACHD mice when the β- and muscarinic receptors were blocked (control: t_{14}= 0.58, P=0.56).

To test the HR response of WT and BACHD mice to decreases in BP, we administered increasing concentrations of NP (LD- 10, MD- 20, HD- 40 μg/kg). By 2-way repeated measures ANOVA, we detected significant interaction between genotype and concentrations of NP drug ($F_{3,55}$=4.079, P=0.014, **Fig. 2-8B**). Post *hoc* analysis detects a significant response to all concentrations of NP in WT mice when compared to the control (control vs. LD: t_{14}= 5.62, P<0.001; control vs. MD: t_{14}= 6.35, P<0.001; control vs. HD: t_{14}= 6.89, P<0.001). BACHD mice, on the other hand, did not show any significant response for any of the concentrations of NP when compared to the control condition (control vs. LD: t_{10}= 1.43, P=0.96; control vs. MD: t_{10}= 2.26, P=0.18; control vs. HD: t_{10}= 1.66, P=0.64). For each of the doses of NP, BACHD had

significantly lower responses compared to WT mice (LD: t_{12}= 3.32, P=0.002; MD: t_{12}= 3.17, P=0.003; HD: t_{12}= 4.05, P<0.001). When mice were primed with β- and muscarinic receptor blockers, there was no difference in ΔHR/ΔBP ratios between WT and BACHD mice after HD NP administration (control: t_{12}= 0.46, P=0.65).

These data suggest that middle-aged BACHD mice have dysfunctional baro-receptor reflexes compared to WT controls. BACHD mice are unable to appropriately modulate their HRs in response to either an increase or decrease in BP.

Morphometry

Increases in BP and changes in baro-receptor reflex function may lead to cardiac hypertrophy. We used a standard measure of heart morphometry by calculating the ratio of heart weight (HW) relative to body weight (BW) or tibia length (TL) in 7-8 mo and 12 mo old WT and BACHD mice.

Table 1:
Morphometry Measurements of WT and BACHD Mice

Genotype	Age	BW (g)	HW (mg)	TL (mm)
WT	7 mo	29.5 ± 2.8*	140.3 ± 6.7*#	17.3 ± 0.2*#
	12 mo	35.3 ± 2.5	161.3 ± 6.1	18.2 ± 0.2
BACHD	7 mo	41.5 ± 2.4	165.6 ± 5.7	18.0 ± 0.2
	12 mo	40.9 ± 2.8	182.0 ± 6.7	18.3 ± 0.2

Table 2-6: *Morphometry measurements of WT and BACHD mice. * significance between genotypes. # significance between ages.*

In comparing the morphometry parameters among the various groups by 2-way ANOVA, we detected a significant effect of genotype on BW ($F_{1,22}$=11.36, P=0.003), with BACHD mice displaying increased BW at 7mo. of age (t_{12}=3.31, P=0.004) when compared to WT mice, but

this difference is no longer detected between genotypes at 12 mo of age (t_{12}=*1.49,* P=0.15; **Table 2-6**). When comparing the HWs, we found a significant effect of genotype ($F_{1,22}$=13.20, P=0.002) and age ($F_{1,22}$=8.78, P=0.008), but no significant interaction between genotype and age ($F_{1,22}$=0.13, P=0.72; **Table 2-6**). The HWs of WT mice increased as they aged (t_{14}=1.31, P=0.032), but at both age groups, the HW of BACHD mice were significantly higher when compared to WT mice (7mo.: t_{12}=*2.87,* P=*0.01;* 12mo*:* t_{12}=2.28, P=0.035). Lastly, we found a significant effect of age ($F_{1,22}$=7.16, P=0.015) when comparing TL (**Table 2-6**). The TL of WT mice increased as they aged (t_{14}=2.88, P=0.01), but this trend was not detected in BACHD mice. Similar to BW, the TLs of BACHD mice were longer at 7mo. (t_{12}= 2.43, P=0.025) compared to WT mice, but not at 12 mo of age (t_{12}= 0.32, P=0.76).

We did not find significant differences in the HW/BW ratios between WT and BACHD mice by 2-way ANOVA (age: $F_{1,22}$=0.66, P=0.43; genotype: $F_{1,22}$=2.85, P=0.108; age X genotype: $F_{1,22}$=2.22, P=0.15), but measured significant differences in the HW/TL ratios between the two genotypes (**Fig. 2-9**). By 2-way ANOVA, we find a significant effect of genotype ($F_{1,22}$=10.50, P=0.004) and age ($F_{1,22}$=5.31, P=0.033), but do not detect an interaction between genotype and age ($F_{1,22}$=0.001, P=0.97). The HW/TL ratios did not change as BACHD or WT mice aged (WT: t_9=0.131, P>0.05; BACHD: t_{10}=0.108, P>0.05), but the HW/TL ratios were significantly higher in BACHD mice compared to WT mice at both ages (7mo: t_{10}=2.30, P=0.033; 12mo: t_9=2.28, P=0.034). These data indicate that the hearts of BACHD mice are increased in weight in relation to body frame and may be undergoing some form of remodeling.

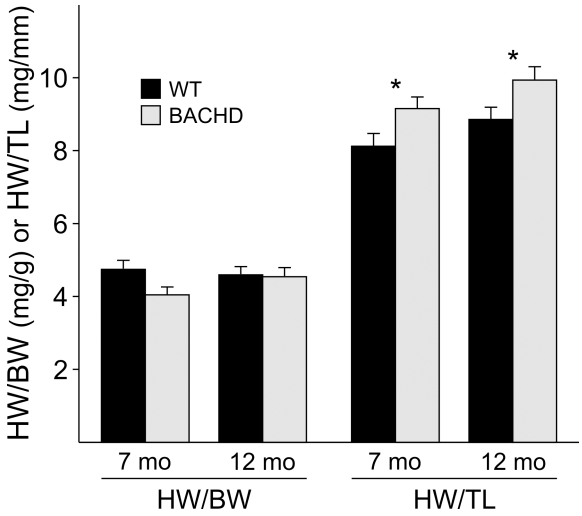

Figure 2-9: *Heart Morphometry comparisons between WT and BACHD mice at 7 mo and 12 mo of age. HW/BW or HW/TL were calculated for all genotypes and age groups and compared using a 2-way ANOVA. * significant difference between genotypes.*

Echocardiographic Analysis

Changes in the morphology of the hearts of BACHD mice, could cause aberrant modifications in heart function. Therefore, we subjected BACHD and WT mice to echocardiographic analysis at about 12 mo of age in order to assess heart function. We found no significant differences in any of the parameters measured (**Table 2-7**). Though not statistically significant, the wall thicknesses and LV mass were slightly higher in the BACHD mice consistent with the morphometry data. Despite indications of abnormal regulation of BP and baroreflex, the hearts of BACHD mice continue to function normally at this age as assessed by echocardiogram.

Table 2:
Echocardiogram Parameters in 12 mo old WT and BACHD Mice

Echocardiogram Parameters	WT	BACHD
HR (bpm)	531 ± 26	512 ± 23
VST (mm)	0.53 ± 0.01	0.58 ± 0.02
EDD (mm)	4.18 ± 0.09	4.16 ± 0.09
PWT (mm)	0.53 ± 0.03	0.59 ± 0.03
ESD (mm)	2.80 ± 0.13	2.74 ± 0.05
A0-ET (ms)	49.4 ± 2.1	48.3 ± 1.5
LV % FS	33.2 ± 2.3	34.1 ± 1.2
Vcf	6.75 ± 0.50	7.07 ± 0.30
LvEF	67.6 ± 3.2	68.4 ± 1.4
LvMass	75.3 ± 4.5	83.9 ± 4.7
E	0.82 ± 0.05	0.85 ± 0.11
A	0.39 ± 0.03	0.42 ± 0.02
E/A	2.11 ± 0.10	2.02 ± 0.13

Table 2-7: *Echocardiogram parameters in 12 mo old WT and BACHD mice. No significant differences were detected between genotypes using a Student's t-test. HR- Heart Rate; VST-Ventricular Septal Thickness, EDD- End Diastolic Diameter, PWT- Posterior Wall Thickness, ESD- End Systolic Diameter, Ao-ET- Aortic Ejection Time, LV%FS- Left Ventricular percent Fractional Shortening, LvEF- Left Ventricular Ejection Fraction, LVMass- Left Ventricular Mass, and E/A- Early Diastole/Atrial contraction ratio.*

Discussion

We report dysfunction of the ANS in BACHD mice, as measured by the baroreceptor reflex. Furthermore, baseline measurements of BP and HR were higher in BACHD mice compared to WT controls. Lastly, we find changes in the morphometry of the heart, but echocardiography did not detect any functional changes at 12 mo of age.

The increased baseline BP levels measured in lightly anesthetized BACHD mice indicate changes in the overall regulation of BP tone. Importantly, these BP recordings were taken during the day, a time in the resting period of mice when BP is expected to be low. These increased BP levels parallel the reported increase in HR of BACHD mice also measured during the day (Kudo *et al.*, 2011), suggesting a global dysregulation of the cardiovascular system

causing it to be hyperactive during the rest period. The blunted depression in BP levels during rest would be similar to a nondipping pressure profile observed in humans, which in many cases is an indication of dysautonomia (Kanbay *et al.*, 2008; Myredal *et al.*, 2010). Nondippers have a higher risk for future cardiovascular events, as well as damage to other organs (White, 2007; Kanbay *et al.*, 2008). Published reports of BP in Huntington's disease patients do not detect significant differences compared to control groups, however BP measurements were taken during the day when patients are in a more active state, which could mask the higher levels of BP tone (Andrich *et al.*, 2002; Bär *et al.*, 2008). This appears to be the case for HR in BACHD mice, as HR levels are not significantly different between WT and BACHD mice during the active period (Kudo *et al.*, 2011). Therefore, it may be valuable to examine nighttime BP and HR in Huntington's disease patients, as well as pursue circadian studies of BP in awake and freely moving BACHD mice, which would further explore the extent of dysregulation in BP. It is important to note that the BWs of BACHD mice are significantly increased at 7 mo of age compared to WT mice, possibly due to hypoactivity (Oakeshott *et al.*, 2011; Kudo *et al.*, 2011), which may contribute to the observed increase in BP in BACHD mice. This increased BW is transient, as the BWs are no longer significantly different at 12 mo of age. Comparisons of BP at this older age may indicate whether heavier BW and/or other mechanisms of BP regulation are factors involved in the increase of BP observed in BACHD mice.

The BACHD mice showed deficits in the baroreceptor reflex, whereby the response in HR to the transient hyper- and hypotension induced by ATII and NP, respectively, is blunted compared to WTs. This blunted response in both directions of the reflex suggests that both branches of the ANS may be affected. The primary deficit in the baroreceptor reflex in BACHD mice is unknown, as this process is mediated by various regions of the brain that include the

brainstem and hypothalamus, along with possible deficits in the outputs from the central autonomic nervous system (Kobal *et al.*, 2004; Benarroch, 2008; Oakeshott *et al.*, 2011). *Htt* deposits are found globally in BACHD mice, which could disrupt function among cells in the baroreceptor pathway, even without evidence for gross degeneration of these brain regions (Gray *et al.*, 2008). In HD patients, the detection of alterations in the baroreceptor pathway, such as the vagal nuclei and cerebral cortex, are establishing structural cause for the dysfunction (Benarroch, 1993; Squitieri *et al.*, 2001; Andrich *et al.*, 2002; Ma *et al.*, 2002; Kobal *et al.*, 2004). Ideally, identification of the site of dysfunction could be used to devise an appropriate therapeutic approach to manage symptomatic HD patients (Izzo & Taylor, 1999). In humans, similar studies have been conducted to test the response of the baroreceptor reflex. Results have been mixed, however recent studies report deficits during the Valsalva maneuver, hand-grip test, and the head up tilt test (Den Heijer *et al.*, 1988; Izzo & Taylor, 1999; Sharma *et al.*, 1999; Andrich *et al.*, 2002). Furthermore, patients complain of dizziness and light-headedness upon standing, which are symptoms of baroreceptor dysregulation resulting in orthostatic hypotension (Kobal *et al.*, 2004; Aziz *et al.*, 2010*a*). Other measurements such as Heart Rate Variability and sympathetic skin response suggest that both branches of the ANS are disrupted in HD patients (Sharma *et al.*, 1999; Andrich *et al.*, 2002; Kobal *et al.*, 2004). During the very early stages of HD, the sympathetic nervous system appears to be hyperactive (Kobal *et al.*, 2004, 2010; Bär *et al.*, 2008). As the disease advances, parasympathetic activity progressively decreases (Sharma *et al.*, 1999; Andrich *et al.*, 2002; Bär *et al.*, 2008). In our experiments, the blunted increase in HR after NP administration in BACHD mice may be a result of a ceiling effect for sympathetic activity, in that the range for further activation is limited due to an already hyperactive sympathetic nervous system. The blunted decrease in HR after ATII administration may be a

result of the dysfunction of both branches of the autonomic nervous system. The hyperactivity of the sympathetic nervous system may not allow the HR to fully depress and in addition, the progressive dysfunction of the parasympathetic nervous system may be inadequate to slow HR. Tests to measure both the sympathetic and parasympathetic nervous system activity in BACHD mice would be able to determine the extent of the dysfunction of each of the branches.

There is a high prevalence of autonomic dysfunction in Huntington's disease patients that manifest as various clinical symptoms and signs such as gastrointestinal complaints, urinary difficulties and postural dizziness (Aziz *et al.*, 2010*a*). More profound may be the increased risk of cardiac arrhythmias, and the development of coronary heart disease, that result in a significant number of deaths within the Huntington's disease population (Aminoff & Gross, 1974; Chiu & Alexander, 1982; Lanska *et al.*, 1988; Andrich *et al.*, 2002). Importantly, these autonomic symptoms occur before any motor deficits, therefore measures of autonomic dysfunction could be a valuable tool in Huntington's disease diagnosis and staging (Kobal *et al.*, 2010; Aziz *et al.*, 2010*a*). Upon diagnosis, vigilant monitoring of the cardiovascular system may help deter the incidence of fatal events. We were able to measure changes in the morphometry of the heart in BACHD mice relative to body frame size (TL), which could indicate the start of cardiac remodeling in response to the increased BP and aberrant autonomic signaling. Echocardiogram results do not show functional changes in the hearts of BACHD mice, suggesting that the hearts at this stage of the disease are still able to compensate despite the morphological and physiological changes in the cardiovascular system. The R6/2 Huntington disease mouse model, which display a more rapid disease progression, develop serious cardiac dysfunction suggesting a cardiotoxic effect of *htt* deposits in the heart (Sassone *et al.*, 2009), and we speculate that BACHD mice may develop cardiac dysfunction at an older age. Future work can be directed to

study the susceptibility of this BACHD model to cardiovascular stresses as well as design management strategies focused on cardiovascular health to offset and reduce the chances of serious cardiovascular events in HD patients.

vi. Bibliography

Algra A, Tijssen JG, Roelandt JR, Pool J & Lubsen J (1993). Heart rate variability from 24-hour electrocardiography and the 2-year risk for sudden death. *Circulation* **88,** 180–185.

Aminoff MJ & Gross M (1974). Vasoregulatory activity in patients with Huntington's chorea. *J Neurol Sci* **21,** 33–38.

Andrich J, Schmitz T, Saft C, Postert T, Kraus P, Epplen JT, Przuntek H & Agelink MW (2002). Autonomic nervous system function in Huntington's disease. *J Neurol Neurosurg Psychiatr* **72,** 726–731.

Aziz NA, Anguelova GV, Marinus J, van Dijk JG & Roos RAC (2010). Autonomic symptoms in patients and pre-manifest mutation carriers of Huntington's disease. *Eur J Neurol* **17,** 1068–1074.

Bär KJ, Boettger MK, Andrich J, Epplen JT, Fischer F, Cordes J, Koschke M & Agelink MW (2008). Cardiovagal modulation upon postural change is altered in Huntington's disease. *Eur J Neurol* **15,** 869–871.

Benarroch EE (1993). The central autonomic network: functional organization, dysfunction, and perspective. *Mayo Clin Proc* **68,** 988–1001.

Benarroch EE (2008). The arterial baroreflex: functional organization and involvement in neurologic disease. *Neurology* **71,** 1733–1738.

Chiu E & Alexander L (1982). Causes of death in Huntington's disease. *Med J Aust* **1,** 153.

Dekker JM, Schouten EG, Klootwijk P, Pool J, Swenne CA & Kromhout D (1997). Heart rate variability from short electrocardiographic recordings predicts mortality from all causes in middle-aged and elderly men. The Zutphen Study. *Am J Epidemiol* **145,** 899–908.

Gray M, Shirasaki DI, Cepeda C, André VM, Wilburn B, Lu X-H, Tao J, Yamazaki I, Li S-H, Sun YE, Li X-J, Levine MS & Yang XW (2008). Full-length human mutant huntingtin with a stable polyglutamine repeat can elicit progressive and selective neuropathogenesis in BACHD mice. *J Neurosci* **28,** 6182–6195.

Den Heijer JC, Bollen WL, Reulen JP, van Dijk JG, Kramer CG, Roos RA & Buruma OJ (1988). Autonomic nervous function in Huntington's disease. *Arch Neurol* **45,** 309–312.

Izzo JL Jr & Taylor AA (1999). The sympathetic nervous system and baroreflexes in hypertension and hypotension. *Curr Hypertens Rep* **1,** 254–263.

Jordan MC, Henderson SA, Han T, Fishbein MC, Philipson KD & Roos KP (2010). Myocardial function with reduced expression of the sodium-calcium exchanger. *J Card Fail* **16,** 786–796.

Kanbay M, Turgut F, Uyar ME, Akcay A & Covic A (2008). Causes and mechanisms of nondipping hypertension. *Clin Exp Hypertens* **30,** 585–597.

Kobal J, Meglic B, Mesec A & Peterlin B (2004). Early sympathetic hyperactivity in Huntington's disease. *Eur J Neurol* **11,** 842–848.

Kobal J, Melik Z, Cankar K, Bajrovic FF, Meglic B, Peterlin B & Zaletel M (2010). Autonomic dysfunction in presymptomatic and early symptomatic Huntington's disease. *Acta Neurol Scand* **121,** 392–399.

Kudo T, Schroeder A, Loh DH, Kuljis D, Jordan MC, Roos KP & Colwell CS (2011). Dysfunctions in circadian behavior and physiology in mouse models of Huntington's disease. *Experimental Neurology* **228,** 80–90.

Lanska DJ, Lanska MJ, Lavine L & Schoenberg BS (1988). Conditions associated with Huntington's disease at death. A case-control study. *Arch Neurol* **45,** 878–880.

Ma X, Abboud FM & Chapleau MW (2002). Analysis of afferent, central, and efferent components of the baroreceptor reflex in mice. *Am J Physiol Regul Integr Comp Physiol* **283,** R1033–1040.

Margolis RL & Ross CA (2003). Diagnosis of Huntington disease. *Clin Chem* **49,** 1726–1732.

Mihm MJ, Amann DM, Schanbacher BL, Altschuld RA, Bauer JA & Hoyt KR (2007). Cardiac dysfunction in the R6/2 mouse model of Huntington's disease. *Neurobiol Dis* **25,** 297–308.

Myredal A, Friberg P & Johansson M (2010). Elevated myocardial repolarization lability and arterial baroreflex dysfunction in healthy individuals with nondipping blood pressure pattern. *Am J Hypertens* **23,** 255–259.

Oakeshott S, Balci F, Filippov I, Murphy C, Port R, Connor D, Paintdakhi A, Lesauter J, Menalled L, Ramboz S, Kwak S, Howland D, Silver R & Brunner D (2011). Circadian Abnormalities in Motor Activity in a BAC Transgenic Mouse Model of Huntington's Disease. *PLoS Curr* **3,** RRN1225.

Pattison JS, Sanbe A, Maloyan A, Osinska H, Klevitsky R & Robbins J (2008). Cardiomyocyte expression of a polyglutamine preamyloid oligomer causes heart failure. *Circulation* **117,** 2743–2751.

Pilowsky PM & Goodchild AK (2002). Baroreceptor reflex pathways and neurotransmitters: 10 years on. *J Hypertens* **20,** 1675–1688.

Sassone J, Colciago C, Cislaghi G, Silani V & Ciammola A (2009). Huntington's disease: the current state of research with peripheral tissues. *Exp Neurol* **219,** 385–397.

Sharma KR, Romano JG, Ayyar DR, Rotta FT, Facca A & Sanchez-Ramos J (1999). Sympathetic skin response and heart rate variability in patients with Huntington disease. *Arch Neurol* **56,** 1248–1252.

Squitieri F, Cannella M, Giallonardo P, Maglione V, Mariotti C & Hayden MR (2001). Onset and pre-onset studies to define the Huntington's disease natural history. *Brain Res Bull* **56,** 233–238.

Timmers HJLM, Wieling W, Karemaker JM & Lenders JWM (2003). Denervation of carotid baro- and chemoreceptors in humans. *J Physiol (Lond)* **553,** 3–11.

Tsuji H, Venditti FJ Jr, Manders ES, Evans JC, Larson MG, Feldman CL & Levy D (1994). Reduced heart rate variability and mortality risk in an elderly cohort. The Framingham Heart Study. *Circulation* **90,** 878–883.

White WB (2007). Importance of blood pressure control over a 24-hour period. *J Manag Care Pharm* **13,** 34–39.

CHAPTER 3

i. Introduction

In the published paper entitled "Circadian Regulation of Cardiovascular Function: a role for Vasoactive Intestinal Peptide" by Schroeder et al 2011, we found a disruption in the diurnal and circadian rhythms of ECG parameters, Heart Rate Variability, HR, body temperature and cage activity in VIP-deficient mice. The QT interval of the ECG waveform was significantly elongated in the VIP-deficient mice. Acute HR responses appear to be intact in VIP-deficient mice but respond differently compared to WT. Lastly, we found robust rhythms in clock gene expression in the hearts of VIP-deficient mice under LD conditions, but these rhythms were significantly phase advanced compared to WT mice.

ii. Circadian Regulation of Cardiovascular Function: a role for vasoactive intestinal peptide.

Abstract

The circadian system, driven by the suprachiasmatic nucleus (SCN), regulates properties of cardiovascular function. The dysfunction of this timing system can result in cardiac pathology. The neuropeptide vasoactive intestinal peptide (VIP) is crucial for circadian rhythms in a number of biological processes including SCN electrical activity and wheel running behavior. Anatomical evidence indicates that SCN neurons expressing VIP are well-positioned to drive circadian regulation of cardiac function through interactions with the autonomic centers. In this study, we tested the hypothesis that loss of VIP would result in circadian deficits in heart rate (HR) and clock gene expression in cardiac tissue. We implanted radio-telemetry devices into VIP-deficient mice and wildtype (WT) controls and continuously recorded HR, body temperature and cage activity in freely moving mice. In light/dark conditions, VIP-deficient mice displayed weak rhythms in HR, body temperature and cage activity, with onsets that were advanced in phase compared to WTs. Similarly, clock gene expression in cardiac tissue was rhythmic but phase advanced in the mutant mice. In constant darkness, the normal circadian rhythms in HR were lost in the VIP-deficient mice; however, most mutant mice continued to exhibit circadian rhythms of body temperature with shortened free-running period. The loss of VIP altered, but did not abolish, autonomic regulation of HR. Analysis of the echocardiograms did not find any evidence for a loss of cardiac function in the VIP-deficient mice, and the size of the hearts did not differ between genotypes. These results demonstrate that VIP is an important regulator of physiological circadian rhythmicity in the heart.

Introduction

Circadian rhythms are an endogenous timing mechanism that coordinates behavioral, physiological, and biochemical processes with the 24-hour environment of light and dark (Takahashi *et al.*, 2008). The site of the core circadian clock lies in a bilaterally paired nucleus located in the hypothalamus called the suprachiasmatic nucleus (SCN). Neurons from this region have the intrinsic ability to generate circadian rhythms in electrical activity, secretion, and metabolism. These intrinsic rhythms are generated by a cell-autonomous molecular feedback loop driving rhythmic transcription and translation of key clock genes such as *Period (Per1, Per2), Cryptochrome (Cry1, Cry2), Clock (Clk)* and *Bmal1* (Ko & Takahashi, 2006).

Recently, it has become clear that mammals exhibit robust circadian rhythms in cardiovascular function that are dependent upon signals from the SCN. Cardiovascular parameters such as heart rate (HR) and blood pressure are elevated during periods of wake and depressed during periods of sleep in anticipation of the level of physical activity and physiological demands of the organism (Guo & Stein, 2003). Cardiac tissue also exhibits rhythmic expression of clock genes (Oishi *et al.*, 1998; Sakamoto & Ishida, 2000; Martino *et al.*, 2004; Guo *et al.*, 2005). The function of such oscillations in the heart is unknown, but a reasonable assumption is that these molecular oscillations serve to gate information from the SCN to heart-specific rhythmic outputs. Circadian rhythms of HR and clock gene expression in the heart disappear when the SCN is lesioned (Witte *et al.*, 1998; Scheer *et al.*, 2001; Martino *et al.*, 2008).

In humans, the onset of cardiovascular events such as myocardial ischemia, infarctions, and arrhythmias cluster around the morning period suggesting influence by the circadian system (Muller *et al.*, 1985, 1989; Marler *et al.*, 1989; Hu *et al.*, 2004). Furthermore, disruptions in the circadian system caused by shiftwork, is associated with increased incidence of cardiovascular

disease and mortality (Knutsson *et al.*, 1986; Tüchsen, 1993; Stoynev & Minkova, 1998; Brown *et al.*, 2009). Work using animal models supports the view that circadian rhythmicity may be a critical aspect of cardiovascular health. Circadian perturbations have been shown to exacerbate heart disease and decrease survival in cardiomyopathic hamsters (Martino *et al.*, 2007, 2008). It has also been shown that the deletion of *mPer2* in all tissues provided a protective measure against myocardial infarction (Virag *et al.*, 2010). These studies suggest a complex interaction between circadian rhythms and cardiovascular function exists that influences cardiovascular disease progression.

The neuropeptide VIP and its receptor $VPAC_2R$ are critical for normal circadian function. The loss of VIP signaling has been shown to abolish electrical rhythmicity in a subgroup of SCN neurons, while those that remain rhythmic exhibit a decrease in cellular coupling (Aton *et al.*, 2005; Maywood *et al.*, 2006; Brown *et al.*, 2007; Vosko *et al.*, 2007). Many SCN neurons that project to extra-SCN tissues and peripheral outputs are VIPergic and therefore, VIP may be required for communication between the SCN and peripheral tissues to drive rhythms in behavior and other biological processes (Kalsbeek *et al.*, 1993; Ban *et al.*, 1997; Sollars & Pickard, 1998). Indeed, studies of circadian output in VIP-deficient mice demonstrate that VIP is critical for normal circadian rhythms in wheel running behavior, metabolic processes and plasma corticosterone levels (Colwell *et al.*, 2003; Loh *et al.*, 2008; Bechtold *et al.*, 2008; Pantazopoulos *et al.*, 2010). This study examines the effect of the loss of VIP on rhythms and function of the heart. In addition, we concurrently measure rhythms of body temperature and cage activity, which enables comparison of the effects of the loss of VIP on various physiological measurements.

Materials and Methods

Experimental Animals

To study the effects of the loss of VIP on circadian rhythms of HR, body temperature, and cage activity, we utilized adult male C57BL/6J mice lacking the genes encoding for VIP and PHI (VIP-/-). As controls, littermate or age-matched mice from other litters were used. All animal experimentations were conducted in accordance to the recommendations and guidelines of the UCLA Division of Laboratory Animals and the National Institutes of Health.

Mice were placed in a cage in the absence of a running wheel. Under light/dark (LD) conditions, Zeitgeber (ZT) 0 is defined as the time of lights on and ZT 12 as the time of lights off. Under constant darkness (DD), Circadian Time (CT) 12 is defined as the onset of increased activity (point of half-maximal rise) in heart rate (HR), body temperature or cage activity. In VIP-deficient mice, we often find circadian arrhythmicity of HR and cage activity, but concurrently detect rhythms in body temperature in the same animal. In order to produce group mean waveforms and analyze subjective day/night differences in these cases, we utilized the onset of body temperature to define CT 12 for HR and cage activity.

Telemetry Measurements

WT and VIP-deficient mice (3-4 mo) were surgically implanted with a wireless radiofrequency transmitter (ETA-F20, Data Sciences International, St. Paul, MN). Mice were housed in individual cages in the absence of a running wheel. Cages were placed atop telemetry receivers (Data Sciences International) in a light and temperature-controlled chamber. Standard rodent chow was provided ad libitum. Data collection began 2 weeks post-surgery, to allow mice to recover in the 12:12 LD cycle. We recorded 20 sec of ECG and measured average body

temperature and cage activity every 10 min for approximately 15 days. Lights were then turned off and measurements continued in DD for another 15-20 days. HR is extrapolated from ECG waveforms using the RR interval. Upon completion of LD and DD recordings, the mice (5-6 mo old) were used for the light exposure and exercise experiments described below.

ECG and Circadian Analysis

A 20 sec ECG recording every hour was used to calculate ECG intervals (RR, PR, QRS, QT and QTc) using Ponemah Analysis Software (Data Sciences International) at timepoints ZT 2-4 and ZT 14-16 (LD conditions). Heart Rate Variability (HRV) in the time-domain (standard deviation of all normal R-R intervals, SDNN) was calculated using the Data Science International Analysis software. Circadian rhythms of HR, body temperature and cage activity were analyzed by periodogram analysis combined with a χ^2 test (El Temps software, Barcelona Spain). The strongest amplitude (=power) of periodicities (within 20 and 31 hr limits) was compared between WT and VIP-deficient mice. The amplitude of the χ^2 test determines the period of a rhythm and its robustness.

Acute effects of Light

In order to examine the acute, photic regulation of HR, we adapted a protocol previously described in rats (Scheer *et al.*, 2001). Six days of 8-hr HR recording from ZT 13 to 20 were averaged and served as control. On the seventh day, mice were exposed to light starting at ZT14 and then returned to dark conditions at ZT 15. Recording continued until HR returned to baseline levels. During this experiment, ECG, body temperature and cage activity data were recorded every min.

Acute effects of Exercise

Baseline HR was recorded for 20 min prior to forced exercise. Mice were placed on a motorized running wheel (Rota Rod, Ugo Basile Comerio, Italy) for 20 min at a constant speed of approximately 4 meters/min. Recording continued for 20 min after exercise. Forced exercise was administered at ZT 2 and ZT 14 and an infrared viewer (FJW Industries, Ohio, USA) was used to visualize the mice during the dark. Data were recorded continuously.

Echocardiography and Heart Size

Middle aged (12 mo) WT and VIP-deficient mice were subject to functional analysis using two-dimensional, M-mode echocardiography and spectral Doppler images acquired by a Siemens Acuson Sequoia C256 equipped with a 15L8 15MHz probe (Siemens Medical Solutions, Mountain View, CA). Mice were lightly anesthetized with 1% isoflurane and HRs were maintained between 450 and 600 during the procedure. Parameters measured include: Ventricular Septic Thickness (VST), End Diastolic Diameter (EDD), Posterior Wall Thickness (PWT), End Systolic Diameter (ESD), Aortic Ejection Time (Ao-ET), Left Ventricular percent Fractional Shortening (LV%FS), Left Ventricular Ejection Fraction (LvEF), Left Ventricular Mass (LVmass), and Early Diastole/Atrial contraction ratio (E/A). Heart weights and Tibia lengths were measured from middle aged mice (12 mo) perfused with PFA.

Real-Time PCR of Clock Genes

RNA extraction and Real-Time PCR were carried out as previously described (Loh *et al.*, 2008). Briefly, RNA was extracted from heart tissue of young mice (3-6 mo) using the Trizol (Invitrogen) procedure and treated with DNase (Turbo DNA-free, Ambion Austin TX).

cDNA was produced from 1ug of total mRNA (High Capacity cDNA Reverse Transcription Kit, Applied Biosystems, Foster City CA) and an equivalent of 50 ng of starting total RNA was used for real-time PCR using SyBr Green (SYBR Green PCR Master Mix, Applied Biosystems Austin, TX). Oligonucleotide primer sequences used were *Per2*-sense: 5'-GGGCATTACCTCCGAGTATA -3' and *Per2*-antisense: 5'-GGCCACTTGGTTAGAGATGTA -3'; *Bmal1*-sense: 5'- CTCAACCATCAGCGACTTCA -3'; and *Bmal1*-antisense: 5'-CTGCCTTTCCTCTTGCGATT -3'; *Gapdh*-sense: 5'- GGCCTTCCGTGTTCCTAC -3' and *Gapdh*-anti-sense: 5'- TGTCATCATACTTGGCAGGTT -3'. Primers for *Per2* were designed using Oligo6 (Molecular Biology Insights, Cascade CO) and Mfold programs (Zuker, 2003) to cross intron-exon boundaries and prevent contaminants in the subsequent RT-PCR. The relative levels of *Per2,* and *Bmal1* transcripts were determined using the $2^{-\Delta\Delta Ct}$ method, using *Gapdh* as the normalizing reference gene. We sampled mRNA at ZT 2, 6, 10, 14, 18 and 22, so only large phase differences could be detected. The time of peak expression was determined for each gene and compared between WT and VIP-deficient mice.

Statistics

Genotypic comparisons were analyzed using a Student's *t*-Test while, day/night comparisons were analyzed using a paired Student's *t*-Test. We used the Student's *t*-Test to compare the onset of HR, body temperature, cage activity between WT and VIP-deficient mice. We also used the Student's *t*-Test to compare maximum HR during forced exercise, HR responses to light exposure between WT and VIP-deficient mice, echocardiogram parameters, and Heart Weight/Tibia Length ratios. To analyze the clock gene expression, we used a one-way ANOVA statistical test. Data were tested for normal distribution and variance, but in cases where

the data did not pass these tests, we used non-parametric statistical tests (ex. Wilcoxon-Signed Rank Test or Mann-Whitney Rank Sum Test) to determine significance. Statistical analyses were performed using Sigma Stat 3.5 software (San Jose, CA). We report the appropriate *t*, *Z*, *F* or *H* statistics and include the degrees of freedom for each analysis.

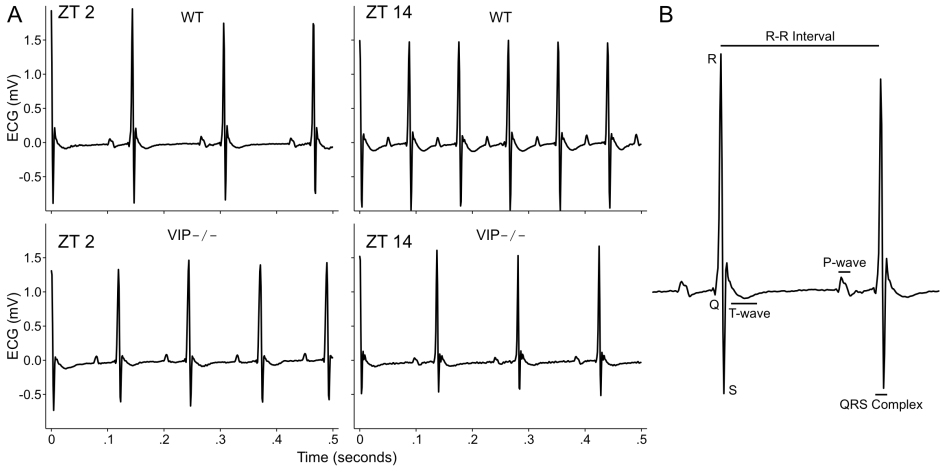

Figure 3-1: *In vivo ECG recordings from freely behaving mice. A: representative examples of ECG tracings from wild-type (WT; top) and VIP-deficient (bottom) mice at Zeitgeber (ZT) 2 and ZT 14. B: magnified example of an ECG tracing labeled with features and intervals of the waveform.*

Results

Analysis of ECG Features

Surgical implantation of a telemetric device into the abdomen allows for continuous recording of ECG waveforms (**Fig. 3-1A**), body temperature and cage activity in freely-moving WT and VIP-deficient mice. We compared and analyzed a number of ECG features (RR, PR, QRS, QT, QTc intervals; **Fig. 3-1B**) between WT and VIP-deficient mice under LD conditions to detect any day/night and genotypic differences (**Table 3-1**). WT mice displayed significant day/night differences in the RR (Z_5=2.20, P= 0.031), PR (Z_5=2.20, P= 0.031) and QRS (t_5=3.05 P=0.029) intervals while, VIP-deficient mice showed differences only in the PR interval

(t_4=3.67, P=0.021). A significant elongation of the QTc interval during the day period (t_9= 2.37, P=0.042) was detected in VIP-deficient mice compared to WT mice. These results indicate disruption in the diurnal regulation of HR and a number of ECG intervals in VIP-deficient mice. Furthermore, the significant elongation of the QTc interval during the light phase in VIP-deficient mice suggests changes in the regulation of electrical activity, particularly in the repolarization of the heart.

ECG Parameters		WT(n=6)	VIP−/−(n=5)
RR (ms)	Day	129.9 ± 5.5	117.5 ± 4.3
	Night	107.6 ± 2.8*	111.2 ± 6.8
PR (ms)	Day	39.3 ± 1.1	37.4 ± 0.6
	Night	36.0 ± 0.5*	35.5 ± 0.9*
QRS (ms)	Day	14.1 ± 0.4	14.3 ± 0.5
	Night	13.0 ± 0.6*	13.2 ± 0.8
QT (ms)	Day	41.9 ± 4.2	54.0 ± 3.8
	Night	45.4 ± 3.6	53.0 ± 4.9
QTc (ms)	Day	118.7 ± 13.0	159.5 ± 10.5‡
	Night	139.8 ± 10.5	160.6 ± 14.2

Table 3-1: *Average duration of ECG features (RR, PR, QRS, QT, and QTc intervals) in WT and VIP-deficient mice under LD condition. Values are means ± SE; n = 6 wild-type (WT) mice and 5 VIP-deficient mice. ECG intervals at two time points, day [Zeitgeber (ZT) 2–4] and night (ZT 14–16) were calculated and averaged over 8 days. *Significant difference in intervals between day and night (P < 0.05), as analyzed by a paired Student's t-test; †significant difference in intervals between WT and VIPdeficient mice (P < 0.05), as analyzed by an unpaired Student's t-test.*

Circadian Analysis of HR, Body Temperature and Cage Activity

In order to examine the circadian component of HR, body temperature and cage activity of individual animals, we plotted the raw data to produce graphs similar to an actogram (**Fig. 3-2 A-C**). The raw data was subjected to periodogram analysis (**Table 3-2**) and the resulting amplitude was used as an index of rhythm strength. To examine rhythms at a population level, we produced group mean waveforms under LD and DD conditions (**Fig. 3-2 D-F**) and compared average values between the day or subjective day (ZT or CT 0-11) and the night or subjective

night (ZT or CT 12-23). Under LD conditions, WT mice exhibited robust daily rhythms of HR, body temperature and cage activity (**Table 3-2**) that were synchronized to the LD cycle. The onset of these measurements occurred minutes after lights off (ZT 12): HR onset 11.5 ± 20 min; body temperature onset 27 ± 17 min; cage activity onset 23.9 ± 12 min (**Fig. 3-2 D-F**). Significant day/night differences in HR (t_6=-11.54, P<0.001), body temperature (t_6=-8.693, P<0.001) and cage activity (t_6=-5.238; P=0.002) were detected (**Table 3-3**). When WT mice were placed in DD, circadian rhythms of HR, body temperature, and cage activity remained robust with a free-running period of 23.7 ± 0.1 hrs (**Fig. 3-2, Table 3-2**). Subjective day/night differences in average HR (t_6=9.085, P<0.001), body temperature (t_6=-19.684, P<0.001) and cage activity (t_6=-5.588, P<0.001) remained significant (**Table 3-3**).

	LD		DD	
Rhythm Amplitude	WT	VIP−/−	WT	VIP−/−
HR	28.6 ± 2.4	12.0 ± 0.8*	24.5 ± 3.0	10.0 ± 0.5*
Body Temperature	70.5 ± 4.1	32.5 ± 3.4*	75.7 ± 3.3	17.7 ± 1.4*
Cage Activity	24.5 ± 3.5	11.3 ± 0.8*	23.3 ± 2.3	10.9 ± 0.9*

Table 3-2: *Periodogram analysis using 10 days of HR, body temperature, and cage activity data. Values are means ± SE. LD, light-dark; DD, constant darkness; HR, heart rate. Peak amplitudes (% power) were compared between WT (n =7) and VIP-deficient mice (n =8) under LD and DD conditions. Genotypic comparisons were analyzed by Student's t-test (*P < 0.05)*

VIP-deficient mice displayed weak diurnal rhythms in HR, body temperature and cage activity (**Table 3-2**). The onset of all three physiological measurements were significantly advanced in VIP-deficient mice compared to WTs (HR: -215 ± 71.8 min, T=56.6, P=0.035; body temperature: -244 ± 50.6 min, t_{12}=7.165, P<0.001; cage activity: -194 ± 51.8 min T=69.06, P<0.001) indicating an advanced phase angle of entrainment (Fig. 2D-F). Day/night differences in cage activity (Z_7=2.521, P=0.008) were significant in VIP-deficient mice but no differences

were detected for HR (t_7=2.325; P=0.058) and body temperature (t_7=1.497, P=0.18). Under DD conditions, HR was arrhythmic in all VIP-deficient mice tested (8/8 mice; **Table 3-2**). Rhythms in cage activity were detected in only 2/8 mice, and these rhythms were weak with a shortened free-running period (22.3 ± 0.17 hrs). Most VIP-deficient mice maintained circadian rhythms in body temperature (7/8) but with shortened periodicity (22.7 ± 0.25 hrs). In order to produce average waveforms of HR and activity despite the absence of a detectable rhythm in individual mice, we used the half-maximal rise of body temperature, which remained rhythmic in VIP-deficient mice, to determine CT12 for HR and cage activity. We detected significant subjective day/night differences in body temperature (t_7=-6.693, P<0.001) and cage activity (t_7=-3.636, P=0.008) but no difference was detected for HR (t_7=-1.511, P=0.175; **Table 3-3**). Under both LD and DD conditions, there were no significant differences in average HR, body temperature and cage activity between WT and VIP-deficient mice, except for a significant decrease of average cage activity in VIP-deficient mice under DD conditions (WT: 6.47 ± 0.73 a.u.,VIP-/-: 3.75 ± 0.322 a.u., T=76, P=0.021). These data indicate that the temporal patterning of HR, body temperature and cage activity is impacted in VIP-deficient mice.

HR and Body Temperature rhythms during periods of no/low activity

While levels of motor activity and HR are closely coupled, previous work has attempted to separate these parameters by measuring HR during times of low activity (Scheer *et al.*, 2001; Sheward *et al.*, 2007). We undertook a similar analysis and extracted HR and body temperature data during periods of low/or no activity (<1% of average activity). In WT mice, there were still clear rhythms in HR and body temperature under both LD and DD conditions during times at which the mice were inactive (**Sup. Fig. 3-1**). In contrast, VIP-deficient mice

showed no day/night differences in HR under LD or DD conditions in the absence of activity. However, the rhythms in body temperature in the VIP-deficient mice persisted under these conditions. This data indicates that, even if we factor out acute activity, we can still measure clear rhythms in body temperature but not HR in the VIP-deficient mice.

Rhythms of HRV

HRV is an index of the balance of sympathovagal signals to the heart and measures the variability of the time between individual heartbeats (Massin *et al.*, 2000). We assessed the temporal patterning of neural signals to the heart by calculating HRV from WT and VIP-deficient mice under LD and DD conditions (**Fig. 3-3**). WT mice exhibited significant day/night differences in HRV under LD (WT: t_6=3.60, P=0.01) and significant subjective day/night differences under DD conditions (t_6=4.582, P=0.005). VIP-deficient mice did not exhibit a day/night difference in HRV under LD conditions (t_7=1.88, P=0.10). Under DD conditions, there was no rhythm evident in the average waveform (**Fig. 3-3B**); however, if we used body temperature rhythm to define CT, we did find a low amplitude rhythm of HRV in VIP-deficient mice (**Fig. 3-3D**; t_7=3.96, P=0.005). HRV was higher during the subjective day compared to the subjective night in all of the VIP-deficient mice (**Sup. Fig. 3-2**) although the difference is small compared to WT mice. The average HRV (measured over 24 hrs) did not vary between the genotypes so the autonomic system is still functioning but the temporal patterning is altered. These results suggest that circadian regulation of sympathovagal signals is dampened but not completely eliminated in VIP-deficient mice.

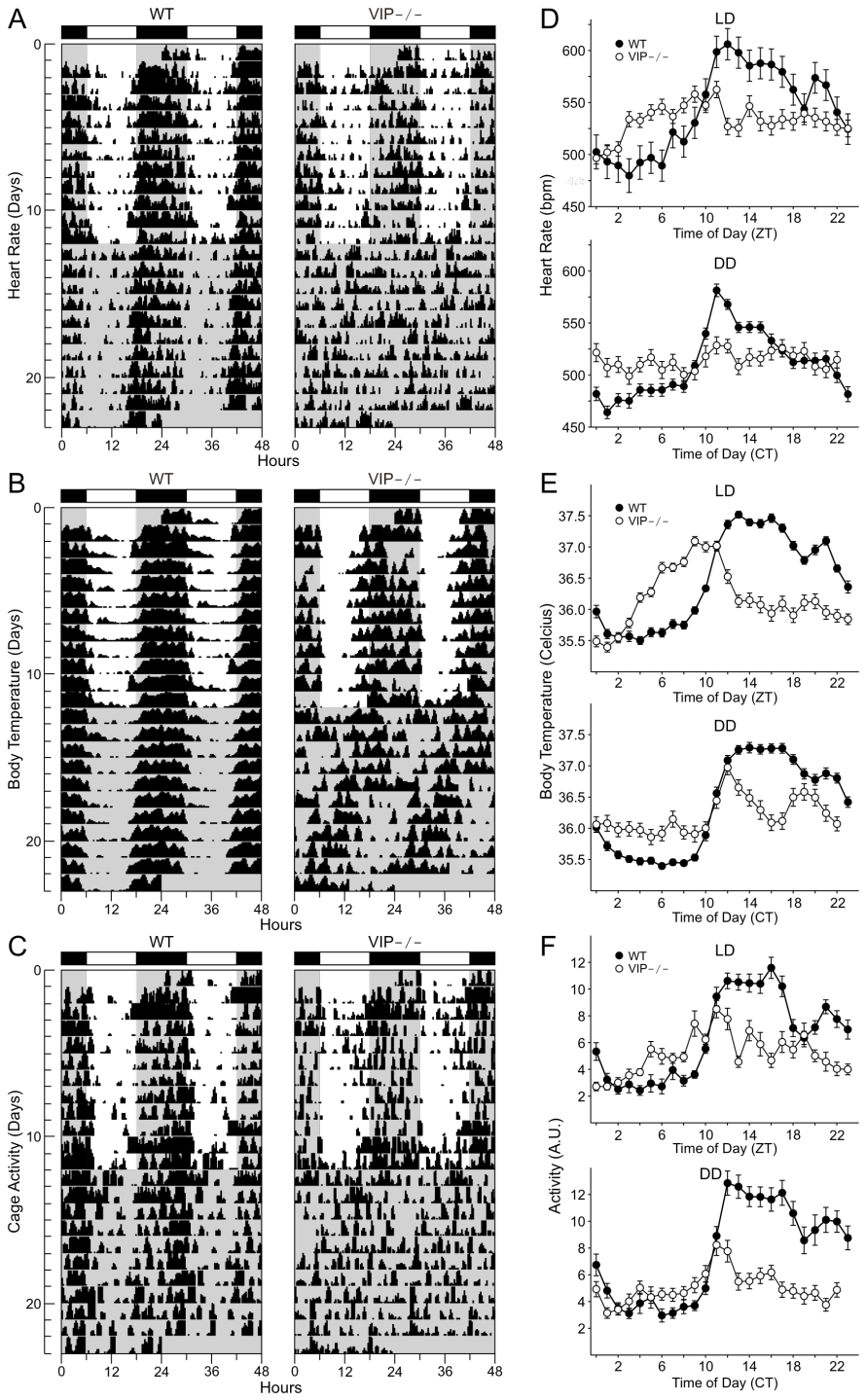

Figure 3-2: *Daily pattern of heart rate [HR; in beats/min (bpm)], body temperature, and cage activity [in arbitrary units (AU)] in WT and VIP-deficient mice. Double-plotted raster plots of HR (A), body temperature (B), and cage activity (C) from WT (left) and VIPdeficient mice (right) were created. Mice were trained in 12:12 light-dark (LD) conditions and then placed in constant darkness (DD). Shaded regions indicated when mice were in the dark. Each horizontal row represents a 24-h period that was*

plotted twice, and each day/row was plotted in succession. Ten days of HR, body temperature, and cage activity were averaged to produce group mean waveforms of HR (D), body temperature (E), and cage activity (F) for WT (n _ 7) and VIPdeficient (n _ 8) mice under LD (top) and DD (bottom) conditions. All of the WT mice showed strong diurnal and circadian rhythms of HR, body temperature, and cage activity (7 of 7 mice) under LD and DD conditions. VIP-deficient mice displayed dampened diurnal rhythms in HR (6 of 8 mice), body temperature (8 of 8 mice), and cage activity (7 of 8 mice) under LD conditions. Under DD conditions, VIP-deficient mice displayed a dampened circadian rhythm of body temperature (7 of 8 mice) and cage activity (2 of 8 mice). VIP-deficient mice did not display a circadian rhythm of HR under DD conditions (0 of 8 mice), as assessed by periodogram analysis.

	WT (n=7)		VIP−/− (n=8)	
LD	day	night	day	night
HR (bpm)	508 ± 15	580 ± 16**	517 ± 14	532 ± 16
Body Temperature	35.8 ± 0.13	37.2 ± 0.09**	36.2 ± 0.06	36.4 ± 0.13
Cage Activity	3.6 ± 0.3	8.7 ± 1.1*	4.2 ± 0.4	5.6 ± 0.8*
DD	s. day	s. night	s. day	s. night
HR (bpm)	486 ± 10	549 ± 10**	504 ± 6	510 ± 7
Body Temperature	35.6 ± 0.05	37.2 ± 0.09**	36.1 ± 0.07	36.5 ± 0.05**
Cage Activity	3.4 ± 0.4	9.3 ± 1.3**	4.1 ± 0.1	5.4 ± 0.1*

Table 3-3: *Day/night differences in HR, body temperature, and cage activity under LD and DD conditions. Values are means ± SE; n = 7 WT mice and 8 VIP-deficient mice. Day/subjective day (ZT or CT 0–11) and night/subjective night (ZT or CT 12–23) values of HR, body temperature, and cage activity were averaged over 10 days and compared using a paired Student's t-test (*P < 0.05).*

We also challenged the cardiovascular system to respond to an exercise protocol. The HR of WT and VIP-deficient mice increased when mice were forced to run at two timepoints: ZT 2 and ZT 14 (**Fig. 3-4C,D**). We compared the HRs of WT and VIP-deficient mice during exercise (20 min in duration) at both time points (WT ZT2: 751 ± 6 bpm, ZT 14: 790 ± 2 bpm; VIP-/- ZT2: 773 ± 2 bpm, ZT 14: 801 ± 2 bpm). The VIP-deficient mice exhibited significantly higher HRs during exercise in both the light (t_{10}= 2.43, P=0.036) and the dark (t_{10} = 3.40, P=0.007) when compared to WT mice. These data suggest that acute signaling to the heart is intact in VIP-deficient mice, although their response to exercise is larger than WT mice.

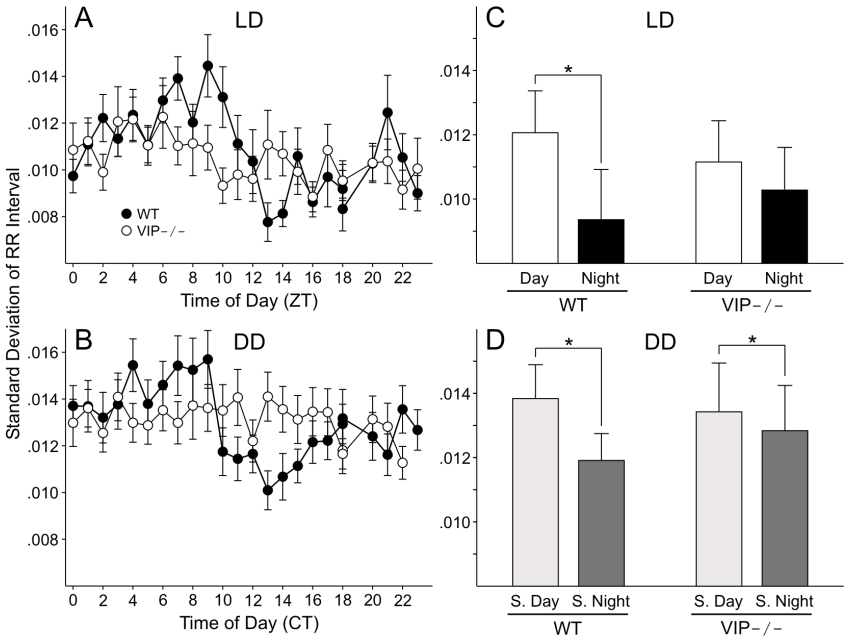

Figure 3-3: *Daily pattern of HR variability (HRV) in WT and VIP-deficient mice. HRV was determined by calculating the variance of the time between individual beats, also known as the interbeat interval (IBI). Group mean waveforms of HRV using 10 days of data were produced for WT (n = 7) and VIP-deficient (n = 8) mice under LD (A) and DD (B) conditions. WT mice displayed significant day/night differences under LD (C) and DD (D) conditions. No significant day/night differences were measured for VIP-deficient mice under LD conditions (C), but significance was detected under DD conditions (D). HRV was consistently decreased during the subjective night (S. night) compared with the subjective day (S. day) in both WT and VIPdeficient mice. These data were analyzed using a paired Student's t-test (*P < 0.05).*

Cardiac Function and Morphology

To determine whether the loss of VIP may have functional consequences on the heart, we performed echocardiograms on WT and VIP-deficient mice at 12 months of age. Our results show no significant differences in any of the measurements by this assay between the various groups (**Table 3-4**) indicating that the hearts of VIP-deficient mice are functionally intact. Previous work suggests that the hearts of these mice exhibit hypertrophy (Said *et al.*, 2007), therefore we calculated the heart weight/tibia length (HW/TL) ratio to provide an index for hypertrophy (**Sup. Fig. 3-3A,B**). We did not find significant differences in the HW/TL ratio between WT and VIP-deficient mice at this age.

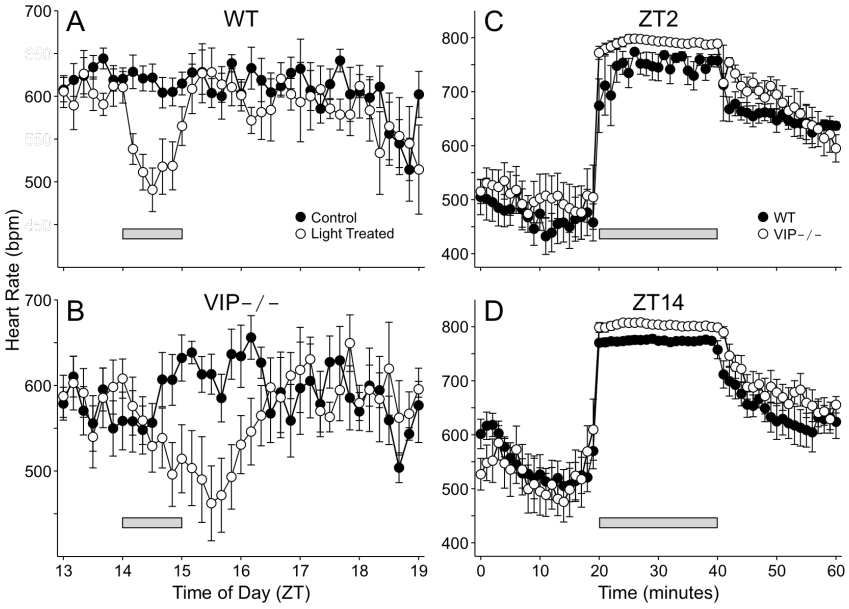

Figure 3-4: *Acute regulation of HR in WT and VIP-deficient mice. A: light exposure (1 h) administered at ZT 14 elicited a precipitous drop of HR in WT mice (n = 7). B: VIP-deficient mice (n = 6) responded to the light treatment, but at a rate that was significantly delayed (P < 0.001). Forced exercise triggered the significant increase of HR in WT (n = 5) and VIP-deficient (n = 5) mice at ZT 2 (C) and ZT 14 (D) time points. VIP-deficient mice exhibited an increase in HR that was larger than WT controls. Bars indicate the times of treatment.*

	YOUNG	
	WT (n=7)	VIP -/- (n=4)
HR (bpm)	529 ± 17	527 ± 34
VST (mm)	0.60± 0.02	0.65 ± 0.02
EDD (mm)	4.37 ± 0.05	4.43 ± 0.12
PWT (mm)	0.61 ± 0.02	0.62 ± 0.03
ESD (mm)	2.94 ± 0.09	2.88 ± 0.15
Ao-ET (ms)	51.4 ± 1.8	55.5 ± 1.1
LV % FS	32.7 ± 2.0	35.1 ± 2.7
Vcf	6.4 ± 0.5	6.3 ± 0.5
LvEF	67.2 ± 2.6	70.6 ± 3.4
LvMass	96.0 ± 3.1	105.5 ±4.6
E	0.99 ± 0.18	0.71 ± 0.02
A	0.53 ± 0.10	0.41 ± 0.04
E/A	1.87 ± 0.05	1.80 ± 0.14

Table 3- 4: *Echocardiogram analysis of young WT and VIP-deficient mice. Values are means ± SE; n = 7 WT mice and 4 VIP-deficient mice. LV, left ventricular; E, early diastole contraction; A, atrial contraction. There were no significant differences between the genotypes.*

Clock Gene Expression in the Heart

Most peripheral tissues, including the heart, possess a molecular clock and display circadian rhythms in core clock gene expression. To determine the condition of the molecular clock in the heart of VIP-deficient mice, we measured mRNA expression levels of the clock genes *Per2* and *Bmal1* under LD conditions at ZT 2, 6 10, 14, 18 and 22 (**Fig. 3-5**). As measured by a one-way ANOVA, *Per2* and *Bmal1* were rhythmic in both WT (*Per2*: H_5 =21.08, P<0.001; *Bmal1*: H_5 =19.56, P=0.002) and VIP-deficient mice (*Per2*: H_6 =21.54, P=0.001; *Bmal1*: H_5 =18.43, P=0.002). We also found a clear advance in the phase of peak expression of both genes (*Per2* peak phase: WT ZT 13; VIP-/- ZT 6; t_6=3.656 P=0.011; *Bmal1* peak phase: WT ZT 1; VIP-/- ZT 20; T_7=10.00 P=0.029) compared to WT controls. These results indicate that the loss of VIP does not disrupt molecular rhythms in the heart but alters the phase of these rhythms under LD conditions.

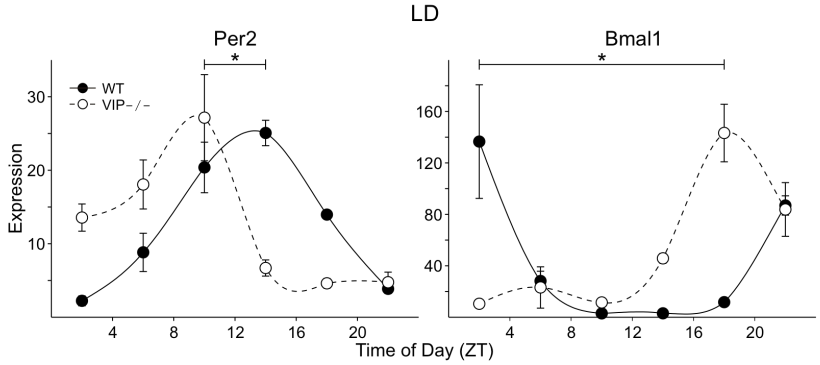

Figure 3-5: *Expression profiles of clock genes period 2 (Per2) and Bmal1 in heart tissues of WT and VIP-deficient mice under LD conditions using RT-PCR techniques. Each time point shows mean results of 3–4 hearts. A one-way ANOVA statistical test was used to determine whether there were significant differences in expression. Bars indicate differences in peak expression between WT and VIP-deficient mice; results were analyzed using Student's t-test (*P < 0.05).*

Discussion

In this set of experiments, we used a telemetry system to measure the impact of the loss of VIP on daily and circadian rhythms in HR, body temperature, and cage activity in freely-moving mice. We found that the loss of VIP differentially disrupted these physiological and behavioral rhythms. Most dramatically, VIP-deficient mice exhibited weak rhythms in HR under LD, which were completely lost under DD conditions, confirming a central role for VIP in the circadian regulation of HR. Rhythms of cage activity in VIP-deficient mice were weak under LD conditions and most mice were arrhythmic in DD. In contrast, VIP-deficient mice exhibited daily rhythms in body temperature albeit with an altered phase compared to WT controls, and continued to display robust rhythms in body temperature under DD with a shortened free-running period. The changes in profile and the reduction in the amplitude of the average waveform of physiological outputs may also be impacted by the imprecise onset of activity observed in VIP-deficient mice (Colwell *et al.*, 2003). All three peripheral outputs displayed onsets (half maximal rise) that were phase advanced under an LD cycle, which has also been described for feeding behavior and metabolism in VIP-deficient mice (Bechtold *et al.*, 2008). This phase advance in onset under LD is absent when measuring activity using a running wheel (Colwell *et al.*, 2003). Furthermore, the wheel appears to improve rhythms in activity under DD conditions, raising the possibility that running on the wheel may be able to temporally organize activity rhythms in VIP-deficient mice (Colwell *et al.*, 2003; Power *et al.*, 2010). Overall, it appears that the impact of the loss of VIP on circadian rhythms varies with the output being measured. Within the SCN, the genetic loss of VIP or $VPAC_2R$ disrupts circadian rhythms in neural activity in the SCN population (Cutler *et al.*, 2003; Brown *et al.*, 2007), where the loss of VIP decreases the number of electrically rhythmic SCN neurons and appears to weaken the

coupling among the remaining rhythmic SCN neurons (Aton *et al.*, 2005; Ciarleglio *et al.*, 2009). Circadian regulation of peripheral tissues may be specialized at the level of the SCN, an idea that has been suggested by a number of studies (Kalsbeek *et al.*, 2006*b*, 2006*a*). In the case of VIP-deficient mice, SCN neurons that regulate body temperature may be among those that do not require VIP to generate daily rhythms. In contrast, arrhythmic physiological processes in VIP-deficient mice, such as the regulation of plasma corticosterone levels (Loh *et al.*, 2008) and HR, may have circuitry coupled to the arrhythmic SCN neurons. Running on the wheel running may provide feedback to the SCN that aids in the coupling of individual neurons. Models considering the role of VIP as a coupling molecule within the SCN (To *et al.*, 2007; Vasalou & Henson, 2010) will need to take into account the findings that not all outputs are arrhythmic in the VIP-deficient mice.

The telemetry system enabled us to record ECG waveforms from WT and VIP-deficient mice under LD conditions. While most of the ECG parameters were not different between WT and VIP-deficient mice, there was a significant increase in the duration of the QTc interval in the VIP-deficient mice during the light phase. A long QTc interval indicates a delay in the repolarization of the ventricle after contraction, which is a risk factor for ventricular arrhythmias and sudden death in humans (Priori *et al.*, 2003; Sauer *et al.*, 2007). In most cases, long QT syndrome (LQTS) is caused by an ion channelopathy associated with loss-of-function mutations in genes encoding for repolarizing potassium channels or proteins that interact with these channels (Hedley *et al.*, 2009). Expression levels of potassium channels have been shown to fluctuate depending on the time of day (Storch *et al.*, 2002; Yamashita *et al.*, 2003), and pharmacological administration of Nicroandil, a K^+ channel opener, can selectively disrupt rhythms in HR, but not body temperature or cage activity (Gantenbein *et al.*, 1998). VIP

regulates potassium channels in a variety of tissues including the colon, coronary arteries and trachea (Shuttleworth *et al.*, 1996; Thirstrup *et al.*, 1997; Sawmiller *et al.*, 2006). Within the heart, VIP has effects on neuroexcitability of intracardiac neurons and can increase the rate and strength of contraction (Chang *et al.*, 1994; Accili *et al.*, 1996; Halimi *et al.*, 1997). Based on these data, a reasonable hypothesis is that the disruption of circadian rhythms in HR in VIP-deficient mice may be in part due to the mis-regulation of potassium ion channel activity within the heart.

Neurons in the SCN containing VIP are well positioned to drive the rhythms in cardiac output through the regulation of the ANS (Buijs *et al.*, 2003; Kalsbeek *et al.*, 2006*b*). Previous anatomical studies have shown that VIP is expressed in SCN efferents projecting onto pre-autonomic neurons of the PVN (Teclemariam-Mesbah *et al.*, 1997) as well as in the parasympathetic postganglion neurons that innervate the heart (Halimi *et al.*, 1997). In order to assess the ANS and determine the effect of the loss of VIP, we examined HRV in WT and VIP-deficient mice. In WT mice, we found clear evidence for circadian regulation in HRV while this rhythmicity appeared to be lost in the VIP-deficient mice. However, a closer inspection using the animal's own rhythm in body temperature to mark phase indicated that a low amplitude rhythm in HRV persisted even in the absence of VIP. Furthermore, the acute autonomic regulation of HR is still functional in VIP-deficient mice as determined by their response to light exposure and exercise, although these responses are different compared to WT. In rodents, the light-evoked decrease in HR is largely driven by an increase in parasympathetic tone (Scheer *et al.*, 2001) while the exercise-evoked increase in HR is driven by sympathetic activity (Miller, 2008). In the present study, we found that the VIP-deficient mice were able to decrease their HR in response to light to the same level as WT albeit at a more sluggish rate. The VIP-deficient

mice also showed a rapid exercise induced increase in HR that was even larger than WT controls. VIP's localization in the parasympathetic neurons may result in some reduction in parasympathetic function in the mutant mice. Overall, the HRV data as well as the ability of the mice to respond to environmental challenges suggest that the autonomic regulation of HR is altered but still functional in the absence of VIP.

Interacting molecular feedback loops driving rhythmic transcription and translation of key clock genes such as *Period* and *Bmal1* (Hastings *et al.*, 2003) are at the core of the oscillatory mechanism. Several studies have now shown that cardiac tissue exhibits rhythmic expression of clock genes (Oishi *et al.*, 1998; Sakamoto & Ishida, 2000; Guo & Stein, 2003; Guo *et al.*, 2005). These molecular rhythms persist in isolated cardiomyocyte cultures, including persistent circadian oscillations in *Per1*-driven bioluminescence (Davidson *et al.*, 2005; Durgan *et al.*, 2005). These data are consistent with the conclusion that cardiovascular tissue contains molecular circadian oscillators that are independent from the SCN. The function of such oscillations in the heart is unknown, but a reasonable assumption is that these molecular oscillations serve to gate information from the SCN to heart-specific rhythmic outputs. Micro-array studies have found that hundreds of genes (~10-15% of total genome) oscillate in the heart (Storch *et al.*, 2002; Martino *et al.*, 2004; Rudic *et al.*, 2005). These rhythmic genes code for proteins such as ion channels, neurotransmitter receptors, and proteins involved in calcium flux, which are likely to have substantial effects on function. In LD conditions, we found robust rhythms in the expression of *Per2,* and *Bmal1* genes within the heart of WT mice. These genes were also rhythmic in VIP-deficient mice, but showed advancement in the phase of peak expression, which nicely parallels the advanced onset of HR, body temperature and cage activity under LD conditions. The data demonstrate that the loss of VIP can alter, but not eliminate, the

daily rhythms in gene expression that underlie circadian oscillations in this peripheral organ. Prior work reported the loss of clock gene expression rhythms in the SCN of $VPAC_2R$ KO mice, yet these mice continue to display gene expression rhythms in peripheral tissues such as the heart and liver (Harmar *et al.*, 2002; Sheward *et al.*, 2007). Given the present data demonstrating that clock gene expression are still rhythmic in the hearts of VIP-deficient mice, the impact of the loss of VIP on the central clock and other peripheral organs will need to be re-visited.

Several recent studies have found evidence that disruption of the circadian system alone is sufficient to lead to the development of cardiovascular disease in circadian compromised animals (Penev *et al.*, 1998; Martino *et al.*, 2007, 2008; Bray *et al.*, 2008). Echocardiogram and heart weight to tibia length ratio data indicate that the hearts of the VIP-deficient mice are normal in size and function in a normal range despite the loss of rhythms in activity, HR, and corticosterone. Perhaps the presence of rhythms in clock gene expression and body temperature in VIP-deficient mice protects the cardiovascular system in some way. More work on the inter-relationships between VIP, disruption of circadian function and cardiac morphology are clearly needed. We propose that the VIP- as well as the $VPAC_2R$-deficient mice may provide important models to look at these relationships.

iii. Supplemental Data

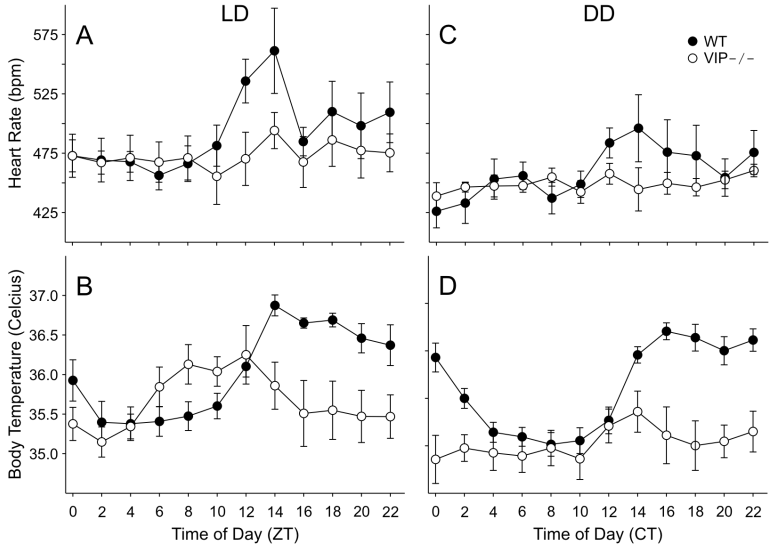

Supplemental Figure 3-1*: Baseline HR and body temperature rhythms. HR (A,C) and body temperature (B, D) data from WT (n=5) and VIP-deficient mice (n=6) during periods of low/no activity (<1% of mean activity) were plotted to produce a group mean waveform under LD and DD conditions. Robustness of the rhythm in HR and body temperature is reduced in the absence of activity, however the profile of the rhythms remains unchanged.*

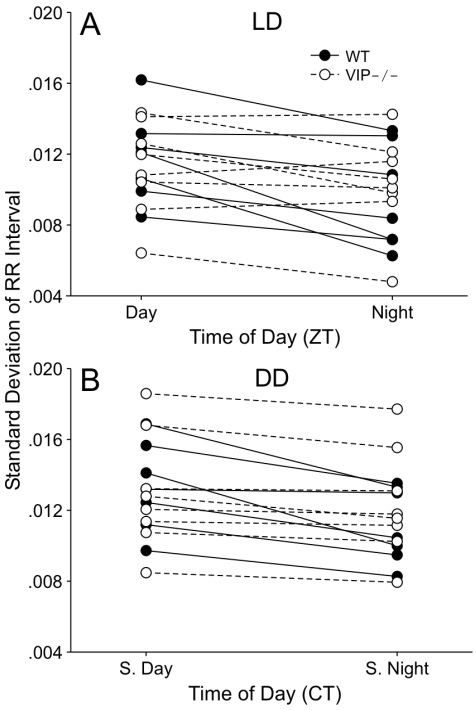

Supplemental Figure 3-2: *HRV of individual WT and VIP-deficient mice under LD and DD conditions. In order to show trends in HRV, we plotted the data of individual mice during the day or subjective day and night or subjective night. VIP-deficient mice showed a mixed trend in HRV when placed under LD (A), but HRV was consistently decreased in all WT and VIP-deficient mice in the subjective night compared to the subjective day (B).*

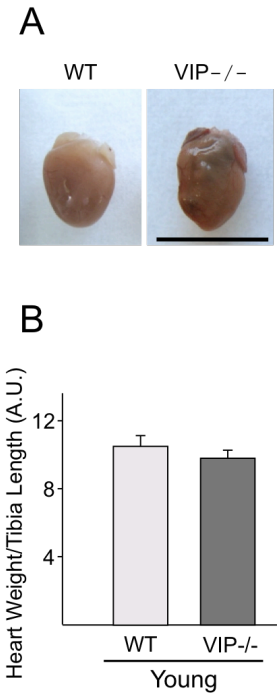

Supplemental Figure 3-3: *Cardiac Size in WT and VIP-deficient mice. (A) Photomicrographs of hearts from young adult (2-4 mo) WT and VIP-deficient mice. (B) Heart Weight to Tibia length ratios (HW/TL) were measured in WT (n=6) and VIP-deficient mice (n=8) to determine heart dimension relative to body size.*

iv. Bibliography

Accili EA, Redaelli G & DiFrancesco D (1996). Activation of the hyperpolarization-activated current (if) in sino-atrial node myocytes of the rabbit by vasoactive intestinal peptide. *Pflugers Arch* **431,** 803–805.

Aton SJ, Colwell CS, Harmar AJ, Waschek J & Herzog ED (2005). Vasoactive intestinal polypeptide mediates circadian rhythmicity and synchrony in mammalian clock neurons. *Nat Neurosci* **8,** 476–483.

Ban Y, Shigeyoshi Y & Okamura H (1997). Development of vasoactive intestinal peptide mRNA rhythm in the rat suprachiasmatic nucleus. *J Neurosci* **17,** 3920–3931.

Bechtold DA, Brown TM, Luckman SM & Piggins HD (2008). Metabolic rhythm abnormalities in mice lacking VIP-VPAC2 signaling. *Am J Physiol Regul Integr Comp Physiol* **294,** R344–351.

Bray MS, Shaw CA, Moore MWS, Garcia RAP, Zanquetta MM, Durgan DJ, Jeong WJ, Tsai J-Y, Bugger H, Zhang D, Rohrwasser A, Rennison JH, Dyck JRB, Litwin SE, Hardin PE, Chow C-W, Chandler MP, Abel ED & Young ME (2008). Disruption of the circadian clock within the cardiomyocyte influences myocardial contractile function, metabolism, and gene expression. *Am J Physiol Heart Circ Physiol* **294,** H1036–1047.

Brown DL, Feskanich D, Sánchez BN, Rexrode KM, Schernhammer ES & Lisabeth LD (2009). Rotating night shift work and the risk of ischemic stroke. *Am J Epidemiol* **169,** 1370–1377.

Brown TM, Colwell CS, Waschek JA & Piggins HD (2007). Disrupted neuronal activity rhythms in the suprachiasmatic nuclei of vasoactive intestinal polypeptide-deficient mice. *J Neurophysiol* **97,** 2553–2558.

Buijs RM, la Fleur SE, Wortel J, Van Heyningen C, Zuiddam L, Mettenleiter TC, Kalsbeek A, Nagai K & Niijima A (2003). The suprachiasmatic nucleus balances sympathetic and parasympathetic output to peripheral organs through separate preautonomic neurons. *J Comp Neurol* **464,** 36–48.

Chang F, Yu H & Cohen IS (1994). Actions of vasoactive intestinal peptide and neuropeptide Y on the pacemaker current in canine Purkinje fibers. *Circ Res* **74,** 157–162.

Ciarleglio CM, Gamble KL, Axley JC, Strauss BR, Cohen JY, Colwell CS & McMahon DG (2009). Population encoding by circadian clock neurons organizes circadian behavior. *J Neurosci* **29,** 1670–1676.

Colwell CS, Michel S, Itri J, Rodriguez W, Tam J, Lelievre V, Hu Z, Liu X & Waschek JA (2003). Disrupted circadian rhythms in VIP- and PHI-deficient mice. *Am J Physiol Regul Integr Comp Physiol* **285,** R939–949.

Cutler DJ, Haraura M, Reed HE, Shen S, Sheward WJ, Morrison CF, Marston HM, Harmar AJ & Piggins HD (2003). The mouse VPAC2 receptor confers suprachiasmatic nuclei cellular rhythmicity and responsiveness to vasoactive intestinal polypeptide in vitro. *Eur J Neurosci* **17,** 197–204.

Davidson AJ, London B, Block GD & Menaker M (2005). Cardiovascular tissues contain independent circadian clocks. *Clin Exp Hypertens* **27,** 307–311.

Durgan DJ, Hotze MA, Tomlin TM, Egbejimi O, Graveleau C, Abel ED, Shaw CA, Bray MS, Hardin PE & Young ME (2005). The intrinsic circadian clock within the cardiomyocyte. *Am J Physiol Heart Circ Physiol* **289,** H1530–1541.

Guo H, Brewer JM, Champhekar A, Harris RBS & Bittman EL (2005). Differential control of peripheral circadian rhythms by suprachiasmatic-dependent neural signals. *Proc Natl Acad Sci USA* **102,** 3111–3116.

Guo Y-F & Stein PK (2003). Circadian rhythm in the cardiovascular system: chronocardiology. *Am Heart J* **145,** 779–786.

Halimi F, Piot O, Guize L & Le Heuzey JY (1997). Electrophysiological effects of vasoactive intestinal peptide in rabbit atrium: a modulation of acetylcholine activity. *J Mol Cell Cardiol* **29,** 37–44.

Harmar AJ, Marston HM, Shen S, Spratt C, West KM, Sheward WJ, Morrison CF, Dorin JR, Piggins HD, Reubi JC, Kelly JS, Maywood ES & Hastings MH (2002). The VPAC(2) receptor is essential for circadian function in the mouse suprachiasmatic nuclei. *Cell* **109,** 497–508.

Hastings MH, Reddy AB & Maywood ES (2003). A clockwork web: circadian timing in brain and periphery, in health and disease. *Nat Rev Neurosci* **4,** 649–661.

Hedley PL, Jørgensen P, Schlamowitz S, Wangari R, Moolman-Smook J, Brink PA, Kanters JK, Corfield VA & Christiansen M (2009). The genetic basis of long QT and short QT syndromes: a mutation update. *Hum Mutat* **30,** 1486–1511.

Hu K, Ivanov PC, Hilton MF, Chen Z, Ayers RT, Stanley HE & Shea SA (2004). Endogenous circadian rhythm in an index of cardiac vulnerability independent of changes in behavior. *Proc Natl Acad Sci USA* **101,** 18223–18227.

Kalsbeek A, Palm IF, La Fleur SE, Scheer FAJL, Perreau-Lenz S, Ruiter M, Kreier F, Cailotto C & Buijs RM (2006*a*). SCN outputs and the hypothalamic balance of life. *J Biol Rhythms* **21,** 458–469.

Kalsbeek A, Perreau-Lenz S & Buijs RM (2006*b*). A network of (autonomic) clock outputs. *Chronobiol Int* **23,** 521–535.

Kalsbeek A, Rikkers M, Vivien-Roels B & Pévet P (1993). Vasopressin and vasoactive intestinal peptide infused in the paraventricular nucleus of the hypothalamus elevate plasma melatonin levels. *J Pineal Res* **15,** 46–52.

Knutsson A, Akerstedt T, Jonsson BG & Orth-Gomer K (1986). Increased risk of ischaemic heart disease in shift workers. *Lancet* **2,** 89–92.

Ko CH & Takahashi JS (2006). Molecular components of the mammalian circadian clock. *Hum Mol Genet* **15 Spec No 2,** R271–277.

Loh DH, Abad C, Colwell CS & Waschek JA (2008). Vasoactive intestinal peptide is critical for circadian regulation of glucocorticoids. *Neuroendocrinology* **88,** 246–255.

Marler JR, Price TR, Clark GL, Muller JE, Robertson T, Mohr JP, Hier DB, Wolf PA, Caplan LR & Foulkes MA (1989). Morning increase in onset of ischemic stroke. *Stroke* **20,** 473–476.

Martino T, Arab S, Straume M, Belsham DD, Tata N, Cai F, Liu P, Trivieri M, Ralph M & Sole MJ (2004). Day/night rhythms in gene expression of the normal murine heart. *J Mol Med* **82,** 256–264.

Martino TA, Oudit GY, Herzenberg AM, Tata N, Koletar MM, Kabir GM, Belsham DD, Backx PH, Ralph MR & Sole MJ (2008). Circadian rhythm disorganization produces profound cardiovascular and renal disease in hamsters. *Am J Physiol Regul Integr Comp Physiol* **294,** R1675–1683.

Martino TA, Tata N, Belsham DD, Chalmers J, Straume M, Lee P, Pribiag H, Khaper N, Liu PP, Dawood F, Backx PH, Ralph MR & Sole MJ (2007). Disturbed diurnal rhythm alters gene expression and exacerbates cardiovascular disease with rescue by resynchronization. *Hypertension* **49,** 1104–1113.

Massin MM, Maeyns K, Withofs N, Ravet F & Gérard P (2000). Circadian rhythm of heart rate and heart rate variability. *Arch Dis Child* **83,** 179–182.

Maywood ES, Reddy AB, Wong GKY, O'Neill JS, O'Brien JA, McMahon DG, Harmar AJ, Okamura H & Hastings MH (2006). Synchronization and maintenance of timekeeping in suprachiasmatic circadian clock cells by neuropeptidergic signaling. *Curr Biol* **16,** 599–605.

Miller TD (2008). Exercise treadmill test: estimating cardiovascular prognosis. *Cleve Clin J Med* **75,** 424–430.

Muller JE, Stone PH, Turi ZG, Rutherford JD, Czeisler CA, Parker C, Poole WK, Passamani E, Roberts R & Robertson T (1985). Circadian variation in the frequency of onset of acute myocardial infarction. *N Engl J Med* **313,** 1315–1322.

Muller JE, Tofler GH & Stone PH (1989). Circadian variation and triggers of onset of acute cardiovascular disease. *Circulation* **79,** 733–743.

Oishi K, Sakamoto K, Okada T, Nagase T & Ishida N (1998). Antiphase circadian expression between BMAL1 and period homologue mRNA in the suprachiasmatic nucleus and peripheral tissues of rats. *Biochem Biophys Res Commun* **253,** 199–203.

Pantazopoulos H, Dolatshad H & Davis FC (2010). Chronic stimulation of the hypothalamic vasoactive intestinal peptide receptor lengthens circadian period in mice and hamsters. *Am J Physiol Regul Integr Comp Physiol* **299,** R379–385.

Penev PD, Kolker DE, Zee PC & Turek FW (1998). Chronic circadian desynchronization decreases the survival of animals with cardiomyopathic heart disease. *Am J Physiol* **275,** H2334–2337.

Power A, Hughes ATL, Samuels RE & Piggins HD (2010). Rhythm-promoting actions of exercise in mice with deficient neuropeptide signaling. *J Biol Rhythms* **25,** 235–246.

Priori SG, Schwartz PJ, Napolitano C, Bloise R, Ronchetti E, Grillo M, Vicentini A, Spazzolini C, Nastoli J, Bottelli G, Folli R & Cappelletti D (2003). Risk stratification in the long-QT syndrome. *N Engl J Med* **348,** 1866–1874.

Rudic RD, McNamara P, Reilly D, Grosser T, Curtis A-M, Price TS, Panda S, Hogenesch JB & FitzGerald GA (2005). Bioinformatic analysis of circadian gene oscillation in mouse aorta. *Circulation* **112,** 2716–2724.

Said SI, Hamidi SA, Dickman KG, Szema AM, Lyubsky S, Lin RZ, Jiang Y-P, Chen JJ, Waschek JA & Kort S (2007). Moderate pulmonary arterial hypertension in male mice lacking the vasoactive intestinal peptide gene. *Circulation* **115,** 1260–1268.

Sakamoto K & Ishida N (2000). Light-induced phase-shifts in the circadian expression rhythm of mammalian period genes in the mouse heart. *Eur J Neurosci* **12,** 4003–4006.

Sauer AJ *et al.* (2007). Long QT syndrome in adults. *J Am Coll Cardiol* **49,** 329–337.

Sawmiller DR, Ashtari M, Urueta H, Leschinsky M & Henning RJ (2006). Mechanisms of vasoactive intestinal peptide-elicited coronary vasodilation in the isolated perfused rat heart. *Neuropeptides* **40,** 349–355.

Scheer FA, Ter Horst GJ, van Der Vliet J & Buijs RM (2001). Physiological and anatomic evidence for regulation of the heart by suprachiasmatic nucleus in rats. *Am J Physiol Heart Circ Physiol* **280,** H1391–1399.

Sheward WJ, Maywood ES, French KL, Horn JM, Hastings MH, Seckl JR, Holmes MC & Harmar AJ (2007). Entrainment to feeding but not to light: circadian phenotype of VPAC2 receptor-null mice. *J Neurosci* **27,** 4351–4358.

Shuttleworth CW, Koh SD, Bayginov O & Sanders KM (1996). Activation of delayed rectifier potassium channels in canine proximal colon by vasoactive intestinal peptide. *J Physiol (Lond)* **493 (Pt 3),** 651–663.

Sollars PJ & Pickard GE (1998). Restoration of circadian behavior by anterior hypothalamic grafts containing the suprachiasmatic nucleus: graft/host interconnections. *Chronobiol Int* **15,** 513–533.

Storch K-F, Lipan O, Leykin I, Viswanathan N, Davis FC, Wong WH & Weitz CJ (2002). Extensive and divergent circadian gene expression in liver and heart. *Nature* **417,** 78–83.

Stoynev AG & Minkova NK (1998). Effect of forward rapidly rotating shift work on circadian rhythms of arterial pressure, heart rate and oral temperature in air traffic controllers. *Occup Med (Lond)* **48,** 75–79.

Takahashi JS, Hong H-K, Ko CH & McDearmon EL (2008). The genetics of mammalian circadian order and disorder: implications for physiology and disease. *Nat Rev Genet* **9,** 764–775.

Teclemariam-Mesbah R, Kalsbeek A, Pevet P & Buijs RM (1997). Direct vasoactive intestinal polypeptide-containing projection from the suprachiasmatic nucleus to spinal projecting hypothalamic paraventricular neurons. *Brain Res* **748,** 71–76.

Thirstrup S, Nielsen-Kudsk JE & Mellemkjaer S (1997). Involvement of K+ channels in the relaxant effect of vasoactive intestinal peptide and atrial natriuretic peptide in isolated guinea-pig trachea. *Eur J Pharmacol* **319,** 253–259.

To T-L, Henson MA, Herzog ED & Doyle FJ 3rd (2007). A molecular model for intercellular synchronization in the mammalian circadian clock. *Biophys J* **92,** 3792–3803.

Tüchsen F (1993). Working hours and ischaemic heart disease in Danish men: a 4-year cohort study of hospitalization. *Int J Epidemiol* **22,** 215–221.

Vasalou C & Henson MA (2010). A multiscale model to investigate circadian rhythmicity of pacemaker neurons in the suprachiasmatic nucleus. *PLoS Comput Biol* **6,** e1000706.

Virag JAI, Dries JL, Easton PR, Friesland AM, DeAntonio JH, Chintalgattu V, Cozzi E, Lehmann BD, Ding JM & Lust RM (2010). Attenuation of myocardial injury in mice with functional deletion of the circadian rhythm gene mPer2. *Am J Physiol Heart Circ Physiol* **298,** H1088–1095.

Vosko AM, Schroeder A, Loh DH & Colwell CS (2007). Vasoactive intestinal peptide and the mammalian circadian system. *Gen Comp Endocrinol* **152,** 165–175.

Witte K, Schnecko A, Buijs RM, van der Vliet J, Scalbert E, Delagrange P, Guardiola-Lemaître B & Lemmer B (1998). Effects of SCN lesions on circadian blood pressure rhythm in normotensive and transgenic hypertensive rats. *Chronobiol Int* **15,** 135–145.

Yamashita T, Sekiguchi A, Iwasaki Y, Sagara K, Iinuma H, Hatano S, Fu L-T & Watanabe H (2003). Circadian variation of cardiac K+ channel gene expression. *Circulation* **107,** 1917–1922.

Zuker M (2003). Mfold web server for nucleic acid folding and hybridization prediction. *Nucleic Acids Res* **31,** 3406–3415.

CHAPTER 4

i. Introduction

In the submitted manuscript entitled "Scheduled exercise alters diurnal rhythms of behaviour, physiology and gene expression in WT and Vasoactive Intestinal Peptide-deficient mice" by Schroeder et al., we used scheduled access to a running wheel to induce a level of exercise at different times and durations of the active/dark phase. This manipulation altered the rhythms of cage activity, HR, body temperature as well as Per2:LUC expression in WT and VIP-deficient mice. Many of the diurnal deficits of VIP-deficient mice were rescued using late night wheel access suggesting that the scheduling of exercise could be used as a tool to temporally structure and organize diurnal rhythms.

ii. Scheduled exercise alters diurnal rhythms of behaviour, physiology and gene expression in WT and Vasoactive Intestinal Peptide-deficient mice.

Abstract

The circadian system coordinates the temporal patterning of behaviour and many underlying biological processes. In some cases, the regulated outputs of the circadian system, such as activity, may be able to feedback to alter core clock processes. In our studies, we used 4 wheel access conditions to manipulate the duration and timing of activity while under the influence of a light/dark cycle: no access, free access, early (ZT12-18) and late (ZT 18-24) night. In WT mice, scheduled wheel access was able to increase cage activity levels inducing a level of exercise driven at various phases of the LD cycle. Scheduled exercise also manipulated the magnitude and phasing of the circadian regulated outputs of heart rate and body temperature. At a molecular level, the phasing and amplitude of PER2:LUC expression rhythms in the SCN and peripheral tissues of *Per2*:*luc* knockin mice were altered by scheduled exercise. We then tested whether scheduled wheel access could improve deficits observed in VIP-deficient mice under an LD cycle. We found that scheduled wheel access during the late night improved many of the behavioural, physiological and molecular deficits previously described in VIP-deficient mice. Our results raise the possibility that scheduled exercise could be used as a tool to modulate daily rhythms and when applied may counter-act some of the negative impacts of ageing and disease on the circadian system.

Introduction

The endogenous circadian system drives coordinated rhythms of behaviour, physiology and gene expression and responds to a variety of external cues in order to synchronize to the changing environment. Photic input is the primary driver that resets the circadian clock by directly modulating the function of the central oscillator located in the hypothalamus, called the Suprachiasmatic Nucleus (SCN; (Reppert & Weaver, 2002)). Light can alter the molecular feedback loop found in the individual neurons of the SCN, by shifting the timing of expression of its clock gene components (i.e. *Period*, *Cryptochrome*, *Bmal1;* (Yamazaki *et al.*, 2000; Davidson *et al.*, 2008)). The SCN, through neural, humoral and paracrine mechanisms, drives the molecular clock and rhythms of individual cells in various peripheral tissues that enable the coordination of biological processes (Kalsbeek *et al.*, 2006; Dibner *et al.*, 2010). In addition to light, the circadian system is responsive to changes in its environment, resources and condition. Activity for example, is a behavioural output regulated by the circadian system and at altered intensities or timing, can feedback and modulate circadian regulation of outputs (Yamada *et al.*, 1988; Reebs & Mrosovsky, 1989; Edgar & Dement, 1991; Mrosovsky, 1996).

In rodents, the effects of stimulated activity induced by wheel access on the circadian system have been demonstrated by a variety of studies. The phase of the circadian system shifts in response to wheel access administered at certain times of the day (Reebs & Mrosovsky, 1989; Van Reeth *et al.*, 1994; Buxton *et al.*, 1997, 2003). Wheel access scheduled at 24 hour (hr) intervals under constant dark conditions synchronized rhythms of WT mice (Edgar & Dement, 1991) and helped improve behavioural rhythms in circadian compromised mouse models (Power *et al.*, 2010). Furthermore, reentrainment to a shifted LD (light/dark) cycle can be accelerated or delayed depending on whether wheel access is allowed in-phase or out-of-phase of the new LD

cycle, respectively (Mrosovsky & Salmon, 1987; Dallmann & Mrosovsky, 2006; Castillo *et al.*, 2011). Activity during the subjective day has also been shown to acutely decrease the expression of clock genes (*period1* and *period2*) in the SCN (Maywood *et al.*, 1999; Yannielli *et al.*, 2002), indicating an effect of activity on the central pacemaker. Furthermore, recent *in* vivo studies have described close correlations between the firing rate of neurons in the SCN and the level of behavioural activity, supporting a direct interaction between the two processes (Schaap & Meijer, 2001; Houben *et al.*, 2009).

In our studies, we measured rhythms of behaviour, physiology and gene expression in wild type (WT) mice subject to wheel access conditions that manipulate the timing and duration of activity, under a 12:12hr LD cycle. We first examined the effects of free wheel access on activity and then restricted the opportunity to run, by providing scheduled wheel access during the first or second half of the dark phase. Scheduled wheel access better reflects the limited time humans spend active or exercising. Furthermore, examining the effects of wheel access under an LD cycle takes into account interactions of photic and nonphotic input, conditions in which the circadian system has evolved. We also measured the ability of the wheel access conditions to reorganize daily rhythms of heart rate (HR), body temperature and gene expression. Lastly, to test whether activity alters or rescues a disrupted circadian system, we extended our studies and examined the effects of wheel access on VIP-deficient mice, a model that exhibits circadian deficits.

Materials and Methods

Ethical Approval and Experimental Animals

All experimentations were conducted under the recommendations and guidelines of the UCLA Division of Laboratory Animals and the National Institutes of Health. We examined the effects of wheel access in male mice homozygous for the PER2::LUC fusion gene (Yoo *et al.*, 2004), crossed into the *Vip-/-* line on a C57BL/6J background. As controls, age-matched *Vip+/+; Per2::Luc* littermates were used.

Telemetry Measurements

WT (*n*=7) and VIP-deficient mice (*n*=7; 4-5 months) were anaesthetized with isoflurane and surgically implanted with a wireless radiofrequency transmitter (ETA-F20, Data Sciences International, St. Paul, MN USA) and housed in individual cages. These cages contained running wheels equipped with an automated wheel-locking device that prohibit/allow wheel running at specified times of the day without human stimulation or arousal. Cages were placed atop telemetry receivers (Data Sciences International) in a light and temperature-controlled chamber where mice were provided standard rodent chow *ad libitum*. Data collection began 2 weeks post-surgery, to allow mice to recover in the 12:12 LD cycle. Throughout the experiment, we recorded 20 seconds of the ECG waveform every 10 minutes, which was used to extrapolate heart rate (HR; beats per minute, bpm) using the RR interval. Average body temperature (ºCelcius, ºC) and cage activity (arbitrary units, a.u.) were measured every 10 minutes.

Under a 12:12 LD cycle, 4 WT and 3 VIP-deficient mice were subject to no wheel access, free wheel access, followed by wheel access between Zeitgeber (ZT) 12-18 and 18-24. ZT 0 is defined as lights on. For the remaining mice (3 WT and 4 VIP-deficient mice) the order

of the conditions were altered (no access, free access, ZT 18-24, ZT 12-18) to minimize any order effects of scheduled wheel access. Each mouse was subject to all of the wheel access conditions and remained in each condition for a minimum of 16 days.

Behavioural Analysis

We produced average waveforms by binning 3hr averages of HR, body temperature and cage activity and aligned 10 consecutive days of data using the time of lights. Rhythms of HR, body temperature and cage activity were analyzed by periodogram analysis combined with a χ^2 test (El Temps software, Barcelona Spain) using the strongest amplitude (=power) of periodicities (within 20 and 31hr limits) to reflect the robustness of the rhythm. We used ClockLab software to calculate the acrophase of daily rhythms, which is the phase in the cycle during which the cycle peaks. Data from the last 10 days in each condition were used for all analyses.

Bioluminescence

WT and VIP-deficient mice (4-6months; *n*=6-9) were subject to each of the wheel access conditions for at least two weeks before they were deeply anesthetized with isoflurane and sacrificed for bioluminescence recording using a photomultiplier tube photodetector (Actimetrics, Wilmette, IL USA). For these studies, wheels were locked manually. Our culture conditions are as described in Yamazaki and Takahashi (2005) and dissections are detailed in Loh et al. (2011). Briefly, mice were sacrificed between ZT 10-12 and the SCN, liver, heart and adrenals were dissected and placed on Millicell membranes (0.4 um, PICMORG50, Millipore, Bedford, MA USA) in 35-mm dishes with 1.2 mL of recording media containing 0.1mM

luciferin (sodium salt monohydrate, Biosynth Staad, Switzerland). Heart explants were taken from atrial tissue using a single cut with a sterile scalpel. The dishes were sealed using high vacuum grease (Dow Corning , Midland, MI USA) placed in the lumicycler maintained at 37°C. Bioluminescence was recorded for at least 7 days. Using the Lumicycler analysis software (Actimetrics, Wilmette, IL USA), raw data were normalized by subtraction of the recorded baseline followed by the subtraction of the 24hr running average. Peaks and troughs were identified to calculate amplitude, period and timing of PER2:LUC peaks. To calculate the timing of PER2:LUC peaks, we calculated the number of hours from ZT12 of dissection day, and compared the average timing of the peak that occurred between 36-60hr from the time of dissection. Period was calculated by averaging the time interval between 4 peaks, starting from the first peak that occurred after 36hr of recording. Amplitude was calculated by measuring the bioluminescence value at the peak of the waveform that occurred between 36-60hr and subtracted the bioluminescence value of the subsequent trough.

Statistics

For all analyses, we compared free access and scheduled access against no wheel access conditions, separately. For within genotype analysis, we used a paired Student's *t*-Test to compare average cage activity, HR and body temperature, as well as rhythmic power and acrophase between no access and free wheel access conditions. We used a one-way repeated measures analysis of variance (ANOVA) to compare these same parameters between no access and the two scheduled wheel access conditions. Average waveform comparisons between no access and free access conditions and between no access and scheduled access conditions were analyzed using a two-way repeated measures ANOVA. Comparisons of period, amplitude and

timing of PER2:LUC peaks between no wheel and free wheel conditions were analyzed using a Student's *t*-Test, while comparisons between no wheel and scheduled access were analyzed using a one-way ANOVA.

For genotypic comparisons between WT and VIP-deficient mice, we used a two-way repeated measures ANOVA to compare the power and acrophase of cage activity, HR and body temperature between no access and free access or between no access and scheduled wheel access. A two-way ANOVA was used to compare period, amplitude and timing of PER2:LUC peaks between genotypes.

Statistical analyses were performed using Sigma Plot 10.0 software (San Jose, CA USA). All data were tested for normal distribution and variance, but in cases where the data did not pass these tests, we used non-parametric statistical tests (ex. Wilcoxon-Signed Rank Test or Mann-Whitney Rank Sum Test) to determine significance. Following ANOVA analysis, post hoc tests (Holm-Sidak or Student Newman Keuls Method) were used to identify significantly different groups. We report the appropriate *t*, *Q*, *F* or *H* statistics and included the degrees of freedom for each analysis. We reported some of the post-*hoc* statistics for comparisons that were not significant.

Results

Cage activity in WT mice provided free access to the wheel.

Using telemetry, we recorded cage activity in freely moving WT mice given either no access or free access to the running wheel (**Fig. 4-1A**). Free access increased the 24hr averages of cage activity compared to conditions without access (t_6= -4.22, P=0.006; **Table 4-1**). In comparing the average waveforms of cage activity (**Fig. 4-1B**), we found that cage activity

increased selectively during the dark phase of the LD cycle (**Table 4-2**), demonstrating an induction of exercise during the normal active phase of WT mice. Lastly, the power of cage activity rhythms was improved with free access to the wheel (t_6=-4.86, P=0.003, **Fig. 4-1C**), while acrophase was not altered (t_6=2.053, P=0.086, **Fig. 4-1D**).

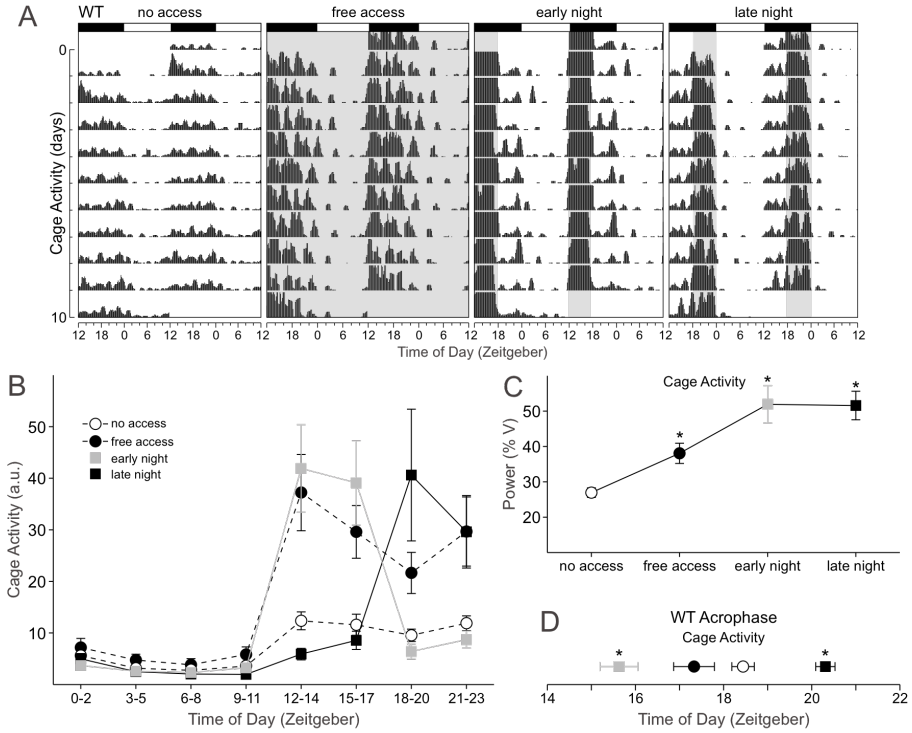

Figure 4-1: *Wheel access increased levels and altered rhythmic properties of cage activity in WT mice. (A) Double plotted raster plot using 10 consecutive days of cage activity recording from the same WT mouse subject to the four wheel-access conditions under a 12:12 LD cycle. In this and other figures, each horizontal row represents a 24hr period plotted twice with each day/row plotted in succession. The LD cycle is specified by the white and black bars above each graph. Shaded areas indicate when the wheel was available. The profile of cage activity rhythms is clearly altered by the various wheel access conditions. (B) Group mean waveforms using 10 days of cage activity data from WT mice (n=7) subject to the various wheel access conditions. Cage activity data were grouped into 3hr bins. Cage activity levels increased when wheel access was available. For statistical results, see Table 4- 2. (C) Increased power of cage activity rhythms in WT mice subject to wheel access conditions. Power measurement was produced by periodogram analysis using 10 days of behavioral data. (D) Shifts in the acrophase of cage activity rhythms were induced by scheduled wheel access. Early night access advanced while late night access delayed the acrophase of cage activity. For this and the other figures: average acrophase from 10 days of data were calculated using the ClockLab Software, average waveform comparisons were analyzed using a two-way repeated measures ANOVA, power and acrophase comparisons were analyzed using a one-way repeated-measures ANOVA. Error bars are SEM. (*=P<0.05).*

Cage activity in WT mice provided scheduled access to the wheel.

We shortened the duration of wheel access at two different phases of the LD cycle to test whether the limited opportunity for running would alter the levels and timing of cage activity in WT mice when compared to no access conditions. Wheel access restricted to 6hrs a day scheduled either during the early night (ZT12-18) or the late night (ZT 18-24; **Fig. 4-1A**), did not change the 24hr averages of activity (**Table 4-1**). However, we detected significant increases in cage activity that was dependent on the time of day (**Fig. 4-1B**, **Table 4-2**). Compared to no access conditions, cage activity was significantly increased during the times of wheel availability. The power of cage activity rhythms was significantly improved ($F_{2,20}$=21.0, P<0.001) with access in the early night (t_{12}=5.65, P<0.001) and late night (t_{12}=5.57, P<0.001; **Fig. 4-1C**). Lastly, scheduled wheel access shifted the acrophase of cage activity rhythms ($F_{2,20}$=74.0, P<0.001). Access in the early night advanced the acrophase (t_{12}=7.27,P<0.001) whereas, access in the late night (t_{12}=4.82, P<0.001) delayed the acrophase of activity (**Fig. 4-1D**). We demonstrate that scheduled wheel access altered levels of activity, improved cage activity rhythms and shifted its acrophase, indicating that manipulation of wheel access can induce exercise at specified times of the LD cycle.

Effect of wheel access on HR and body temperature of WT mice.

We recorded HR (**Fig. 4-2A**) and body temperature (**Fig. 4-3A**) from WT mice subject to the various exercise schedules to determine if other circadian-regulated physiological outputs were altered. Compared to no wheel access conditions, 24hr averages of HR were increased with free access (t_6=-3.66, P=0.011) as well as scheduled wheel access ($F_{2,20}$=13.2, P<0.001), either during the early night (t_{12}=4.31, P=0.001) or late night (t_{12}=4.59, P<0.001; **Table 4-1**).

Free access increased HR at all timepoints of the day except between ZT 12-14 (**Fig. 4-2B, Table 4-2**). Wheel access during the early night increased HR at all timepoints except for the few hours before lights off. Late night access increased HR starting at ZT18, when the wheel was available and throughout most of the light phase up until ZT8. Free access did not alter the power of HR rhythms, but scheduled wheel access ($F_{2,20}$=4.41, P=0.037) during the early night (t_{12}=2.79, P=0.017) significantly increased power (**Fig. 4-2C**). The acrophase of HR rhythms was not shifted by free access, but scheduled access ($F_{2,20}$=24.7, P<0.001) during the late night effectively delayed the acrophase (t_{12}=5.77, P<0.001, **Fig. 4-2D**).

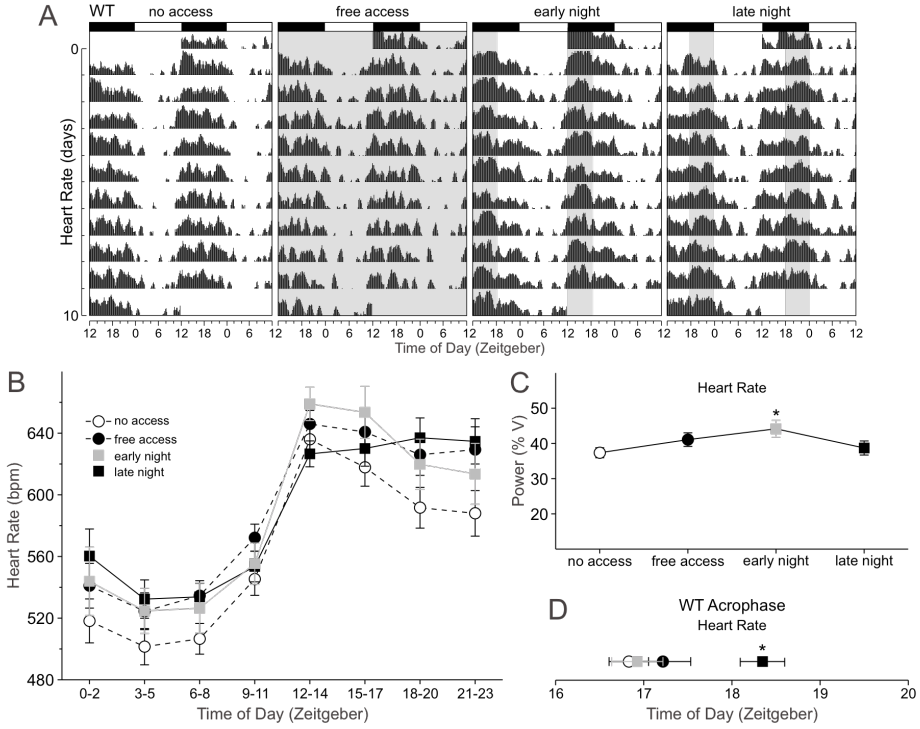

Figure 4-2: *Wheel access altered daily rhythms of HR in WT mice. (A) Double plotted raster plot of HR using 10 consecutive days of HR recording from the same WT mouse subject to the four wheel-access conditions under a 12:12 LD cycle. (B) Group mean waveforms using 10 days of HR recordings from WT mice (n=7) subject to the various wheel access conditions. HR data were grouped into 3hr bins. HRs were increased at most timepoints of the LD cycle, including periods when the wheel was available. For statistical results, see Table 4- 1. (C) Increased power of HR rhythms in WT mice subject to early night wheel access. Power measurement was produced by periodogram analysis using 10 days of HR data. (D) Late night access delayed the acrophase of HR rhythms of WT mice.*

Average body temperatures of WT mice were decreased by free access (t_6=3.15, P=0.02), as well as scheduled access ($F_{2,20}$=7.43, P=0.008) in both early night (t_{12}=3.12, P=0.009) and late night (t_{12}=3.52, P=0.004) when compared to no wheel access (**Table 4-1**). Free access decreased body temperatures during most of the light phase and increased body temperature during the first few hours of dark (**Fig. 4-3B, Table 4-2**). Wheel access in the early night resulted in significantly higher temperatures at the time of wheel access and a decrease in temperature in the hours following the end of the wheel access period. Access in the late night increased body temperature at the beginning of wheel access, and decreased body temperatures in the late part of the day and early night. The power of body temperature rhythms was not changed with either free or scheduled wheel access (**Fig. 4-3C**). Lastly, free wheel access did not change the acrophase of body temperature rhythms, but scheduled access (χ^2_2=10.3, P=0.004) during the early night advanced the acrophase (q_{12}=3.21, P<0.05), while access in the late night delayed the acrophase (q_{12}=3.21, P<0.05, **Fig. 4-3D**).

Effect of wheel access on PER2:LUC rhythms in the SCN and peripheral tissues of WT mice.

In WT mice, manipulating the timing of wheel access altered properties of behaviour and physiology. We wanted to explore whether wheel access would also change properties of the molecular clock by recording bioluminescence rhythms of SCN (**Fig. 4-4A**), heart, liver and adrenals from *Per2:luc* mice subject to the various wheel access conditions.

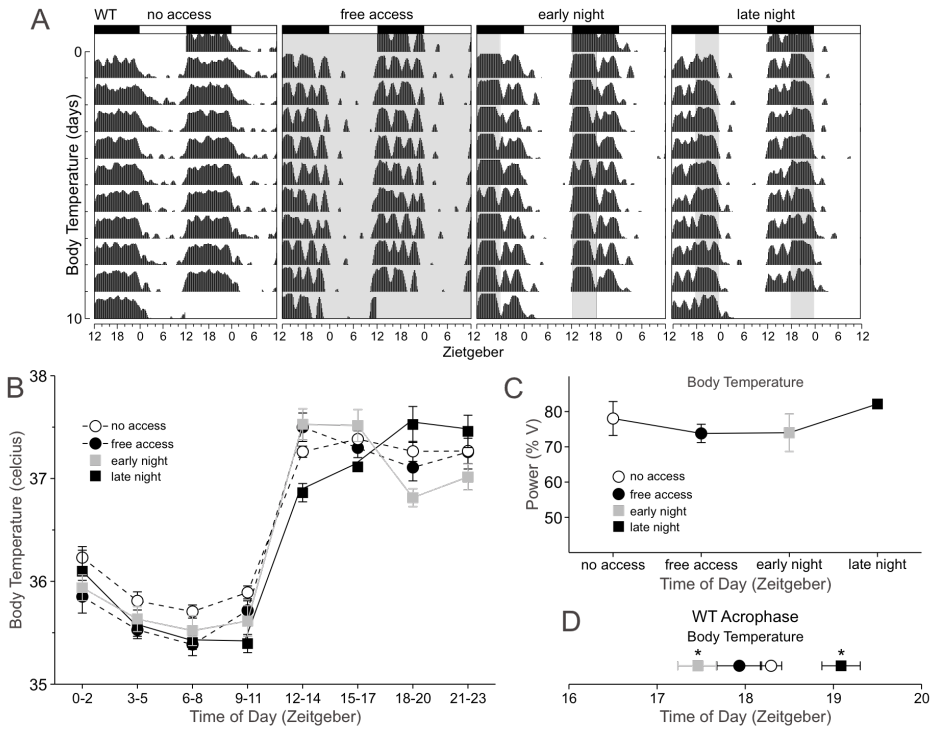

Figure 4-3: *Wheel access altered daily rhythms of body temperature in WT mice. (A) Double plotted raster plot of body temperature using 10 consecutive days of temperature recording from the same WT mouse subject to the four wheel-access conditions under a 12:12 LD cycle. (B) Group mean waveforms using 10 days of temperature recordings from WT mice (n=7) subject to the various wheel access conditions. Temperature data were grouped into 3hr bins. Wheel access increased temperature when wheel access was available, but also decreased temperatures at certain timepoints of their rest phase. For statistical results see Table 4- 2. (C) Wheel access did not alter the power of body temperature rhythms in WT mice. Power measurement was produced by periodogram analysis using 10 days of temperature data. (D) Wheel access altered the acrophase of body temperature rhythms. Early night access advanced while late night access delayed the acrophase of body temperature. Average acrophase from 10 days of data were calculated using the ClockLab Software.*

We first examined the effect of wheel access on the timing of PER2:LUC peaks, which would reflect the phasing of gene expression in the various tissues. In the adrenals (t_{14}=-2.97, P=0.01) and livers (t_{14}=-2.17, P=0.047) of WT mice, free access delayed the timing of PER2:LUC peaks (**Fig. 4-4B**). Scheduled wheel access also had a significant effect on the timing of PER2:LUC in both the liver ($F_{2,23}$=8.05, P=0.003) and adrenals ($F_{2,23}$=6.73, P=0.006). In the liver, early night (t_{14}=3.54, P=0.002) and late night access (t_{14}=3.41, P=0.003) delayed the timing of peaks, whereas in the adrenals only early night access (t_{14}=3.61, P= 0.002) caused a

significant delay. In the heart, free access (t_{13}=-1.34, P=0.20) and scheduled wheel access ($F_{3,31}$=2,23, P=0.092) had no significant effect on timing (**Fig. 4-4B**). In the SCN, the average timing of PER2:LUC peaks were not significantly different between mice subject to the various wheel conditions (free access: T=76, P=0.44; scheduled access: $F_{2,23}$=0.60, P=0.56), however the range of peak times was increased when allowed any amount of running (no access 2.48 hr, free access: 7.28 hr; early night: 9.0 hr; late night: 6.0 hr; **Fig. 4-4C**).

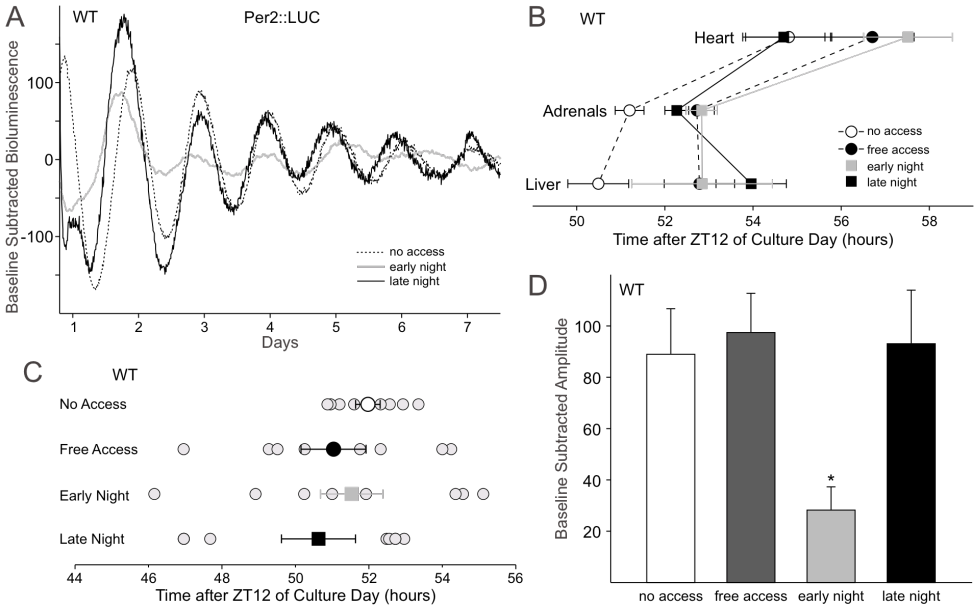

Figure 4-4: *Wheel access effects on PER2:LUC rhythms in the SCN and peripheral tissues of WT mice. (A) Example bioluminescence waveforms from the SCN of WT mice subject to wheel access conditions. (B) Average timing of PER2:LUC peaks in the peripheral tissues of WT mice. Significant delays in timing were detected in the adrenals and livers. (C) Average timing of PER2:LUC peaks in the SCN of WT mice (larger symbols with error bars) did not significantly differ between wheel access groups, however when examining individual samples (smaller grey circles), the variability of the timing was increased when mice were provided any form of wheel access. The x-axis represents the number of hours after ZT12 of culture day. (D) Effects of wheel access on the amplitude of PER2:LUC rhythms in the SCN of WT mice, where early night wheel access significantly dampened the amplitude of PER2:LUC rhythms compared to no access conditions. Average PER2:LUC timing and amplitude were analyzed using a one-way ANOVA. For statistical results see text. Error bars are SEM. (*=P<0.05).*

We next examined the effect of wheel access on the period of PER2:LUC rhythms in the various tissues (**Table 4-4**). Free access conditions lengthened the period of PER2:LUC in the SCN (t_{14}=-2.22, P=0.04) as well as in the heart (t_{12}=-2.29, P=0.04), but there was no effect in the

liver or adrenals. Early night (t_{14}=4.79, P<0.001) and late night (t_{14}= 3.07, P=0.006) wheel access lengthened the period of PER2:LUC bioluminescence in the adrenals ($F_{2,23}$=11.8, P<0.001) but not in the SCN, heart or the liver.

Lastly, we examined the effect of wheel access on the amplitude of PER2:LUC rhythms in the SCN and peripheral tissues. In the adrenals, free access had no effect but, scheduled wheel access (H_2=12.35, P=0.002) during the early (q_{14}=3.12, P<0.05) and late night (q_{14}=4.95, P<0.05) increased the amplitude of rhythms (**Table 4-5**). We did not find a significant change in amplitude in any of the other tissues. In the SCN, free access did not change the amplitude of PER2:LUC rhythms compared to no access (**Fig. 4-4D**). Scheduled wheel access on the other hand, had a significant effect on SCN PER2:LUC amplitude (H_2=9.3, P=0.01), whereby wheel access in the early night (Q_{13}=2.73, P<0.05) decreased amplitude.

In summary, wheel access delayed the timing of PER2:LUC rhythms in some of the peripheral tissues and produces a variable effect on the timing in the SCN of WT mice. There are also effects on amplitude and period in the SCN and some peripheral tissues.

Late night access rescues circadian parameters of behaviour, physiology and gene expression in VIP-deficient mice.

We subjected VIP-deficient mice to the four wheel access conditions (**Fig. 4-5A**) to explore whether we could alter or rescue circadian parameters, which are disrupted in these mice. Consistent with previous reports, VIP-deficient mice without wheel access displayed an advanced acrophase in cage activity (t_{12}=7.21; P<0.001; **Fig.5C**), HR (t_{12}=3.38, P=0.002; **Fig. 4-5D**) and body temperature (t_{12}=9.22, P<0.001, **Fig. 4-5E**) as well as lower power of HR (t_{12}=3.93, P=0.001;**Fig. 4-2C** vs. **Supp. Fig. 4-1B**) and body temperature rhythms (t_{12}=3.41,

P=0.002; **Fig. 4-3C** vs. **Supp. Fig. 4-1C**) when compared to WT controls (**Table 6**; Schroeder *et al.*, 2011). At a molecular level, we previously reported that the timing of PER2:LUC peaks was advanced in the heart (t_{14}=2.28, *P*=0.03) and adrenals (t_{14}=2.14, *P*=0.041) with a measured trend in the liver (t_{14}=1.89, *P*=0.069; **Supp. Fig. 4-2A**; **Table 4- 7**; Loh *et al.*, 2011). In the SCN, there were no significant differences in the timing of PER2:LUC peaks between genotypes (**Suppl. Fig. 4-2B**), but the amplitude of the rhythm was significantly dampened in VIP-deficient mice (t_{14}=3.37, *P*=0.002; **Fig. 4-6A,B; Table 4- 7**).

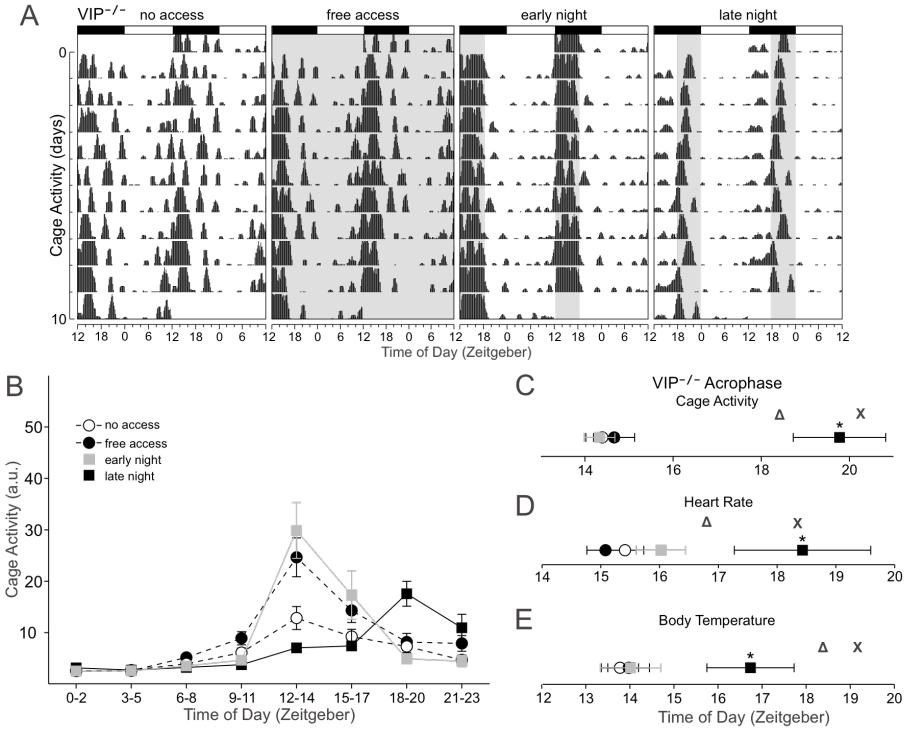

Figure 4-5: *Wheel access altered daily rhythmic properties of cage activity, HR and body temperature in VIP-deficient mice. (A) Double plotted raster plot using 10 consecutive days of cage activity from the same VIP-deficient mouse subject to the four wheel-access conditions under a 12:12 LD cycle. The profile of cage activity rhythms is altered by wheel access. (B) Group mean waveforms using 10 days of cage activity data from VIP-deficient mice (n=7) subject to the various wheel access conditions. Cage activity data were grouped into 3hr bins. Wheel access increased cage activity levels at certain timepoints of the LD cycle including periods when wheel access was provided. For statistical results see Table 4- 3. Late night wheel access delayed and rescued the acrophase of cage activity (C) and HR (D) in VIP-deficient mice. Body temperature acrophase was also delayed but only partially rescued (E; see text and Table 4- 5). Δ represent WT acrophase subject to no access while X's represent WT acrophase subject to late night access.*

When VIP-deficient mice were provided free wheel access, 24hr average cage activity significantly increased (t_6=-3.827, P=0.009; **Table 4- 1**), the power of cage activity rhythm was improved (t_6=-3.97, P=0.007; **Supp. Fig. 4-1A**) and the daily profile of cage activity was altered (**Fig. 4-5A,B**; **Table 4-3**). Scheduled wheel access did not change 24hr average activity in VIP-deficient mice (**Table 4-1**), however, we did find alterations in cage activity levels dependent on the time of day (**Fig.5 A,B**; **Table 4-3**). Only late night wheel access was able to delay the acrophase of cage activity (χ^2_2:11.1, P=0.001; q_{12}=4.54, P<0.05), effectively rescuing the advanced acrophase when compared to WT mice (**Fig. 4-5C**). Scheduled wheel access improved the power of cage activity rhythms (χ^2_2=8.86, P=0.008) in the early night (q_{12}=4.16, P<0.05) and late night (q_{12}=3.74, P<0.05) in VIP-deficient mice, but the increase in power brought about by late night access was significantly decreased when compared to WT mice (t_{12}=3.90, P<0.001; **Fig.1C**, **Supp. Fig. 4-1A**, **Table 4- 6**). Overall, by scheduling wheel access in VIP-deficient mice, we increased levels of cage activity at certain phases of an LD cycle when wheel access was provided, improved the power of cage activity rhythms and rescued its timing by providing late night wheel access.

We found that wheel access altered the profile of HR (**Supp. Fig 3A,B**) and body temperature rhythms (**Supp. Fig. 4-4A,B**) in VIP-deficient mice (**Table 4- 3**). Similar to cage activity, late night wheel access delayed the acrophase of HR (χ^2_2=8.00, P=0.016; q_{12}=3.806, P<0.05; **Fig. 4-5D**), and body temperature ($F_{2,20}$=6.46, P=0.012; t_{12}=3.24, P=0.007; **Fig. 4-5E**) in VIP-deficient mice, which eliminated the differences in acrophase of HR when compared to WT mice, while improving the relative phasing of body temperature (t_{12}=3.12, P=0.004; **Table 4- 6**). The acrophase resulting from free wheel access remained advanced in VIP-deficient mice (cage activity: t_{12}=2.58, P=0.013; HR: t_{12}=5.28,P<0.001; body temperature: t_{12}=8.08, P<0.001),

whereas early night running eliminated differences between genotypes because WT mice advanced their acrophase (**Table 4-6**).

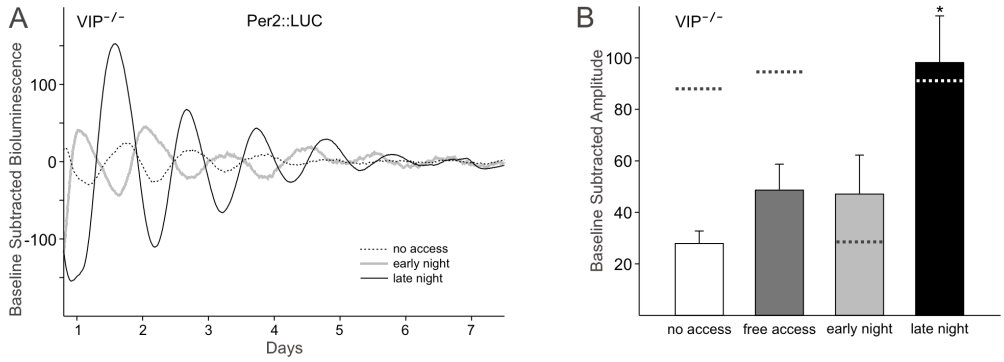

Figure 4-6: *Wheel access effects on amplitude of PER2:LUC rhythms in the SCN of VIP-deficient mice. (A) Example bioluminescence waveforms from VIP-deficient mice subject to the wheel access conditions. (B) Effects of wheel access on the amplitude of PER2:LUC rhythms in the SCN of VIP-deficient mice, where late night wheel access significantly improved the amplitude of PER2:LUC rhythms such that the amplitude was no longer significantly different when compared to WT mice (see text and Table 4- 7). Dashed lines represent WT levels. Average PER2:LUC amplitude was analyzed using a one-way ANOVA. Genotypic comparisons were analyzed using a two-way ANOVA. Error bars are SEM. (*=P<0.05).*

At a molecular level, free (T=46, P=0.024) and scheduled wheel access (H_2=8.21, P=0.017; early night: q_{14}=4.05, P<0.05; late night: q_{14}=2.90, P<0.05), significantly delayed the timing of PER2:LUC peaks in the heart, such that the differences in phasing between WT and VIP-deficient mice were eliminated (**Supp Fig. 4-2A**, **Table 4-7**). In the liver, we did not detect changes in the timing of peaks in VIP-deficient mice subject to either free or scheduled wheel access (**Supp. Fig. 4-2A**). When compared to WT, PER2:LUC timing in the livers of VIP-deficient mice was different under free access (t_{14}=2.76, P=0.01), but no differences were detected when subject to scheduled wheel access (**Table 4-7**). In the adrenals, only free access delayed PER2:LUC peaks (t_{15}=3.32, P=0.005) eliminating genotypic differences in timing, but PER2:LUC phasing remained advanced in VIP-deficient mice subject to scheduled access (early night: t_{14}=4.12, P<0.001; late night t_{14}=2.80, P=0.008; **Supp. Fig. 4-4A**; **Table 4-7**). We also

detected some changes in period (**Table 4-4**) and amplitude (**Table 4-5**) of PER2:LUC rhythms in peripheral tissues of VIP-deficient mice as a result of wheel access (**Table 4-7**).

In the SCN, free and scheduled access did not change the average timing of PER2:LUC peaks in VIP-deficient mice (**Supp. Fig. 4-2B**), and no differences were detected between genotypes (**Table 4-7**). However, there was an increase in the range of timing of PER2:LUC peaks in mice subject to early night access (no access 5.5 hrs; early night: 19.2 hrs). Lastly, the amplitude of PER2:LUC rhythms in the SCN of VIP-deficient mice was increased when mice were subject to late night access (q_{14}=4.15, P<0.05; **Fig. 4-6B**), which eliminated the differences between genotypes and rescued the amplitude in VIP-deficient mice (**Table 4-7**).

Discussion

The effects of stimulated activity on the circadian system have been previously studied, most under conditions of controlled constant environments or examining responses to single bouts of stimulated activity (Reebs & Mrosovsky, 1989; Edgar & Dement, 1991; Marchant & Mistlberger, 1996; Kas & Edgar, 2001; Maywood & Mrosovsky, 2001; Buxton *et al.*, 2003; Canal & Piggins, 2006; Koletar *et al.*, 2011). However, most of life and the circadian pacemaker have evolved under the entrainment effects of daily LD cycles, raising the issue that circadian properties should be examined under the influence of an LD cycle as responses to environmental factors may differ when studied under constant conditions (Mrosovsky, 1996; Roenneberg *et al.*, 2010). In our studies, we examined the ability of stimulated activity induced by wheel access to modify rhythms while entrained to an LD cycle. We altered the duration and timing of wheel access for at least two weeks to drive wheel running activity at different phases within the dark period in WT mice and examined whether this scheduled wheel access could reorganize rhythms

in behaviour, physiology and gene expression. Lastly, we subjected VIP-deficient mice to scheduled wheel access in an attempt to improve their abnormal entrainment to an LD cycle.

Our studies demonstrated that scheduled wheel access increased levels of cage activity, thereby inducing a level of exercise at specified times of the LD cycle in WT mice (Aufradet *et al.*, 2012). Consistent with previous studies, we found that free access to the running wheel under an LD cycle increased the levels of cage activity throughout the dark phase (Visser *et al.*, 2005). We also showed that scheduled wheel access restricted to 6 hrs during the early or late night, increased activity levels during the period of wheel availability, thereby advancing and delaying the acrophase of cage activity, respectively. Alterations in the phasing of activity onset under an LD cycle were observed in hamsters aroused with a novel wheel at the end of the dark phase (Mistlberger, 1991). This daily stimulation of activity is encoded within the circadian system whereby the effects on behaviour are sustained for many days after removal of the stimulus (SUGIMOTO *et al.*, 1994; Reebs & St-Coeur, 1994; Mistlberger & Holmes, 2000). Furthermore, when animals entrained to various phases of stimulated activity are deprived of arousal and placed in constant conditions, the period of activity diverges suggesting that encoding of activity within the circadian system is dependent on its timing (Mistlberger, 1991; Reebs & St-Coeur, 1994). The observed modulation of circadian properties by stimulated activity under an LD cycle suggests that this manipulation could potentially drive and organize rhythms of other behavioural and physiological outputs regulated by the circadian system.

We were able to effectively induce exercise and alter the timing of cage activity relative to the LD cycle in WT mice, which subsequently altered the daily profile and timing of HR and body temperature rhythms (SUGIMOTO *et al.*, 1994), two physiological outputs whose function is regulated by the circadian system (Abe *et al.*, 1979; Warren *et al.*, 1994). Exercise during the

early night advanced the acrophase of body temperature rhythms, whereas late night exercise delayed the acrophase of both body temperature and HR rhythms. Shifts in the timing of physiological rhythms may be driven by the metabolic cycles induced by scheduled exercise (Kohsaka *et al.*, 2012). Our results demonstrated that even under the strong entrainment effects of an LD cycle, scheduled exercise shifted the timing of physiological rhythms.

In addition to the effects on physiology, scheduled exercise altered properties of the molecular clock in the SCN and peripheral tissues of WT mice, suggesting that daily exercise feeds back to the clock to modulate tissue and cell function and that the changes in behavioural and physiological rhythms are not merely acute responses. Within the SCN, the average timing of PER2:LUC peaks were not significantly different between the four conditions, however rather than improving precision of rhythms among individual mice within a treatment group, the variability in the timing of PER2:LUC peaks was increased. Parallel to previous studies, our data demonstrated that scheduled exercise even in an LD cycle altered molecular phasing in the SCN of WT mice (Maywood *et al.*, 1999; Yannielli *et al.*, 2002). In addition to changes in phasing, we also detected a significant blunting of PER2:LUC amplitude caused by early night running, which could be a result of reduced PER2:LUC protein levels, a loss of synchrony among individual neurons or a combination of both. This result was quite surprising, considering the robust rhythms of activity in mice subject to early night running. Furthermore, mice subject to free access conditions that run during the first 6 hrs of dark, retain robust rhythms in PER2:LUC in the SCN. Therefore, running late at night may be providing cues that maintain robust molecular rhythms.

In peripheral tissues, wheel access delayed the timing of PER2:LUC in the liver and adrenals, but no significant effects were measured in the heart of WT mice. We also detected a

boost in PER2:LUC amplitude in the adrenals of WT mice. Changes in amplitude and timing of the molecular clock were also documented in zebrafish subject to exercise during the day (Egg *et al.*, 2011). The adrenals may be responding directly to the level of exercise (Otawa *et al.*, 2007; Cagampang *et al.*, 2011), whereas the molecular phasing in the liver shifts in response to changes in the timing of feeding, which may reorganize due to scheduled exercise (Hirao *et al.*, 2010). Here, we demonstrated that scheduled wheel access altered molecular properties in the SCN and peripheral tissues under an LD cycle. Studies of other nonphotic input such as feeding can uncouple the central and peripheral oscillators under an LD cycle, effectively altering the molecular clock in the peripheral tissues but leaving the SCN unaffected (Damiola *et al.*, 2000; Honma & Honma, 2009). Our studies demonstrated a clear effect of nonphotic manipulation on properties of the central oscillator in rhythmically robust mice suggesting that exercise mediated changes on daily rhythms involves alterations in SCN function. Furthermore, this implies that exercise could be used as a tool to drive rhythms within the SCN even under the influence of an LD cycle.

VIP is localized to a subset of neurons within the SCN and is thought to promote coupling among single cell oscillators to produce coherent output signals (Vosko *et al.*, 2007). Under an LD cycle and without wheel access, the loss of VIP or its receptor (VIPR2) leads to reduced power of behaviour and physiological rhythms as well as an advancement in their onset (Bechtold *et al.*, 2008; Sheward *et al.*, 2010; Schroeder *et al.*, 2011; Hannibal *et al.*, 2011). The phasing of the molecular clock in peripheral tissues parallels behaviour in VIP-deficient mice, such that Per2 *mRNA* or PER2:LUC protein peak a few hours before WT (Loh *et al.*, 2011). Lastly, within the SCN, although the average phasing of PER2:LUC is not altered, the amplitude of rhythms is significantly depressed in VIP-deficient mice (Loh *et al.*, 2011). Scheduled wheel

access during the late night was able to rescue many of the observed deficits of VIP-deficient mice under an LD cycle. Exercise in the late night increased cage activity levels and improved the power of its rhythm. Late night exercise also delayed the acrophase of cage activity rhythms such that the phase was no longer different when compared to WT mice. This manipulation was also able to significantly delay the acrophase of both HR and body temperature rhythms in VIP-deficient mice, rescuing or improving the phase when compared to WT mice, respectively. This manipulation, however, did not rescue the power of HR and body temperature rhythms. At a molecular level, the average phasing of PER2:LUC peaks in the SCN were not different between genotypes. Notably, late night wheel access increased the amplitude of PER2:LUC rhythms in the SCN of VIP-deficient mice to WT levels, suggesting an improvement of synchrony in the SCN despite the absence of VIP. Lastly, wheel access at night delayed the timing of PER2:LUC in the heart and liver of VIP-deficient mice and were no longer advanced compared to WTs, which also improved the phase relationship of peripheral tissues with the SCN. Overall, we demonstrated an improvement in several properties of diurnal rhythms in circadian compromised VIP-deficient mice. These mice display deficits in the light response pathway, and therefore have poor entrainment under an LD cycle. Exercise specifically in the late night may be altering SCN properties either by promoting better synchrony among neurons and/or delaying clock gene expression that optimizes the phase at which light hits the molecular clock enhancing entrainment to an LD cycle.

Scheduled wheel access alters diurnal rhythms in WT and can improve diurnal rhythms in VIP-deficient mice. Exercise itself has many beneficial effects on the body (Warburton *et al.*, 2006; Mercken *et al.*, 2011), but our studies demonstrated that the timing of exercise is important in altering physiology as well as gene expression in various tissues. Timed exercise could be

applied to humans and used as a tool to manipulate and or stabilize daily rhythms. Coordinated timing of behaviour and physiology as well as their alignment to the LD cycle is important as misalignments are correlated with the development of disease (Navara & Nelson, 2007; Stevens, 2009; Thorpy, 2011; Kivimäki *et al.*, 2011). Under conditions in which entrainment to the LD cycle is disrupted, whether a result of genetics, age or disease (Maywood *et al.*, 2006; Takahashi *et al.*, 2008; Colwell, 2011), timing of exercise could help shift rhythms to better realign with the external environment, which could potentially delay or prevent development of disease.

iii. Supplemental Data

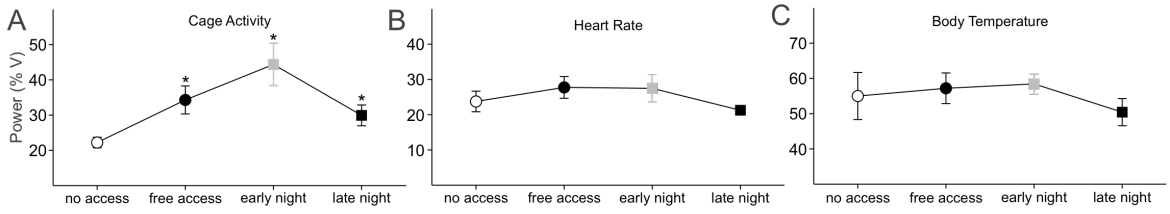

Supplemental Figure 4-1: *Effects of wheel access on power of cage activity, HR and body temperature rhythms in VIP-deficient mice. (A) All four wheel access conditions increased the power of cage activity rhythms in VIP-deficient mice. Wheel access did not improve the power of HR (B) or body temperature (C) rhythms in VIP-deficient mice. Power measurement was produced by periodogram analysis using 10 days of HR data. Power was analyzed by one-way repeated measures ANOVA while genotypic comparisons were analyzed using a two-way repeated measures ANOVA. Error bars are SEM. (*=P<0.05)*

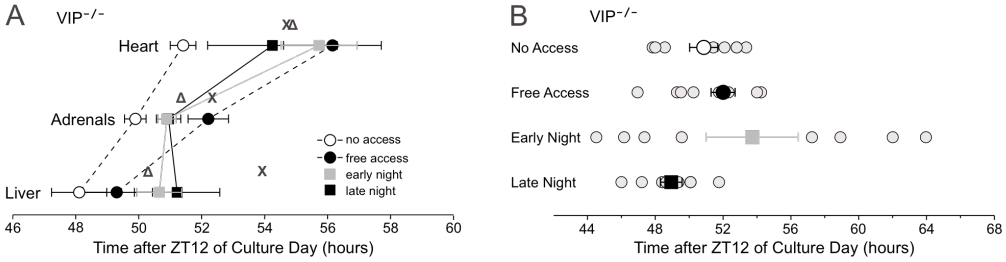

Supplemental Figure 4-2: *Wheel access alters the timing of PER2:LUC peaks in the SCN and peripheral tissues of VIP-deficient mice (A) Average timing of PER2:LUC peaks in the peripheral tissues of VIP-deficient mice. Significant delays in timing were detected in the heart and adrenals. For statistical results see text. (B) Average timing of PER2:LUC peaks in the SCN of VIP-deficient mice (larger symbols with error bars) did not differ between wheel access groups, however when examining individual samples (smaller grey circles), the variability of the timing was increased when mice were provided early night wheel access. The x-axis represents the number of hours after ZT12 of culture day. Average PER2:LUC timing and amplitude were analyzed using a one-way ANOVA. Genotypic comparisons were analyzed using a two-way ANOVA. Error bars are SEM.*

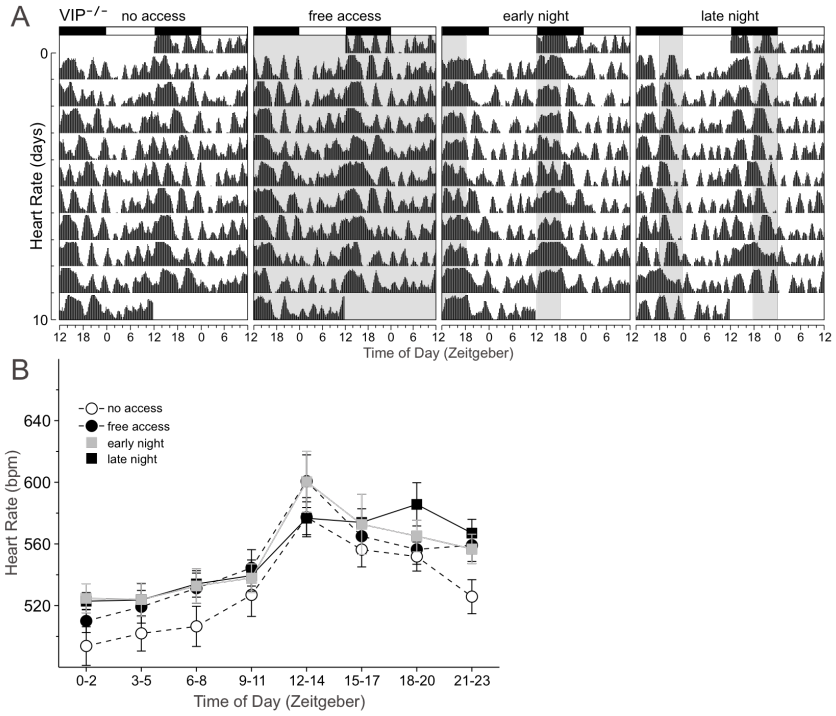

Supplemental Figure 4-3: *Wheel access alters rhythms of HR in VIP-deficient mice. (A) Double plotted raster plot of HR using 10 consecutive days of HR recording from the same VIP-deficient mouse subject to the four wheel-access conditions under a 12:12 LD cycle. (B) Group mean waveforms using 10 days of HR recordings from VIP-deficient mice (n=7) subject to the various wheel access conditions. HR data were grouped into 3hr bins. For statistical results see Table 4- 3. Average waveforms were analyzed using a two-way repeated measures ANOVA. Error bars are SEM.*

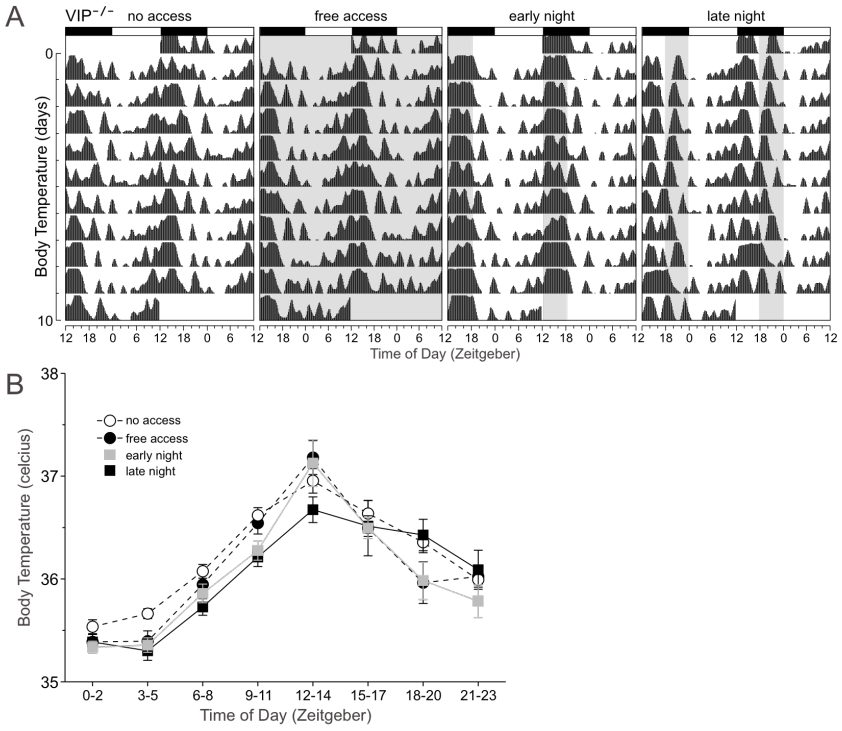

Supplemental Figure 4-4: *Wheel access alters rhythms of body temperature in VIP-deficient mice. (A) Double plotted raster plot of body temperature using 10 consecutive days of temperature recording from the same VIP-deficient mouse subject to the four wheel-access conditions under a 12:12 LD cycle. (B) Group mean waveforms using 10 days of temperature recordings from VIP-deficient mice (n=7) subject to the various wheel access conditions. Temperature data were grouped into 3hr bins. For statistical results see Table 4- 3. Average waveforms were analyzed using a two-way repeated measures ANOVA. Error bars are SEM.*

	Cage Activity (a.u.)		Heart Rate (bpm)		Body Temperature (°C)	
	WT	VIP-/-	WT	VIP-/-	WT	VIP-/-
no access	7.6 ± 1.0	6.17 ± 0.92	563 ± 11	529 ± 10	36.60 ± 0.06	36.23 ± 0.06
free access	17.5 ± 3.1*	9.28 ± 1.35*	589 ± 11*	548 ± 10	36.43 ± 0.08*	36.12 ± 0.08
early night	13.5 ± 2.11	8.73 ± 1.06	587 ± 15*	551 ± 11	36.40 ± 0.10*	36.03 ± 0.09
late night	12.0 ± 7.8	6.98 ± 0.86	589 ± 11*	553 ± 9	36.38 ± 0.10*	36.04 ± 0.09

Supplemental Table 4-1: *Twenty-four hr averages of cage activity, HR and body temperature in WT and VIP-deficient mice subject to wheel access conditions. (*=P<0.05).*

TABLE 2: Two-way repeated measures ANOVA analysis, comparing average waveforms of Cage Activity, Heart Rate and Body Temperature against no wheel access conditions in WT mice

WT	Cage Activity			Heart Rate			Body Temperature		
	Free Access	Scheduled Access		Free Access	Scheduled Access		Free Access	Scheduled Access	
condition	$F1,111$=17.8, P=0.006	$F2,167$=4.22, P=0.041		$F1,111$=13.4, P=0.011	$F2,167$=13.2, $P<0.001$		$F1,111$=5.89, P=0.051	$F2,167$=7.43, P=0.008	
time of day	$F7,111$=24.4, P<0.001	$F7,167$=17.4, P<0.001		$F7,111$=136, P<0.001	$F7,167$=137, P<0.001		$F7,111$=156, P<0.001	$F7,167$=154, P<0.001	
interaction	$F7,111$=10.5, P<0.001	$F14,167$=12.0, P<0.001		$F7,111$=2.32, P=0.043	$F14,167$=6.05, P<0.001		$F7,111$=5.12, P<0.001	$F14,167$=7.40, P<0.001	
Time of day (ZT)		Early Night	Late Night		Early Night	Late Night		Early Night	Late Night
0-2	t_{12}=0.43, P=0.671	t_{12}=0.38, P=0.707	t_{12}=0.12, P=0.901	t_{12}=2.50, P=0.024*	t_{12}=3.04, P=0.004*	t_{12}=4.98, P<0.001*	t_{12}=3.74, P=0.001*	t_{12}=2.36, P=0.021	t_{12}=1.06, P=0.290
3-5	$t_{12}=0.44$, $P=0.662$	t_{12}=0.11, P=0.914	t_{12}=0.13, P=0.900	t_{12}=2.52, P= 0.024*	t_{12}=2.75, P=0.008*	t_{12}=3.65, P=0.001*	t_{12}=2.77, P= 0.009*	t_{12}=1.42, P=0.158	t_{12}=2.00, P=0.048
6-8	$t_{12}=0.27$, $P=0.791$	t_{12}=0.11, P=0.915	t_{12}=0.16, P=0.870	t_{12}=3.07, P=0.008*	t_{12}=2.35, P=0.023*	t_{12}=3.22, P=0.002*	t_{12}=3.15, P= 0.003*	t_{12}=1.49, P=0.139	t_{12}=2.43, P=0.017
9-11	$t_{12}=0.61$, $P=0.547$	t_{12}=0.08, P=0.940	t_{12}=0.32, P=0.750	t_{12}=2.94, P=0.010*	t_{12}=1.18, P=0.242	t_{12}=0.97, P=0.338	t_{12}=1.72, P= 0.095	t_{12}=2.24, P=0.027	t_{12}=4.01, P<0.001*
12-14	$t_{12}=6.89$, $P<0.001$*	t_{12}=5.72, P<0.001*	t_{12}=1.25, P=0.214	t_{12}=1.09, P=0.291	t_{12}=2.72, P=0.009*	t_{12}=1.12, P=0.270	t_{12}=2.34, P= 0.026*	t_{12}=2.15, P=0.034*	t_{12}=3.21, P=0.002*
15-17	$t_{12}=4.99$, $P<0.001$*	t_{12}=5.33, P<0.001*	t_{12}=0.59, P=0.559	t_{12}=2.52, P=0.024*	t_{12}=4.22, P<0.001*	t_{12}=1.44, P=0.155	t_{12}=0.84, P= 0.406	t_{12}=1.06, P=0.292	t_{12}=2.18, P=0.032
18-20	$t_{12}=3.35$, $P=0.002$*	t_{12}=0.61, P=0.546	t_{12}=6.02, P<0.001*	t_{12}=3.77, P=0.002*	t_{12}=3.33, P=0.002*	t_{12}=5.37, P<0.001*	t_{12}=1.54, P= 0.132	t_{12}=3.63, P<0.001*	t_{12}=2.12, P=0.038*
21-23	$t_{12}=4.93$, $P<0.001$*	t_{12}=0.62, P=0.54	t_{12}=3.44, P=0.001*	t_{12}=4.53, P<0.001*	t_{12}=3.03, P=0.004*	t_{12}=5.53, P<0.001*	t_{12}=0.10, P= 0.918	t_{12}=2.04, P=0.044	t_{12}=1.53, P=0.128

Supplemental Table 4-2: *Two-Way repeated measures analysis comparing wheel induced changes in average waveforms of cage activity, HR and body temperature against no wheel access conditions in WT mice.*

TABLE 3:Two-way repeated measures ANOVA analysis, comparing average waveforms of Cage Activity, Heart Rate and Body Temperature against no wheel access conditions in VIP-deficient mice

VIP-/-	Cage Activity			Heart Rate			Body Temperature		
	Free Access	Scheduled Access		Free Access	Scheduled Access		Free Access	Scheduled Access	
condition	$F1,111$=14.6, P=0.009	$F2,167$=2.12, P=0.163		$F1,111$=21.3, P=0.004	$F2,167$=1.28, P=0.313		$F1,111$=8.06, P=0.030	$F2,167$=5.12, P=0.025	
time of day	$F7,111$=31.4, P<0.001	$F7,167$=20.0, P<0.001		$F7,111$=64.7, P<0.001	$F7,167$=62.8, P<0.001		$F7,111$=48.0, P<0.001	$F7,167$=41.6, P<0.001	
interaction	$F7,111$=11.8, P<0.001	$F14,167$=13.1, P<0.001		$F7,111$=1.94, P=0.087	$F14,167$=2.01, P=0.027		$F7,111$=5.76, P<0.001	$F14,167$=3.24, $P<0.001$	
Time of day (ZT)		Early Night	Late Night		Early Night	Late Night		Early Night	Late Night
0-2	$t_{12}=0.01$, P=0.989	t_{12}=0.00, P=0.999	t_{12}=0.25, P=0.803	t_{12}=2.24, P=0.031*	t_{12}=1.74, P=0.099	t_{12}=1.64, P=0.119	t_{12}=1.79, P=0.080	t_{12}=1.50, P=0.138	t_{12}=1.12, P=0.267
3-5	$t_{12}=0.10$, P=0.922	t_{12}=0.05, P=0.962	t_{12}=0.00, P=0.997	t_{12}=2.37, P=0.023*	t_{12}=1.24, P=0.233	t_{12}=1.22, P=0.238	t_{12}=3.25, P=0.002*	t_{12}=2.30, P=0.024*	t_{12}=2.72, P=0.008*
6-8	$t_{12}=0.92$, P=0.367	t_{12}=0.17, P=0.864	t_{12}=0.30, P=0.767	t_{12}=3.40, P=0.002*	t_{12}=1.48, P=0.157	t_{12}=1.55, P=0.138	t_{12}=1.55, P=0.127	t_{12}=1.62, P=0.110	t_{12}=2.61, P=0.011*
9-11	$t_{12}=2.08$, P=0.046*	t_{12}=0.61, P=0.541	t_{12}=0.98, P=0.330	t_{12}=2.42, P=0.021*	t_{12}=0.62, P=0.544	t_{12}=0.71, P=0.487	t_{12}=0.919, P=0.363	t_{12}=2.57, P=0.012*	t_{12}=3.04, P=0.003*
12-14	$t_{12}=8.78$, P<0.001*	t_{12}=7.13, P<0.001*	t_{12}=2.42, P=0.018*	t_{12}=3.21, P=0.003*	t_{12}=1.30, P=0.211	t_{12}=0.04, P=0.971	t_{12}=2.74, P=0.009*	t_{12}=1.30, P=0.198	t_{12}=2.11, P=0.038
15-17	$t_{12}=3.77$, P=0.001*	t_{12}=3.37, P=0.001*	t_{12}=0.76, P=0.451	t_{12}=1.19, P=0.241	t_{12}=0.92, P=0.368	t_{12}=0.99, P=0.334	t_{12}=1.69, P=0.098	t_{12}=1.06, P=0.294	t_{12}=0.91, P=0.366
18-20	$t_{12}=0.63$, P=0.531	t_{12}=1.00, P=0.320	t_{12}=4.29, P<0.001*	t_{12}=0.63, P=0.532	t_{12}=0.75, P=0.465	t_{12}=1.91, P=0.073	t_{12}=4.77, P<0.001*	t_{12}=2.80, P=0.006*	t_{12}=0.54, P=0.594
21-23	$t_{12}=2.37$, P=0.024*	t_{12}=0.10, P=0.918	t_{12}=2.62, P=0.011*	t_{12}=4.57, P<0.001*	t_{12}=1.75, P=0.098	t_{12}=2.34, P=0.032	t_{12}=0.38, P=0.704	t_{12}=1.56, P=0.122	t_{12}=0.74, P=0.464

Supplemental Table 4-3: *Two-Way repeated measures analysis comparing wheel induced changes in average waveforms of cage activity, HR and body temperature against no wheel access conditions in VIP-deficient mice.*

TABLE 4: Period of Per2:LUC rhythms in WT and VIP-deficient mice.

		WT	VIP-/-
SCN			
	no access	24.99 ± 0.28	25.53 ± 0.37
	free access	25.73 ± 0.19*	26.15 ± 0.52
	early night	25.77 ± 0.82	26.19 ± 0.87
	late night	25.00 ± 0.45	24.80 ± 0.55
Heart			
	no access	23.77 ± 0.18	23.69 ± 0.26
	free access	24.64 ± 0.33*	24.30 ± 0.63
	early night	24.26 ± 0.17	24.42 ± 0.25
	late night	23.69 ± 0.51	24.68 ± 0.25*
Liver			
	no access	24.88 ± 0.33	24.26 ± 0.28
	free access	24.79 ± 0.76	24.52 ± 0.7
	early night	25.05 ± 0.65	25.70 ± 0.69
	late night	25.95 ± 0.51	25.27 ± 0.56
Adrenals	no access	22.94 ± 0.15	22.93 ± 0.15
	free access	23.20 ± 0.16	23.12 ± 0.22
	early night	23.69 ± 0.14*	23.35 ± 0.18
	late night	23.61 ± 0.05*	23.47 ± 0.23

Supplemental Table 4-4: *Period of PER2:LUC rhythms in the SCN and peripheral tissues of WT and VIP-deficient mice. *=P<0.05, statistical significance within genotype.*

TABLE 5: Amplitude of Per2:LUC rhythms in the peripheral tissues of WT and VIP-deficient mice.

		WT	VIP-/-
Heart			
	no access	27.4 ± 5.71	20.4 ± 3.46
	free access	16.9 ± 7.81	23.5 ± 6.12
	early night	17.9 ± 4.19	43.6 ± 9.62^
	late night	30.5 ± 5.20	40.3 ± 9.68
Liver			
	no access	84.1 ± 17.9	47.0 ± 8.00
	free access	113.9 ± 49.1	74.7 ± 16.0
	early night	54.8 ± 16.1	49.7 ± 12.0
	late night	66.6 ± 15.0	39.3 ± 6.22
Adrenals			
	no access	76.7 ± 16.1	72.8 ± 13.3
	free access	87.7 ± 20.8	87.6 ± 34.2
	early night	122.1 ± 21.4*	93.0 ± 13.0
	late night	288.2 ± 46.5*	122.4 ± 18.7^

Supplemental Table 4-5: *Amplitude of PER2:LUC rhythms in the peripheral tissues of WT and VIP-deficient mice. *=P<0.05, statistical significance within genotype. ^= P<0.05, statistical significant between genotypes.*

Table 6: Two Way ANOVA analysis comparing wheel access condition and genotypic effect on power and acrophase of cage activity, HR and body temperature rhythms

		Power				Acrophase			
	Factors	Free Access		Scheduled Access		Free Access		Scheduled Access	
Cage Activity	genotype	*F*1,27=1.73	*P*=0.213	*F1,41*=10.1	*P*=0.008*	*F*1,27=59.7	*P*<0.001*	*F1,41*=18.7	*P*<0.001*
	access conditions	*F1,27*=37.1	*P*<0.001*	*F2,41*=21.2	*P*<0.001*	*F1,27*=1.40	*P*=0.26	*F2,41*=52.2	*P*<0.001*
	interaction	*F1,27*=0.065	*P*=0.804	*F2,41*=3.01	*P*=0.068	*F1,27*=3.77	*P*=0.076	*F2,41*=6.56	*P*=0.005*
HR	genotype	*F*1,27=17.7	*P*=0.001*	*F1,41*=64.7	*P*<0.001*	*F1,27*=28.6	*P<0.001**	*F1,41*=3.04	*P*=0.107
	access conditions	*F1,27*=8.67	*P*=0.012*	*F2,41*=3.28	*P*=0.055	*F1,27*=0.19	*P*=0.67	*F2,41*=10.6	*P*<0.001*
	interaction	*F1,27*=0.01	*P*=0.920	*F2,41*=0.33	*P*=0.73	*F1,27*=1.54	*P*=0.24	*F2*,41=1.55	*P*=0.232
Body Temp	genotype	*F*1,27=*9.80*	*P*=0.009*	*F1,41*=37.0	*P*<0.001*	*F1,27*=96.4	*P*<0.001*	*F1,41*=40.1	*P*<0.001*
	access conditions	*F1,27*=0.19	*P*=0.672	*F2,41*=0.00	*P*=0.997	*F1,27*=0.12	*P=0.73*	*F2,41*=12.4	*P*<0.001*
	interaction	*F1,27*=1.85	*P*=0.199	*F2,41*=1.78	*P*=0.190	*F1,27*=1.46	*P*=0.25	*F2*,41=2.57	*P*=0.097

Supplemental Table 4-6: *Two-way ANOVA analysis examining the effect of wheel access condition and genotype on power and acrophase of cage activity, HR and body temperature rhythms. Significant post-hoc statistics are listed in the text.*

Table 7: Two Way ANOVA analysis comparing Wheel Access condition and Genotypic effect on the timing of Per2:LUC peaks in the SCN & Peripheral tissues

		Amplitude				Timing of Per2:LUC peaks			
	Factors	Free Wheel Access		Scheduled Wheel Access		Free Wheel Access		Scheduled Wheel Access	
SCN	genotype	*F1,31*=18.3	*P*<0.001*	*F1,47*=0.99	*P*=0.326	*F1,31*=0.008	*P*= 0.931	*F1,47*=0.04	*P*=0.850
	access conditions	*F1,31*=1.30	*P*=0.265	*F2,47*= 7.42	*P*=0.002*	*F1,31*=0.027	*P*=0.870	*F2,47*= 2.26	*P*=0.117
	interaction	*F1,31*=0.23	*P*=0.636	*F2,47*=3.93	*P*=0.027*	*F1,31*=2.13	*P*=0.155	*F2,47*=1.21	*P*=0.307
Heart	genotype	*F1,31*=0.08	*P*=0.786	*F1,47*=3.40	*P*=0.072	*F1,30*= 4.84	*P*= 0.036*	*F1,47*=3.65	*P*=0.063
	access conditions	*F1,31*=0.16	*P*=0.694	*F2,47*=1.67	*P*=0.200	*F1,20*= 7.47	*P*=0.01*	*F2,47*= 4.31	*P*=0.020*
	interaction	*F1,31*=0.86	*P*=0.362	*F2,47*=3.45	*P*=0.045*	*F1,30*= 0.93	*P*=0.34	*F2,47*=0.75	*P*=0.479
Liver	genotype	*F1,31*=1.91	*P*=0.178	*F1,47*=4.60	*P*=0.038*	*F1,31*=10.8	*P*=0.003*	*F1,47*=7.88	*P*=0.008*
	access conditions	*F1,31*=1.08	*P*=0.307	*F2,47*=0.64	*P*=0.532	*F1,31*=3.82	*P*=0.061	*F2,47*=5.17	*P*=0.010*
	interaction	*F1,31*=0.00	*P*=0.969	*F2,47*=0.76	*P*=0.474	*F1,31*=0.38	*P*=0.54	*F2,47*=0.03	*P*=0.966
Adrenals	genotype	*F1,32*=0.01	*P*=0.928	*F1,48*=11.4	*P*=0.002*	*F1,32*=4.33	*P*=0.046*	*F1,47*=31.9	*P*<0.001*
	access conditions	*F1,32*=0.34	*P*=0.563	*F2,48*=15.9	*P*<0.001*	*F1,32*=19.2	*P*<0.001*	*F2,47*=9.14	*P*<0.001*
	interaction	*F1,32*=0.01	*P*=0.933	*F2,48*=6.52	*P*=0.003*	*F1,32*=0.81	*P=0.37*	*F2,47*=0.60	*P*=0.556

Supplemental Table 4-7: *Two-way ANOVA analysis examining the effect of wheel access condition and genotype on the timing of PER2:LUC peaks and amplitude in the SCN and peripheral tissues. Significant post-hoc statistics are listed in the text.*

iv. Bibliography

Abe K, Kroning J, Greer MA & Critchlow V (1979). Effects of Destruction of the Suprachiasmatic Nuclei on the Circadian Rhythms in Plasma Corticosterone, Body Temperature, Feeding and Plasma Thyrotropin. *Neuroendocrinology* **29,** 119–131.

Aufradet E, Bessaad A, Alsaid H, Schäfer F, Sigovan M, De Souza G, Chirico E, Martin C & Canet-Soulas E (2012). In vivo cardiac anatomical and functional effects of wheel running in mice by magnetic resonance imaging. *Experimental Biology and Medicine (Maywood, NJ)*; DOI: 10.1258/ebm.2011.011034.

Bechtold DA, Brown TM, Luckman SM & Piggins HD (2008). Metabolic rhythm abnormalities in mice lacking VIP-VPAC2 signaling. *Am J Physiol Regul Integr Comp Physiol* **294,** R344–351.

Buxton OM, Frank SA, L'Hermite-Balériaux M, Leproult R, Turek FW & Van Cauter E (1997). Roles of intensity and duration of nocturnal exercise in causing phase delays of human circadian rhythms. *Am J Physiol* **273,** E536–542.

Buxton OM, Lee CW, L'Hermite-Baleriaux M, Turek FW & Van Cauter E (2003). Exercise elicits phase shifts and acute alterations of melatonin that vary with circadian phase. *Am J Physiol Regul Integr Comp Physiol* **284,** R714–724.

Cagampang FR, Poore KR & Hanson MA (2011). Developmental origins of the metabolic syndrome: body clocks and stress responses. *Brain Behav Immun* **25,** 214–220.

Canal MM & Piggins HD (2006). Resetting of the hamster circadian system by dark pulses. *Am J Physiol Regul Integr Comp Physiol* **290,** R785–792.

Castillo C, Molyneux P, Carlson R & Harrington ME (2011). Restricted wheel access following a light cycle inversion slows re-entrainment without internal desynchrony as measured in Per2Luc mice. *Neuroscience* **182,** 169–176.

Colwell CS (2011). Linking neural activity and molecular oscillations in the SCN. *Nature Reviews Neuroscience* **12,** 553–569.

Dallmann R & Mrosovsky N (2006). Scheduled wheel access during daytime: A method for studying conflicting zeitgebers. *Physiol Behav* **88,** 459–465.

Damiola F, Le Minh N, Preitner N, Kornmann B, Fleury-Olela F & Schibler U (2000). Restricted feeding uncouples circadian oscillators in peripheral tissues from the central pacemaker in the suprachiasmatic nucleus. *Genes Dev* **14,** 2950–2961.

Davidson AJ, Yamazaki S, Arble DM, Menaker M & Block GD (2008). Resetting of central and peripheral circadian oscillators in aged rats. *Neurobiology of Aging* **29,** 471–477.

Dibner C, Schibler U & Albrecht U (2010). The mammalian circadian timing system: organization and coordination of central and peripheral clocks. *Annu Rev Physiol* **72,** 517–549.

Edgar DM & Dement WC (1991). Regularly scheduled voluntary exercise synchronizes the mouse circadian clock. *Am J Physiol* **261,** R928–933.

Egg M, Tischler A, Schwerte T, Sandbichler A, Folterbauer C & Pelster B (2011). Endurance Exercise Modifies the Circadian Clock in Zebrafish (Danio rerio) Temperature Independently. *Acta Physiologica (Oxford, England)*; DOI: 10.1111/j.1748-1716.2011.02382.x.

Hannibal J, Hsiung HM & Fahrenkrug J (2011). Temporal phasing of locomotor activity, heart rate rhythmicity, and core body temperature is disrupted in VIP receptor 2-deficient mice. *Am J Physiol Regul Integr Comp Physiol* **300,** R519–530.

Hirao A, Nagahama H, Tsuboi T, Hirao M, Tahara Y & Shibata S (2010). Combination of starvation interval and food volume determines the phase of liver circadian rhythm in Per2::Luc knock-in mice under two meals per day feeding. *Am J Physiol Gastrointest Liver Physiol* **299,** G1045–G1053.

Honma K & Honma S (2009). The SCN-independent clocks, methamphetamine and food restriction. *Eur J Neurosci* **30,** 1707–1717.

Houben T, Deboer T, van Oosterhout F & Meijer JH (2009). Correlation with behavioral activity and rest implies circadian regulation by SCN neuronal activity levels. *J Biol Rhythms* **24,** 477–487.

Kalsbeek A, Palm IF, La Fleur SE, Scheer FAJL, Perreau-Lenz S, Ruiter M, Kreier F, Cailotto C & Buijs RM (2006). SCN outputs and the hypothalamic balance of life. *J Biol Rhythms* **21,** 458–469.

Kas MJH & Edgar DM (2001). Scheduled Voluntary Wheel Running Activity Modulates Free-Running Circadian Body Temperature Rhythms in Octodon degus. *J Biol Rhythms* **16,** 66–75.

Kivimäki M, Batty GD & Hublin C (2011). Shift work as a risk factor for future type 2 diabetes: evidence, mechanisms, implications, and future research directions. *PLoS Med* **8,** e1001138.

Kohsaka A, Waki H, Cui H, Gouraud SS & Maeda M (2012). Integration of metabolic and cardiovascular diurnal rhythms by circadian clock. *Endocrine Journal*. Available at: http://www.ncbi.nlm.nih.gov/pubmed/22361995 [Accessed March 8, 2012].

Koletar MM, Cheng H-YM, Penninger JM & Ralph MR (2011). Loss of dexras1 alters nonphotic circadian phase shifts and reveals a role for the intergeniculate leaflet (IGL) in gene-targeted mice. *Chronobiol Int* **28,** 553–562.

Loh DH, Dragich JM, Kudo T, Schroeder AM, Nakamura TJ, Waschek JA, Block GD & Colwell CS (2011). Effects of vasoactive intestinal peptide genotype on circadian gene expression in the suprachiasmatic nucleus and peripheral organs. *J Biol Rhythms* **26,** 200–209.

Marchant EG & Mistlberger RE (1996). Entrainment and phase shifting of circadian rhythms in mice by forced treadmill running. *Physiology & Behavior* **60,** 657–663.

Maywood ES & Mrosovsky N (2001). A molecular explanation of interactions between photic and non-photic circadian clock-resetting stimuli. *Gene Expression Patterns* **1,** 27–31.

Maywood ES, Mrosovsky N, Field MD & Hastings MH (1999). Rapid down-regulation of mammalian period genes during behavioral resetting of the circadian clock. *Proc Natl Acad Sci USA* **96,** 15211–15216.

Maywood ES, O'Neill J, Wong GKY, Reddy AB & Hastings MH (2006). Circadian timing in health and disease. In *Hypothalamic Integration of Energy Metabolism Proceedings of the 24th International Summer School of Brain Research, held at the Royal Netherlands Academy of Arts and Sciences*, pp. 253–269. Elsevier. Available at: http://www.sciencedirect.com/science/article/pii/S0079612306530158 [Accessed March 15, 2012].

Mercken EM, Carboneau BA, Krzysik-Walker SM & de Cabo R (2011). Of mice and men: The benefits of caloric restriction, exercise, and mimetics. *Ageing Research Reviews*; DOI: 10.1016/j.arr.2011.11.005.

Mistlberger RE (1991). Scheduled daily exercise or feeding alters the phase of photic entrainment in Syrian hamsters. *Physiology & Behavior* **50,** 1257–1260.

Mistlberger RE & Holmes MM (2000). Behavioral feedback regulation of circadian rhythm phase angle in light-dark entrained mice. *Am J Physiol Regul Integr Comp Physiol* **279,** R813–821.

Mrosovsky N (1996). Locomotor Activity and Non‐photic Influences on Circadian Clocks. *Biological Reviews* **71,** 343–372.

Mrosovsky N & Salmon PA (1987). A behavioural method for accelerating re-entrainment of rhythms to new light|[mdash]|dark cycles. *, Published online: 26 November 1987; | doi:101038/330372a0* **330,** 372–373.

Navara KJ & Nelson RJ (2007). The dark side of light at night: physiological, epidemiological, and ecological consequences. *J Pineal Res* **43,** 215–224.

Otawa M, Arai H & Atomi Y (2007). Molecular aspects of adrenal regulation for circadian glucocorticoid synthesis by chronic voluntary exercise. *Life Sci* **80,** 725–731.

Power A, Hughes ATL, Samuels RE & Piggins HD (2010). Rhythm-promoting actions of exercise in mice with deficient neuropeptide signaling. *J Biol Rhythms* **25,** 235–246.

Reebs SG & Mrosovsky N (1989). Effects of induced wheel running on the circadian activity rhythms of Syrian hamsters: entrainment and phase response curve. *J Biol Rhythms* **4,** 39–48.

Reebs SG & St-Coeur J (1994). Aftereffects of scheduled daily exercise on free-running circadian period in Syrian hamsters. *Physiol Behav* **55,** 1113–1117.

Van Reeth O, Sturis J, Byrne MM, Blackman JD, L'Hermite-Balériaux M, Leproult R, Oliner C, Refetoff S, Turek FW & Van Cauter E (1994). Nocturnal exercise phase delays circadian rhythms of melatonin and thyrotropin secretion in normal men. *Am J Physiol* **266,** E964–974.

Reppert SM & Weaver DR (2002). Coordination of circadian timing in mammals. *Nature* **418,** 935–941.

Roenneberg T, Hut R, Daan S & Merrow M (2010). Entrainment concepts revisited. *J Biol Rhythms* **25,** 329–339.

Schaap J & Meijer JH (2001). Opposing effects of behavioural activity and light on neurons of the suprachiasmatic nucleus. *Eur J Neurosci* **13,** 1955–1962.

Schroeder A, Loh DH, Jordan MC, Roos KP & Colwell CS (2011). Circadian regulation of cardiovascular function: a role for vasoactive intestinal peptide. *Am J Physiol Heart Circ Physiol* **300,** H241–250.

Sheward WJ, Naylor E, Knowles-Barley S, Armstrong JD, Brooker GA, Seckl JR, Turek FW, Holmes MC, Zee PC & Harmar AJ (2010). Circadian control of mouse heart rate and blood pressure by the suprachiasmatic nuclei: behavioral effects are more significant than direct outputs. *PLoS ONE* **5,** e9783.

Stevens RG (2009). Light-at-night, circadian disruption and breast cancer: assessment of existing evidence. *Int J Epidemiol* **38,** 963–970.

SUGIMOTO N, SHIDO O, SAKURADA S & NAGASAKA T (1994). Persisting Changes in the 24-Hour Profile of Locomotor Activity by Daily Activity Restriction in Rats. *The Japanese Journal of Physiology* **44,** 735–742.

Takahashi JS, Hong H-K, Ko CH & McDearmon EL (2008). The genetics of mammalian circadian order and disorder: implications for physiology and disease. *Nat Rev Genet* **9,** 764–775.

Thorpy M (2011). Understanding and Diagnosing Shift Work Disorder. *Postgraduate Medicine* **123,** 96–105.

Visser L de, Bos R van den & Spruijt BM (2005). Automated home cage observations as a tool to measure the effects of wheel running on cage floor locomotion. *Behavioural Brain Research* **160,** 382–388.

Vosko AM, Schroeder A, Loh DH & Colwell CS (2007). Vasoactive intestinal peptide and the mammalian circadian system. *Gen Comp Endocrinol* **152,** 165–175.

Warburton DER, Nicol CW & Bredin SSD (2006). Health Benefits of Physical Activity: The Evidence. *CMAJ* **174,** 801–809.

Warren WS, Champney TH & Cassone VM (1994). The suprachiasmatic nucleus controls the circadian rhythm of heart rate via the sympathetic nervous system. *Physiol Behav* **55,** 1091–1099.

Yamada N, Shimoda K, Ohi K, Takahashi S & Takahashi K (1988). Free-access to a running wheel shortens the period of free-running rhythm in blinded rats. *Physiology & Behavior* **42,** 87–91.

Yamazaki S, Numano R, Abe M, Hida A, Takahashi R-I, Ueda M, Block GD, Sakaki Y, Menaker M & Tei H (2000). Resetting Central and Peripheral Circadian Oscillators in Transgenic Rats. *Science* **288,** 682–685.

Yannielli PC, McKinley Brewer J & Harrington ME (2002). Is novel wheel inhibition of per1 and per2 expression linked to phase shift occurrence? *Neuroscience* **112,** 677–685.

Yoo S-H, Yamazaki S, Lowrey PL, Shimomura K, Ko CH, Buhr ED, Siepka SM, Hong H-K, Oh WJ, Yoo OJ, Menaker M & Takahashi JS (2004). PERIOD2::LUCIFERASE real-time reporting of circadian dynamics reveals persistent circadian oscillations in mouse peripheral tissues. *Proc Natl Acad Sci USA* **101,** 5339–5346.

CHAPTER 5

i. Discussion

Huntington's Disease and the Circadian System

The BACHD mouse model of HD displayed diurnal and circadian deficits of behavior and physiology. While day and night expression of PER2 did not differ between WT and BACHD mice, we found a loss of diurnal rhythms in SCN neuron firing rate in BACHD mice, with a significant reduction in the rate of firing during the day/rest period. The loss of diurnal rhythms in firing rate despite the presence of an intact molecular clock, suggests that the disruption in the circadian system is downstream of the molecular clock in the SCN. The absence of rhythms in firing rate may prevent the relay of circadian information from the SCN to peripheral outputs. Indeed, BACHD mice lost day/night differences in Heart Rate Variability (HRV) and were significantly reduced throughout the day and night. The lowered HRV indicates a disruption in the sympathovagal balance of autonomic nervous system (ANS) activity, and a predictor of serious cardiovascular events (Tsuji *et al.*, 1994). Consistent with the decrease in HRV, we measured higher levels of Heart Rate (HR) and body temperature in BACHD mice specifically during the day, which is the same phase when SCN firing rate is depressed. Furthermore, the attenuated baroreceptor reflex response in BACHD mice suggests that signaling from both the parasympathetic and sympathetic branches of the ANS are disrupted.

Despite the loss of day/night differences of HRV in BACHD mice, HR remained rhythmic, although blunted in amplitude, suggesting that factors outside of the ANS may contribute to the daily regulation of HR. However, we don't know yet whether the clock genes in the heart oscillate in BACHD mice or whether external cues are driving the daily

rhythms in cardiovascular function. In the R6/2 mouse model, which have an accelerated disease progression, mice are behaviorally arrhythmic under LD and DD conditions and lack rhythms in expression of clock and metabolic genes in the liver (Maywood *et al.*, 2010). BACHD mice have a milder HD phenotype compared to R6/2 mice, and therefore may display a different pattern of clock gene expression in peripheral tissues. Measurement of clock gene expression in peripheral tissues would provide better understanding of the circadian dysfunction in BACHD mice.

Circadian approaches may be a valuable tool in the management of HD. First, circadian symptoms occur very early in the disease progression and therefore could be used as tool for diagnosis and staging. Also, circadian disruption on its own has been demonstrated to lead to disease and therefore, may further exacerbate symptoms and conditions of HD. The stabilization of the circadian system may be an important strategy in delaying disease progression. In the R6/2 mice, restricted feeding reinstated rhythms of metabolic genes (but not clock genes) in the liver (Maywood *et al.*, 2010). Nonetheless, the reestablished rhythms in metabolic genes may be beneficial. Preliminary studies examining the effect of free wheel access on N171-82Q HD mouse model concluded that exercise did not help in slowing down disease progression; rather the authors observed an acceleration (Potter et al 2010). The issue with this intervention is that these mice were provided free access to the wheel, which may only reinforce the aberrant activity rhythm of BACHD mice. As suggested by results of scheduled exercise (Chapter 4), the timing of exercise may be a valuable component to help temporally structure rhythms to better align endogenous rhythms with the environment. Furthermore, the temporal reorganization may be enhanced by combining both scheduled feeding and scheduled exercise, such that

supply and demands on the metabolic system can be appropriately timed to minimize mismatches that lead to cellular dysfunction.

It would also be interesting to explore the metabolic dysfunction in the SCN and heart of BACHD mice because the metabolic and circadian systems are highly integrated (See Introduction; Asher & Schibler, 2011). In HD, there is an impaired ability to induce transcription and activity of PGC1α (peroxisome proliferator-activated receptor-γ coactivator 1α), which is a gene crucial for the regulation of mitochondrial turnover and biogenesis (Cui *et al.*, 2006; Weydt *et al.*, 2006; Johri *et al.*, 2011; Xiang *et al.*, 2011) and regulates uncoupling protein (UCP) and superoxide dismutase (SOD) 1,2 proteins involved in the conversion of reactive oxygen species to less volatile molecules (Patten & Arany, 2012). Importantly, PGC1α interacts with the circadian system by inducing the transcription of the clock genes *Bmal1* and *Rev-erbα* (Liu *et al.*, 2007; Lin *et al.*, 2008). In addition, PGC1α regulates the activity of PPARγ and α, which also regulate the activity of clock genes. Mice lacking PGC1α expression display disruptions in diurnal rhythms in activity, body temperature and metabolic rates (Liu *et al.*, 2007) further demonstrating the integration of circadian and metabolic pathways. Therefore, pharmacological targeting of the circadian system to improve molecular rhythms by using synthetic ligands (Rev-erb ligand agonist; Solt *et al.*, 2012) may help improve rhythms in BACHD mice in order to properly drive and improve metabolic function with the aim of delaying or deterring disease progression. Also, the temporal targeting of drugs to improve mitochondrial function, such as resveratrol through activation of PGC1α or bezafibrate, a PPARα agonist, would improve metabolic function and be able to recue rhythms in BACHD mice (Lefebvre *et al.*, 2006).

Our studies on the BACHD mouse model enabled us to further explore the deficits of the cardiovascular system, which would have been impossible to pursue using the fragile R6/2 mice. Measurement of circadian and cardiovascular disruption allowed us to suggest additional strategies in the management of HD disease in humans. For example, most published studies that measured autonomic function in humans performed the tests during the day or the active period, and no alterations in blood pressure and HR were detected (Sharma *et al.*, 1999; Kobal *et al.*, 2004, 2010; Bär *et al.*, 2008). In our studies, HR and body temperature did not differ between BACHD and WT mice during the active phase; rather the increased HR and blood pressure were detected during the rest phase. This suggests that BACHD mice may have non-dipping hypertension, known to cause cardiovascular disease. Future studies may determine if this is true in humans and may warrant temporally targeted administration of beta-blockers during the rest phase in order to combat the increased sympathetic drive to the heart.

Another mechanism that may be causing the disruption of the circadian system in HD mice is the decrease in VIP and VIPR2 expression (Fahrenkrug *et al.*, 2007). Other conditions such as aging and Alzheimer's Disease (Zhou *et al.*, 1995; Wu *et al.*, 2007), that include circadian disruption in the list of symptoms, also express VIP at lower levels. The loss of VIP disrupts the synchrony of molecular and firing rate rhythms in the SCN that leads to dampened and sometimes arrhythmic activity in mice under constant conditions (Colwell *et al.*, 2003; Aton *et al.*, 2005). The SCN sends VIPergic efferents to preautonomic neurons of the PVN (Buijs *et al.*, 2003; Kalsbeek *et al.*, 2006) and could therefore be regulating physiological rhythms including HR and cardiovascular function.

Role of VIP in the regulation of circadian rhythms in the heart.

Our results demonstrate that VIP is required for normal diurnal and circadian rhythms in HR, HRV, body temperature, and cage activity. VIP is also important for the phasing of clock gene expression in the heart under LD conditions, as well as the HR responses to acute stimuli. Lastly, VIP-deficient mice display elongated QT intervals suggesting that VIP may regulate ionic mechanisms in the heart.

Whether VIP's effect on rhythms is localized within the SCN alone or contributes to local effects within the heart is not clear. We postulate that in addition to actions within the SCN, VIP may have particular influence in regulating daily oscillations of heart function. This is based on the observation that VIP-deficient mice subject to constant conditions and without wheel access, display arrhythmic HRs despite continued rhythms in body temperature. We don't know yet whether the molecular feedback loop continues to oscillate in the heart under constant conditions, but this would be interesting to pursue. Certain conditions, such as aging and neurodegenerative diseases, display normal oscillations in clock gene expression in the SCN but firing rate rhythms are either dampened or lost (Kudo *et al.*, 2011; Nakamura *et al.*, 2011), indicating that the disruption is downstream of the molecular clock. In the heart, if the molecular clock is arrhythmic, VIP may be necessary in providing temporal cues. However, if the clock genes continue to oscillate in the heart while HR is arrhythmic suggests that VIP's action may be downstream of the molecular clock, by directly regulating proteins and signaling pathways involved in heart function

To further explore whether circadian disruption in VIP-deficient mice is due to disruption of SCN function alone or involves VIP effects on the heart, we can block VIPR2

receptor signaling in the SCN of WT mice by administering the VIPR2 antagonist ([Tyr1,DPhe2]GHRF(1-29; Itri *et al.*, 2004) by cannulation into the SCN region. If the cannulated WT mice display disrupted HR rhythms to the same degree as VIP-deficient mice, then VIP regulation of circadian rhythms in HR is necessary only in the SCN region. In this case, we would further explore the possibility that the loss of VIP disrupts a subpopulation of neurons within the SCN that specifically drives the regulation of cardiovascular output (Buijs *et al.*, 2003). However, if HR continues to oscillate, just as body temperature continues to oscillate despite the loss of VIP signaling in the SCN, then VIP may have functions outside of the SCN mediating temporal information to the heart. Alternatively, we can also perform rescue experiments in VIP-deficient mice, by delivering the VIP peptide to the SCN by cannulation during the middle of the subjective day, when VIP is secreted by SCN neurons (Francl *et al.*, 2010) and determine whether we can drive robust rhythms in behavior and physiology.

VIP plasma concentrations display circadian rhythmicity in humans (Cugini et al. 1991; Opstad 1987) and VIP could bypass the molecular clock and directly drive temporal changes in cell signaling cascades resulting in the rhythms observed in HR and cardiovascular function. VIP is localized in the postganglionic parasympathetic neurons or in the intrinsic VIPergic neuronal population in the heart, most of which, but not all, are cholinergic neurons (Kuncová *et al.*, 2003). Furthermore, VIP immunoreactive nerve fibers have been localized around the sino atrial (SA) and atrial ventricular (AV) nodes, supporting a role for VIP in the regulation of HR (Henning & Sawmiller, 2001). VIP binds to the VIPR1 and VIPR2 G-protein coupled receptors that turn on various signaling cascades including PKA, PKC, IP3 as well as modulating the inward rectifying potassium channel

(Pasyk *et al.*, 1996; Dickson & Finlayson, 2009). In the SA node, VIP increases cAMP levels that leads to the activation of the hyperpolarization activated pacemaker current (I_f) that accelerates the rate of diastolic depolarization and increases HR. In the ventricular myocytes, VIP activation of PKA activity enhances calcium channel phosphorylation, increasing L-type calcium current and the release of calcium from the sarcoplasmic reticulum, enhancing HR and contractility. The temporal regulation of these processes can alter daily HR and heart function. Further studies examining the circadian expression of potassium channels, calcium cycling and electrophysiological properties of cardiomyocytes from WT and VIP-deficient mice may further elucidate mechanisms for the disruption in HR rhythms. The application of VIP onto cardiomyocytes of WT and VIP deficient mice can identify molecular or cellular properties targeted by VIP signaling. We may not see large effects of VIP application alone, instead VIP may be acting as a primer, setting the tone in the heart modulating responses to Ach or NPY released by the parasympathetic nervous system. Alternatively, VIP may be regulating the presynaptic release of signaling molecules from the parasympathetic nervous system, similar to its regulation of GABA release in the SCN (Itri and Colwell). Lastly, a recent study identified a *Bmal1* regulated gene krueppel-like factor 15 (*Klf15*), which regulates the transcription of Kv channel interacting protein 2 (*KChIP2*; Jeyaraj *et al.*, 2012). *KChIP2* modulates the rate of repolarization (QT interval), and its loss leads to increased susceptibility for arrhythmias in mice, demonstrating a mechanism for the circadian regulation of cardiovascular function. In our studies, we also find a disruption in the QT interval (duration of repolarization) in VIP-deficient mice; specifically a lengthening of the QT interval and a loss of day/night differences. Future studies can examine expression levels of *Klf15*, *KChIP2* and *Kv4.2* genes in VIP-deficient

mice, to see if their expression is disrupted, which may be mediating the elongation of the QT interval.

Alternatively, VIP could be modulating the molecular clock in the heart directly. The application of VIP onto SCN explants late at night increases the expression of the *Per1 and Per2* clock genes (Nielsen et al., 2002; Vanecek and Watanabe, 1998). *Period* gene induction could be mediated by activation of the cAMP/PKA (Atkinson *et al.*, 2011; O'Neill & Reddy, 2012) or the CREB signaling pathway (unpublished data), which are two second messenger pathways induced by VIP and stimulate the transcription of *period* genes. Also, the regulation of the molecular clock by VIP may be mediated by nitric oxide (NO) signaling, as VIP can increase NO production (Henning & Sawmiller, 2001) and subsequently induce *Per1* and *Per2* transcription and stabilize BMAL1 protein through s-nitrosylation (Kunieda *et al.*, 2008). Most of these effects were examined within the SCN, and should be tested in cardiomyocytes. Methods to modulate PKA, CREB or NO production at appropriate times of day may be able to improve or rescue the circadian phenotype in VIP-deficient mice.

In addition to the study of dysfunction, methods to improve circadian deficits should be explored. Interventions that lead to the stabilization and alignment of endogenous rhythms with the environment may help deter the development of disease associated with circadian disruption. Just as scheduled feeding has been shown to reinstate rhythmic metabolic genes (Maywood *et al.*, 2010), the scheduling of exercise may be another means of driving and reorganizing the circadian system. Improvements in the daily rhythms of VIP-deficient mice driven by scheduled exercise may have important implications for diseases and conditions shown to have reduced VIP expression.

Exercise effects on the Circadian System

Scheduled exercise altered rhythms of behavior, physiology and gene expression under an LD cycle in WT mice with intact circadian systems, demonstrating that daily exercise could be used as a tool to drive and reorganize rhythms. When VIP-deficient mice, a model with a disrupted circadian system, were subject to scheduled exercise, a number of parameters of daily rhythms were rescued.

Scheduled exercise appears to bypass the loss of VIP and improved rhythmic parameters by realignment of the endogenous rhythms with the light/dark cycle. This improvement in rhythms in VIP-deficient mice induced by scheduled exercise would have important implications for humans who experience circadian deficits, including the aged population. Rhythms of VIP-deficient mice mimic many of the classic circadian disruptions observed in aged individuals, such as advanced phase, fragmentation and low amplitude rhythms (Colwell *et al.*, 2003; Schroeder *et al.*, 2011). Furthermore, levels of VIP are decreased in older humans thereby suggesting a mechanism for the disruption of circadian rhythms as we age (Zhou *et al.*, 1995; Wu *et al.*, 2007). The realignment of rhythms by scheduled exercise in VIP-deficient mice could potentially be applied to humans and deter the development of diseases associated with circadian disruption. However, translation of the effects of scheduled exercise from nocturnal mice to diurnal aged populations may require the identification of signaling pathways induced by exercise (Kohsaka *et al.*, 2012; White & Schenk, 2012) that interact with the circadian system to help predict the appropriate timing of exercise in humans. These pathways could be pharmacologically targeted at appropriate times of day to provide temporal structure and organization for proper alignment to the light/dark cycle.

The effects of exercise on the molecular clock may differ in the peripheral tissues and the SCN. In peripheral tissues, exercise, whether scheduled in the early or late night appears to consistently delay the timing of Per2:LUC peaks. In the SCN however, the effects on the amplitude of Per2:LUC rhythms in both WT and VIP-deficient mice, as well as the effects of dispersion in the phasing of Per2:LUC rhythms in VIP-deficient mice are dependent on the timing of exercise. Therefore, the mechanisms involved in altering the clock may differ depending on the tissue.

There are a number of potential pathways in which exercise could be modulating the circadian system. As mentioned earlier, VIP increases levels of nitric oxide (Henning & Sawmiller, 2001), which could then potentially alter the molecular clock throughout the body (Kunieda *et al.*, 2008), including the SCN. Exercise increases levels of nitric oxide levels and could provide timing signals to the circadian system. Exercise also alters the pyridine nucleotide (NAD+/NADH) ratios in cells, which is crucial for redox control of ATP production. Increased ratios activate SIRT1, a histone deacetylase, that interacts with the molecular feedback loop by deacetylating the clock gene BMAL1 modulating its DNA binding activity when heterodimerized with CLOCK protein (Kohsaka *et al.*, 2012). Exercise can also activate PPARγ (Peroxisome proliferator-activated receptors; (Petridou *et al.*, 2007), which stimulates the transcription of *Bmal1* and *Rev-erb* α genes (Fontaine *et al.*, 2003; Wang *et al.*, 2008). These pathways all influence the positive arm of the molecular clock (*Bmal1* and *Clock*), which normally peak during the dark to light transition. Late night exercise is, therefore, an appropriate intervention in order to reinforce and induce the activation of these genes during the late night.

SCN specific mechanisms may involve the regulation of NPY or serotonergic input from the intergeniculate leaflet (IGL) or raphe nucleus (RN), respectively (Challet *et al.*, 1998; Morin, 1999; Cuesta *et al.*, 2008). Stimulated activity in mice during the middle of the light period can result in a phase advance of behavioral rhythms (Glass *et al.*, 2010). Increased activity causes cellular activation in the IGL and RN regions as measured by c-fos staining that is thought to then relay signals to the SCN (Mrosovsky, 1995). The phase advance as a result of increased activity during the day can be mimicked by the application of NPY (Kallingal & Mintz, 2007) or serotonin (Yamakawa & Antle, 2010) onto the SCN at the same time of day. These studies were conducted during the light phase, however, stimulated activity during the dark to light transition can produce phase delays (Reebs & Mrosovsky, 1989), and it would be interesting to determine the effects of NPY and serotonin application on the SCN during these times, as this coincides with the effects of late night exercise on the circadian system. Also, blocking of NPY and serotonergic signaling in VIP-deficient and WT mice subject to late night exercise, may determine the necessity of these pathways in eliciting the changes in SCN properties induced by late night exercise.

Exercise has been shown to induce epigenetic changes in various genes including PGC1α, BDNF, TFAM, PDK4 (Hsieh *et al.*, 2009; Gomez-Pinilla *et al.*, 2011; Barrès *et al.*, 2012). These genes interact with the circadian system and can alter its function. It would be interesting to determine whether any clock genes are also epigenetically altered during scheduled exercise. If this is the case, exercise may therefore be a practical intervention in humans because epigenetic mechanisms suggest long-term alterations. Once epigenetic

changes have been established, intermittent exercise may be sufficient to retain the effects on the circadian system.

Another interesting result of scheduled exercise on circadian rhythms within the SCN, is the dampened amplitude observed in Per2:LUC expression in WT mice when provided wheel access during the early night. It would be interesting to image these slices using a CCD camera to examine the quality of these rhythms, and whether we find a loss of synchrony among subpopulation of neurons. The Per2:LUC explants capture the state of the SCN at one timepoint and this information is sustained throughout the rest of the recording. Animals were sacrificed shortly before ZT12, which is the start time for early night scheduled wheel access, therefore it is possible that the SCN may be in a state of temporary or transient dysynchrony, as subpopulations of neurons are anticipating the offset of light and the onset of robust activity. We would therefore like to examine Per2 expression in the SCN looking at different timepoints as well as using a different technique, such as immunocytochemistry, which may reveal more robust rhythms. Lastly, because free access, which involves running in the early and late night, does not elicit the same amplitude dampening effects as early night wheel access alone, leads us to speculate that activity during the late night may be an important cue in the synchronization of rhythms in the SCN.

An additional experiment that would further support the improvement of rhythms by late night exercise is the measurement of corticosterone levels in VIP-deficient mice. Under LD conditions and without wheel access, corticosterone levels in VIP-deficient mice are arrhythmic (Loh et al 2011). Therefore, the restorations of rhythms by late night wheel

access would be strong evidence that this manipulation is rescuing various levels of the circadian phenotype in the VIP-deficient.

Summary

The disruption of the circadian system is correlated with an increased incidence of disease that includes cardiovascular disease, cancer and diabetes. It is therefore important to pursue studies that explore the mechanisms of circadian dysfunction as well as develop methods to help improve rhythms in order to deter the development of disease. The BACHD mouse model displayed various levels of circadian disruption that include behavioral, physiological and cellular deficits. In addition to the metabolic dysfunction caused by the *huntingtin* gene, the circadian deficits in HD could be a result of the disruption in VIP signaling. Our studies examining the circadian phenotype in VIP-deficient mice confirmed that VIP is required for normal diurnal and circadian rhythms in HRV, HR, body temperature and cage activity. Lastly, we were able to rescue many of the diurnal deficits of VIP-deficient mice by scheduling exercise during the late night. Whether this intervention will have similar effects on humans and help deter disease will have yet to be determined, but at the moment, scheduled exercise seems to be a promising direction of study.

ii. Bibliography

Asher G & Schibler U (2011). Crosstalk between components of circadian and metabolic cycles in mammals. *Cell Metab* **13,** 125–137.

Atkinson SE, Maywood ES, Chesham JE, Wozny C, Colwell CS, Hastings MH & Williams SR (2011). Cyclic AMP signaling control of action potential firing rate and molecular circadian pacemaking in the suprachiasmatic nucleus. *J Biol Rhythms* **26,** 210–220.

Aton SJ, Colwell CS, Harmar AJ, Waschek J & Herzog ED (2005). Vasoactive intestinal polypeptide mediates circadian rhythmicity and synchrony in mammalian clock neurons. *Nat Neurosci* **8,** 476–483.

Bär KJ, Boettger MK, Andrich J, Epplen JT, Fischer F, Cordes J, Koschke M & Agelink MW (2008). Cardiovagal modulation upon postural change is altered in Huntington's disease. *Eur J Neurol* **15,** 869–871.

Barrès R, Yan J, Egan B, Treebak JT, Rasmussen M, Fritz T, Caidahl K, Krook A, O'Gorman DJ & Zierath JR (2012). Acute Exercise Remodels Promoter Methylation in Human Skeletal Muscle. *Cell Metabolism* **15,** 405–411.

Buijs RM, la Fleur SE, Wortel J, Van Heyningen C, Zuiddam L, Mettenleiter TC, Kalsbeek A, Nagai K & Niijima A (2003). The suprachiasmatic nucleus balances sympathetic and parasympathetic output to peripheral organs through separate preautonomic neurons. *J Comp Neurol* **464,** 36–48.

Challet E, Scarbrough K, Penev PD & Turek FW (1998). Roles of suprachiasmatic nuclei and intergeniculate leaflets in mediating the phase-shifting effects of a serotonergic agonist and their photic modulation during subjective day. *J Biol Rhythms* **13,** 410–421.

Colwell CS, Michel S, Itri J, Rodriguez W, Tam J, Lelievre V, Hu Z, Liu X & Waschek JA (2003). Disrupted circadian rhythms in VIP- and PHI-deficient mice. *Am J Physiol Regul Integr Comp Physiol* **285,** R939–949.

Cuesta M, Mendoza J, Clesse D, Pévet P & Challet E (2008). Serotonergic activation potentiates light resetting of the main circadian clock and alters clock gene expression in a diurnal rodent. *Exp Neurol* **210,** 501–513.

Cui L, Jeong H, Borovecki F, Parkhurst CN, Tanese N & Krainc D (2006). Transcriptional repression of PGC-1alpha by mutant huntingtin leads to mitochondrial dysfunction and neurodegeneration. *Cell* **127,** 59–69.

Dickson L & Finlayson K (2009). VPAC and PAC receptors: From ligands to function. *Pharmacol Ther* **121,** 294–316.

Fahrenkrug J, Popovic N, Georg B, Brundin P & Hannibal J (2007). Decreased VIP and VPAC2 receptor expression in the biological clock of the R6/2 Huntington's disease mouse. *J Mol Neurosci* **31,** 139–148.

Fontaine C, Dubois G, Duguay Y, Helledie T, Vu-Dac N, Gervois P, Soncin F, Mandrup S, Fruchart J-C, Fruchart-Najib J & Staels B (2003). The orphan nuclear receptor Rev-Erbalpha is a peroxisome

proliferator-activated receptor (PPAR) gamma target gene and promotes PPARgamma-induced adipocyte differentiation. *J Biol Chem* **278,** 37672–37680.

Francl JM, Kaur G & Glass JD (2010). Regulation of vasoactive intestinal polypeptide release in the suprachiasmatic nucleus circadian clock. *Neuroreport* **21,** 1055–1059.

Glass JD, Guinn J, Kaur G & Francl JM (2010). On the intrinsic regulation of neuropeptide Y release in the mammalian suprachiasmatic nucleus circadian clock. *Eur J Neurosci* **31,** 1117–1126.

Gomez-Pinilla F, Zhuang Y, Feng J, Ying Z & Fan G (2011). Exercise impacts brain-derived neurotrophic factor plasticity by engaging mechanisms of epigenetic regulation. *Eur J Neurosci* **33,** 383–390.

Henning RJ & Sawmiller DR (2001). Vasoactive Intestinal Peptide: Cardiovascular Effects. *Cardiovasc Res* **49,** 27–37.

Hsieh M-C, Yang S-C, Tseng H-L, Hwang L-L, Chen C-T & Shieh K-R (2009). Abnormal expressions of circadian-clock and circadian clock-controlled genes in the livers and kidneys of long-term, high-fat-diet-treated mice. *International Journal of Obesity* **34,** 227–239.

Itri J, Michel S, Waschek JA & Colwell CS (2004). Circadian Rhythm in Inhibitory Synaptic Transmission in the Mouse Suprachiasmatic Nucleus. *J Neurophysiol* **92,** 311–319.

Jeyaraj D *et al.* (2012). Circadian rhythms govern cardiac repolarization and arrhythmogenesis. *Nature* **483,** 96–99.

Johri A, Starkov AA, Chandra A, Hennessey T, Sharma A, Orobello S, Squitieri F, Yang L & Beal MF (2011). Truncated peroxisome proliferator-activated receptor-γ coactivator 1α splice variant is severely altered in Huntington's disease. *Neurodegener Dis* **8,** 496–503.

Kallingal GJ & Mintz EM (2007). Gastrin releasing peptide and neuropeptide Y exert opposing actions on circadian phase. *Neurosci Lett* **422,** 59–63.

Kalsbeek A, Palm IF, La Fleur SE, Scheer FAJL, Perreau-Lenz S, Ruiter M, Kreier F, Cailotto C & Buijs RM (2006). SCN outputs and the hypothalamic balance of life. *J Biol Rhythms* **21,** 458–469.

Kobal J, Meglic B, Mesec A & Peterlin B (2004). Early sympathetic hyperactivity in Huntington's disease. *Eur J Neurol* **11,** 842–848.

Kobal J, Melik Z, Cankar K, Bajrovic FF, Meglic B, Peterlin B & Zaletel M (2010). Autonomic dysfunction in presymptomatic and early symptomatic Huntington's disease. *Acta Neurol Scand* **121,** 392–399.

Kohsaka A, Waki H, Cui H, Gouraud SS & Maeda M (2012). Integration of metabolic and cardiovascular diurnal rhythms by circadian clock. *Endocrine Journal*. Available at: http://www.ncbi.nlm.nih.gov/pubmed/22361995 [Accessed March 8, 2012].

Kudo T, Schroeder A, Loh DH, Kuljis D, Jordan MC, Roos KP & Colwell CS (2011). Dysfunctions in circadian behavior and physiology in mouse models of Huntington's disease. *Experimental Neurology* **228,** 80–90.

Kuncová J, Slavíková J & Reischig J (2003). Distribution of vasoactive intestinal polypeptide in the rat heart: effect of guanethidine and capsaicin. *Ann Anat* **185,** 153–161.

Kunieda T, Minamino T, Miura K, Katsuno T, Tateno K, Miyauchi H, Kaneko S, Bradfield CA, FitzGerald GA & Komuro I (2008). Reduced nitric oxide causes age-associated impairment of circadian rhythmicity. *Circ Res* **102,** 607–614.

Lefebvre P, Chinetti G, Fruchart J-C & Staels B (2006). Sorting out the roles of PPAR alpha in energy metabolism and vascular homeostasis. *J Clin Invest* **116,** 571–580.

Lin JD, Liu C & Li S (2008). Integration of energy metabolism and the mammalian clock. *Cell Cycle* **7,** 453–457.

Liu C, Li S, Liu T, Borjigin J & Lin JD (2007). Transcriptional coactivator PGC-1alpha integrates the mammalian clock and energy metabolism. *Nature* **447,** 477–481.

Maywood ES, Fraenkel E, McAllister CJ, Wood N, Reddy AB, Hastings MH & Morton AJ (2010). Disruption of peripheral circadian timekeeping in a mouse model of Huntington's disease and its restoration by temporally scheduled feeding. *J Neurosci* **30,** 10199–10204.

Morin LP (1999). Serotonin and the regulation of mammalian circadian rhythmicity. *Ann Med* **31,** 12–33.

Mrosovsky N (n.d.). A Non-Photic Gateway to the Circadian Clock of Hamsters. 154–174.

Nakamura TJ, Nakamura W, Yamazaki S, Kudo T, Cutler T, Colwell CS & Block GD (2011). Age-related decline in circadian output. *J Neurosci* **31,** 10201–10205.

O'Neill JS & Reddy AB (2012). The essential role of cAMP/Ca2+ signaling in mammalian circadian timekeeping. *Biochemical Society Transactions* **40,** 44–50.

Pasyk EA, Cipris S & Daniel EE (1996). A G protein, not cyclic AMP, mediates effects of VIP on the inwardly rectifying K+ channels in endothelial cells. *J Pharmacol Exp Ther* **276,** 690–696.

Patten IS & Arany Z (2012). PGC-1 coactivators in the cardiovascular system. *Trends in Endocrinology & Metabolism* **23,** 90–97.

Petridou A, Tsalouhidou S, Tsalis G, Schulz T, Michna H & Mougios V (2007). Long-term exercise increases the DNA binding activity of peroxisome proliferator-activated receptor gamma in rat adipose tissue. *Metab Clin Exp* **56,** 1029–1036.

Reebs SG & Mrosovsky N (1989). Effects of induced wheel running on the circadian activity rhythms of Syrian hamsters: entrainment and phase response curve. *J Biol Rhythms* **4,** 39–48.

Schroeder A, Loh DH, Jordan MC, Roos KP & Colwell CS (2011). Circadian regulation of cardiovascular function: a role for vasoactive intestinal peptide. *Am J Physiol Heart Circ Physiol* **300,** H241–250.

Sharma KR, Romano JG, Ayyar DR, Rotta FT, Facca A & Sanchez-Ramos J (1999). Sympathetic skin response and heart rate variability in patients with Huntington disease. *Arch Neurol* **56,** 1248–1252.

Solt LA, Wang Y, Banerjee S, Hughes T, Kojetin DJ, Lundasen T, Shin Y, Liu J, Cameron MD, Noel R, Yoo S-H, Takahashi JS, Butler AA, Kamenecka TM & Burris TP (2012). Regulation of circadian behaviour and metabolism by synthetic REV-ERB agonists. *Nature*; DOI: 10.1038/nature11030.

Tsuji H, Venditti FJ Jr, Manders ES, Evans JC, Larson MG, Feldman CL & Levy D (1994). Reduced heart rate variability and mortality risk in an elderly cohort. The Framingham Heart Study. *Circulation* **90,** 878–883.

Wang N, Yang G, Jia Z, Zhang H, Aoyagi T, Soodvilai S, Symons JD, Schnermann JB, Gonzalez FJ, Litwin SE & Yang T (2008). Vascular PPARgamma controls circadian variation in blood pressure and heart rate through Bmal1. *Cell Metab* **8,** 482–491.

Weydt P, Pineda VV, Torrence AE, Libby RT, Satterfield TF, Lazarowski ER, Gilbert ML, Morton GJ, Bammler TK, Strand AD, Cui L, Beyer RP, Easley CN, Smith AC, Krainc D, Luquet S, Sweet IR, Schwartz MW & La Spada AR (2006). Thermoregulatory and metabolic defects in Huntington's disease transgenic mice implicate PGC-1alpha in Huntington's disease neurodegeneration. *Cell Metab* **4,** 349–362.

White AT & Schenk S (2012). NAD+/NADH and skeletal muscle mitochondrial adaptations to exercise. *American journal of physiology Endocrinology and metabolism*; DOI: 10.1152/ajpendo.00054.2012.

Wu Y-H, Zhou J-N, Van Heerikhuize J, Jockers R & Swaab DF (2007). Decreased MT1 melatonin receptor expression in the suprachiasmatic nucleus in aging and Alzheimer's disease. *Neurobiol Aging* **28,** 1239–1247.

Xiang Z, Valenza M, Cui L, Leoni V, Jeong H-K, Brilli E, Zhang J, Peng Q, Duan W, Reeves SA, Cattaneo E & Krainc D (2011). Peroxisome-proliferator-activated receptor gamma coactivator 1 α contributes to dysmyelination in experimental models of Huntington's disease. *J Neurosci* **31,** 9544–9553.

Yamakawa GR & Antle MC (2010). Phenotype and function of raphe projections to the suprachiasmatic nucleus. *Eur J Neurosci* **31,** 1974–1983.

Zhou JN, Hofman MA & Swaab DF (1995). VIP neurons in the human SCN in relation to sex, age, and Alzheimer's disease. *Neurobiol Aging* **16,** 571–576.